OPTIMIZATION OF STAINLESS-STEEL CLADDING ONTO MILD STEEL USING THE GMAW PROCESS

BY

ANCUNGWIRE SHOUDOUR
(19/U/GMEM/18795/PD)

A DISSERTATION SUBMITTED TO THE DIRECTORATE OF RESEARCH AND GRADUATE TRAINING IN PARTIAL FULFILMENT OF THE REQUIREMENTS FOR THE AWARD OF DEGREE OF MASTER OF SCIENCE IN ADVANCED MANUFACTURING SYSTEMS ENGINEERING OF KYAMBOGO UNIVERSITY

SEPTEMBER, 2024

ABSTRACT

Pipe welding is a significant yet demanding technique within welding technology. The Gas Metal Arc Welding (GMAW) cladding method is crucial in metal fabrication, particularly in manufacturing long-lasting materials suitable for extreme acidic and alkaline environments. The advantage of GMAW process is that it eliminates the need for post-weld finishing due to the absence of slag, coupled with a high welding speed that boosts productivity. However, a comprehensive understanding of the equipment is essential, from procurement to production, to effectively monitor and control the welding process and prevent defects. Optimization is critical, given the high demands for accuracy and efficiency stemming from the complexities of welding. The main goal was to identify the best GMAW conditions for applying a corrosion-resistant stainless-steel coating on mild steel substrates. Specific aims included establishing GMAW parameters, identifying factors affecting dilution, and optimizing variables for superior clad welding quality. The study included an experimental approach that followed a thorough literature review to identify suitable materials. The experimental framework utilized multiple trial runs based on the Taguchi design of experiments (DOE). The main parameters targeted for optimization were welding current, wire feed rate, and arc voltage, which were crucial for improving corrosion resistance, bead configuration, and weld dilution. The methodology was systematic, covering factor identification, response characterization, limit determination for process variables, design matrix creation, material selection, experimental execution, data collection, statistical analysis, and result verification. Results indicated significant metrics: bead width at 99.99%, penetration at 95.72%, and reinforcement at 96.4%, with a minimum dilution of 6.67%, all optimized at a 95% confidence level.

Keywords: Gas metal arc welding, Weld cladding, Taguchi (DOE), Response Surface Methodology, Weld bead geometry, Dilution.

DECLARATION

I, **ANCUNGWIRE SHOUDOUR**, hereby affirm that this dissertation report titled "OPTIMIZATION OF STAINLESS-STEEL CLADDING ONTO MILD STEEL USING GMAW PROCESS" is my own original work and has not been submitted for a degree at any other university.

Signature: …… Date: ……..

ANCUNGWIRE SHOUDOUR

19/U/GMEM/18795/PD

APPROVAL

We as University supervisors confirm that the candidate under our supervision has done the dissertation titled “OPTIMIZATION OF STAINLESS-STEEL CLADDING ONTO MILD STEEL USING GMAW PROCESS”.

SIGNATURE_____DATE_____

DR. CATHERINE WANDERA (PhD),

Main supervisor

SIGNATURE_____DATE_____

DR. SAMUEL KANGWAGYE (PhD),

Co-supervisor

TABLE OF CONTENTS

LIST OF TABLES

LIST OF FIGURES

ACKNOWLEDGEMENTS

My sincere appreciation goes to Dr. Catherine Wandera as well as Dr. Samuel Kangwagye, whose supervision and guidance significantly contributed to the success of this research. Professor Paul Kah's technical guidance significantly contributed to the successful preparation of gas metal arc welding (GMAW) experiments, and Mr. Dan Lynge of Northern Alberta Institute of Technology for the hands-on skills he imparted to my mind.

Special thanks to Uganda Technical College Elgon Administration staff (specifically my "Big Brothers Mr. Paul Mulima & Mr. Christopher Ssettuba) for funding part of my tuition, and allowing me to conduct the experiments in their Welding and Fabrication workshop.

I wish to give appreciation specifically to Dr. Catherine for providing critical feedback, especially on the experimental design and setup. Furthermore, I extend my appreciation to colleagues especially Mr. Tyole, not forgetting, Mr. Edenyu, Mr. Onyango, Mr. Eyobeluk, and Mr. Opolot, for their support in the workshop while executing the experiment. Additionally, I wish to thank my colleague "Engineer Eria Namomo" for his kind support in data optimization and interpretation.

I sincerely thank my family for their constant support. I am also grateful for the encouragement and understanding of my friends throughout this journey, particularly my role model, Engineer Denis Sabiiti, my supporter, Engineer Julius Bataringaya, Mr. Apollo Turyakira, and my closest friend, "Engineer" Daniel Okello Ogwal.

Lastly, but most importantly, my daughter Ms. Blessed Viola, and my second-half Ms. Vivian Atuheire plus my ever supportive father Mr. James Bukokosi.

May the Lord bless you.

LIST OF SYMBOLS AND ABBREVIATIONS

ANN	- Artificial Neural Networks
ANOVA	- Analysis of Variance
ANSI	- American National Standards Institute
AOLP	- Automatic Offline Programming
BS	- British Standard
CAD	- Computer-Aided Design
CFH	- Cubic Feet per Hour
CJP	- Complete Joint Penetration
CMT	- Cold Metal Transfer
CNC	- Computer Numerical Control
CO_2	- Carbon dioxide
CP	- Continuous Path
CTWD	- Contact to Work Distance
DC RP-EP	- Direct Current Reverse Polarity-Electrode Positive
DC	- Direct Current
DCEN	- Direct Current Electrode Negative
DOE	- Design of Experiments
DOF	- Degrees of Freedom
DV	- Disturbance Variables
ETWD	- Electrode to Work Distance
FEM	- Finite Element Modeling
HAZ	- Heat Affected Zone
IIW	- International Institute of Welding
ISO	- International Standardization Organization
IWV	- Input Welding Variables
KOBELCO	- Kobe Steel Group
LED	- Light Emitting Diode
M.S.D	- Mean Standard Deviation
NAIT	- Northern Alberta Institute of Technology
NDE	- Non-destructive Testing

NG-GMAW - Narrow gap GMA welding
OA - Orthogonal Array
ODPP - One Drop per Pulse
OLP - Online Programming
OWV - Output Welding Variables
PTP - Point-to-Point
RMD - Regulated Metal Deposition
RSM - Response Surface Methodology
S.D. - Standard Deviation
SAIT - Southern Alberta Institute of Technology
SAW - Submerged Arc Welding
SCC - Stress-Corrosion Cracking
SMAW - Shielded Metal Arc Welding
SNR - Signal-to-Noise Ratio
WBGFs - Weld Bead Geometry Features
WFS - Wire Feed Speed

CHAPTER ONE: INTRODUCTION

1.0 Introduction

Cladding welding is a manufacturing method where a layer of another corrosion resistant material deposited on top of a rusting-prone material (Ranjan & Das, 2023; Kaushik et al., 2021). Gas metal arc welding (GMAW) process can cover very large surfaces with welded deposits in a short time (Farkade & Ravanan, 2015; Fırat Alemdar et al., 2023).

Figure 1-1: Corrosion damage to structural members that ended up collapsing (Fırat Alemdar et al., 2023)

This GMAW weld cladding process with stainless steel on mild steel protects the weldment from acidic/alkaline environments (Ranjan & Das, 2022; Cárcel-Carrasco, 2019) to extend the life of the coated substrate (Preedawiphat et al., 2020). The pulsed metal inert gas welding (PMIGW) method is very effective for cladding than the conventional GMAW process (Ranjan & Das, 2023). PMIGW is one type of gas metal arc welding (GMAW). Clad weldments are used in chemical, petroleum, nuclear, naval, aeronautical, service, and maintenance industries (Saha & Das, 2018; Tang et al., 2024). There are three ways in which GMAW welding is performed: semiautomatic welding, machine welding, and automatic welding (Kah, 2021). The main factors controlling GMAW weld quality, productivity, and cost include arc voltage, welding current, shielding gas flow rate, travel speed, filler metal composition, etc. This study addressed the complexities of weld cladding while analyzing the outcomes of the input welding variables on the resulting joint (Eswaran et al., 2022; Kumar et al., 2023).

GMAW faces significant challenges, with corrosion causing an annual loss of 3.4% (approximately 2.5 trillion US dollars) to the global GDP (Moon et al., 2020). Additionally, defects can occur during and after the welding process (Nele et al., 2022; Abioye et al., 2019; Shin et al., 2020). The key output parameters include corrosion resistance, dilution from the cladded layer, and weld bead geometry, which encompasses bead width, penetration, and reinforcement (Tran et al., 2023; Giarollo et al., 2022; Vora et al., 2022; Madesh et al., 2020).

To enhance GMAW parameters, the Taguchi design of experiments (DOE) approach was employed to assess the impact of various input welding parameters (Odinikuku et al., 2020). The Analysis of Variance (ANOVA) method validated the influence of voltage, welding current, and wire feed rate on weld bead geometry, dilution, and corrosion resistance (Casarini et al., 2020). The optimized parameters were confirmed for application in robotic welding software, indicating that robots could function autonomously using these settings (Wahidi et al., 2024; Curiel et al., 2023).

1.2 Problem Statement

The Cladding Process Challenges are working on nonlinear points that require a lot of care and the Heat Affected Zone (HAZ). This means that using GMAW process in weld cladding can lead to a wider HAZ, which negatively influences the mechanical properties of the substrate. Additionally, large dilution percentage and penetration issues follow the cladded layer. Achieving low dilution while maintaining adequate penetration depth is crucial. Studies

indicate that pulsed current GMAW (PC-GMAW) significantly reduces dilution compared to constant current GMAW (CC-GMAW). In addition, there are the microstructural considerations like the grain structure (the microstructure of the cladded layer is affected by the welding parameters). PC-GMAW promotes finer grain structures, enhancing hardness and wear resistance. The wear performance of cladded specimens is associated to microhardness.

In conclusion, optimizing GMAW parameters is crucial to reduce the heat-affected zone (HAZ), manage dilution, and improve the microstructural integrity of the cladded layer for better wear resistance. While GMAW has its benefits, alternatives like laser cladding may offer different advantages regarding dilution. The researcher focused on parameters such as excellent corrosion resistance, weld bead dilution, and acceptable weld bead geometry. Monitoring and controlling the welding process is necessary to achieve high-quality weldments, and precise measures are required to ensure process accuracy. There is limited research on optimizing GMAW variables. After optimization, the selected parameters were validated using the "Design Expert." Welding operators can then set these optimized parameters for programming robotic manipulators in gas metal arc welding automation (GMAW Robotic Welding).

1.3 Objectives

1.3.1 Main Objective

The main objective of the study was optimization of stainless-steel cladding onto mild steel using GMAW process.

1.3.2 Specific Objectives

Specific Objectives

The specific objectives include:

(i) Identifying the GMAW process variables that affect the geometry of the weld bead when weld cladding stainless steel onto a mild steel substrate.

(ii) Analyzing the GMAW process variables that impact dilution during the welding of stainless steel onto a mild steel substrate.

(iii) Optimizing the GMAW process variables to achieve high-quality welding of stainless steel onto a mild steel substrate.

1.4 Research Questions

The study aimed to explore the following questions:

(i) Which GMAW process parameters affect the geometry of the weld bead when cladding stainless steel onto a mild steel substrate?

(ii) Which GMAW process variables affect the dilution of the interface zone in the welding of stainless steel onto a mild steel substrate?

(iii) What optimal process variables are necessary for producing high-quality weldments in the GMAW weld cladding of stainless steel onto a mild steel substrate?

1.5 Scope

The research concentrated on observing, managing, and optimizing independent variables to address the ongoing corrosion problem in structural steel. Important variables included arc voltage, welding current, torch angle, welding speed, filler wire diameter, preheat temperature, electrode-to-work distance, and wire feed speed. The primary focus was on welding current (I), arc voltage (V), and wire feed rate (S) (m/min). Inductance was not considered since pulsed spray was the chosen metal transfer method. Furthermore, the development of automatic software for robotic welding was outside the scope of this study. The analysis specifically looked at how the three main inputs (I, V, S) influenced weld bead geometry, corrosion resistance, and dilution of the weld bead.

1.6 Significance

The welding cladding process aims at improving the corrosion resistance and hardness of the component. It would also provide scholarly literature on the process optimization of welding cladding by suggesting the best proportions of primary variables needed during the process. These optimized variables will guide other researchers in making the right analyses and the practitioners in executing their jobs perfectly.

1.7 Justification

Given the uncertainties in the GMAW process, it is essential to manage defects and operational disturbances. Optimizing the process is necessary to ensure safe welding practices while meeting environmental regulations. This approach will also boost production rates, improve product quality, and prolong the lifespan of equipment.

1.8 Conceptual Framework

Figure 1-1 illustrates the connections among independent variables, dependent variables, and intervening (noise) variables. The input variables consist of welding current, arc voltage, and wire feed rate. The output variables include surface integrity (such as roughness, cracks, and distortion), corrosion hardness, microstructural features, and weld dilution. Intervening variables (noise factors) encompass elements like air movement (high winds), material density, uniformity, and environmental dirt.

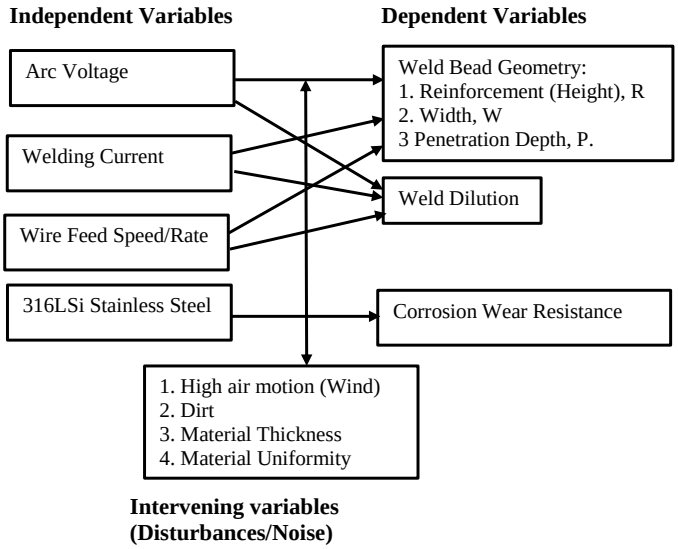

Figure 1-2: Conceptual Framework

1.9 Scope and Limitations of the Study

This research focuses on the cladding of thin mild steel pipes, particularly those with a thickness of up to 5 mm, using stainless steel. The study is confined to examining the physical and mechanical properties at the junction of the stainless-steel coating and the mild steel substrate. It was crucial to eliminate contaminants such as rust, mill scale, dirt, oil, and paint to avoid weld defects like porosity, incomplete fusion, unsatisfactory weld bead appearance, and blow holes. Additionally, it was important to re-clean the substrate after power load shedding to prevent oxide formation on the welding surface.

CHAPTER TWO: LITERATURE REVIEW

2.0 Introduction

This section discusses the application of AISI 316LSi stainless steel cladding on A36 mild steel pipes using Gas Metal Arc Welding (GMAW) for corrosion protection. Cladding involves layering one material over another to improve specific properties, which differs from hard-facing. According to Manney (2024), “hard facing deposits wear-resistant layers on components, while cladding deposits corrosion-resistant layers on components.” A literature review was performed to explore existing research on GMAW cladding and related topics. The study focuses on weld bead geometry, dilution, microstructural characteristics, and the corrosion and wear resistance of AISI 316LSi stainless steel cladding applied to mild steel via the P-GMAW process.

2.1 Gas Metal Arc Welding (GMAW) Processes

As stated in AWS B2.1/B2.1M-BMG (2021), "welding is a fabrication technique that joins two or more material components using heat, pressure, or a combination of both." This process creates a joint as the materials cool and is commonly used for metals, thermoplastics, and wood, resulting in a finished weldment. However, welding is intricate, involving various chemical, physical, and mechanical interactions. The concurrent presence of solid, liquid, and gas phases in a confined space and brief time frame presents significant challenges. Measuring parameters in real-time is challenging, which requires analyzing optimal variables for successful automated and robotic arc welding to achieve the desired bead shape and weldability (Giron-Cruz et al., 2022).

2.1.1 Types of GMAW Processes

In Gas Metal Arc Welding (GMAW), a wire electrode is continuously supplied from a spool to the welding arc at a rate that corresponds to the welding current. At the same time, a shielding gas is delivered through the welding gun to protect the weld area from atmospheric impurities, particularly oxygen and nitrogen, which can lead to issues like porosity, fusion defects, and embrittlement. Additionally, hydrogen and moisture can negatively affect the welds and cause oxidation (Giron-Cruz et al., 2022). GMAW is a flexible welding method that can be easily automated for robotic applications; however, it is not ideal for outdoor conditions due to the instability of the shielding gas mixture caused by air movement. This is particularly

problematic during high wind conditions, which cannot be effectively managed with shielding walls (Zhai et al., 2020).

2.1.2 GMAW Equipment

Gas Metal Arc Welding (GMAW) requires more advanced equipment than Shielded Metal Arc Welding (SMAW), leading to higher initial costs. However, rapid welding metal deposition yields significant labor and overhead savings, quickly offsetting costs. The GMAW setup consists of several key components, illustrated in Figure 2-1, with the main components being the wire feeder, the gas shielding system, and the power circuit. They are further broken down into:

(a) Power source
(b) Wire electrode reel/ spool (Filler metal feeding mechanism)
(c) Wire electrode feeder
(d) Welding gun
(e) Shielding gas cylinder
(f) Welding cables or leads and gas hose pipes

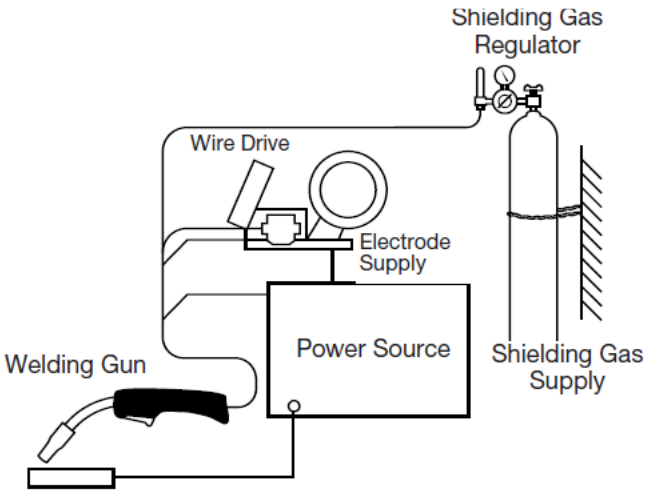

Figure 2-1: Gas Shielded Metal Arc Welding (Arnand, 2022)

GMAW Parts

(a) Power Source

The Telwin Mastermig 400 is a multifunctional MIG-MAG/Flux/Brazing welding machine that runs on a 3-phase 230/400V power supply. It can weld various materials, including mild and stainless steel, and is capable of joining different metals, such as mild steel to stainless steel and vice versa. Key features of the Mastermig 400 include:

1. Robust construction
2. Multiple settings for arc voltage adjustment
3. Control over spot welding duration
4. Two reactance settings
5. Thermostatic protection

Figure 2-2: Mastermig 230/400 welding machine (Telwin Spa, 2020)

(b) Wire electrode reel/ spool (Filler metal feeding mechanism)

The Mastermig welding machine has a removable wire feeder and the optional extensions it has can increase the working distance between the wire feeder and power source up to 10 meters (Figure 2-3).

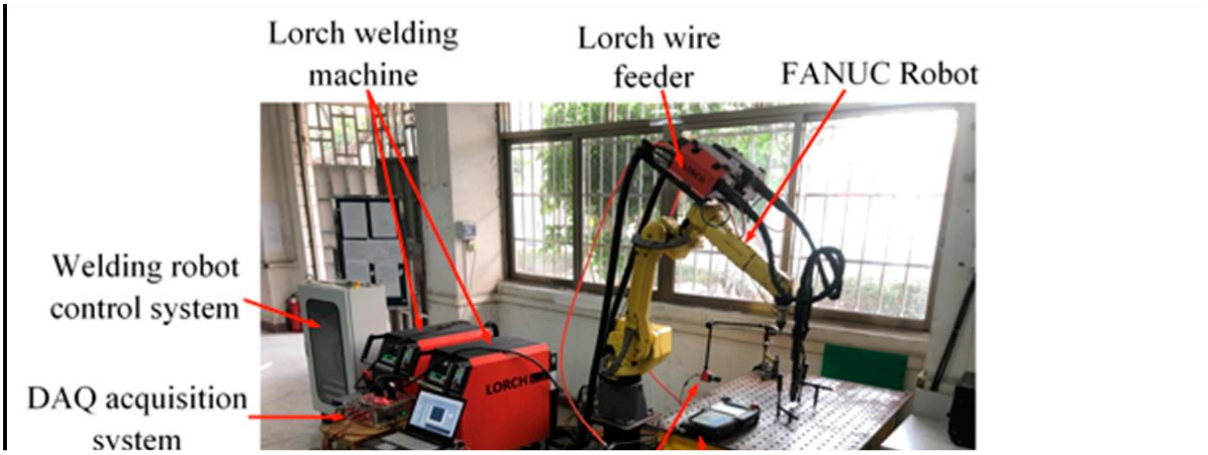

Figure 2-3: Wire electrode feeder (Yao et al. 2021)

(c) Wire Filler Electrode

In Gas Metal Arc Welding (GMAW), a wire electrode is continuously supplied from a spool to the welding arc at a rate that corresponds to the welding current. At the same time, a shielding gas is delivered through the welding gun to protect the weld area from atmospheric impurities, particularly oxygen and nitrogen, which can lead to issues like porosity, fusion defects, and embrittlement. Additionally, the shielding gas must complement the electrode to affect the weld's physical and mechanical traits (Hadžihafizović, Dževad, 2023).

Commercial welding electrodes typically contain small quantities of de-oxidizing metals like silicon, manganese, and aluminum to prevent porosity from oxygen. To mitigate nitrogen-related porosity, elements such as titanium and zirconium may also be included. A cladded weld joint comprises three primary zones:

1. Base metal (substrate – mild steel)
2. Cladded metal (filler wire – stainless steel)
3. Weld zone (a mixture of the filler wire and substrate), encircled by the heat-affected zone (HAZ) (Bunaziv et al., 2019).

The selection of filler wire for MIG welding is influenced by several factors, including:

1. The chemical makeup of the base metal.
2. The mechanical characteristics of the base metal.
3. Type of shielding gas used

4. Service type or specification requirements
5. Weld joint design (Saha and Santanu, 2013; Singh Singhal & Kumar Jain, 2020).

The distance from the electrical contact point to the end of the wire electrode, referred to as wire extension or stick-out, experiences I^2R heating. The distance from the tip to the workpiece affects the necessary welding current; increasing this distance can lower the current requirements but may also lead to arc instability (Giron-Cruz et al., 2022; Punales & Alfaro, 2021).

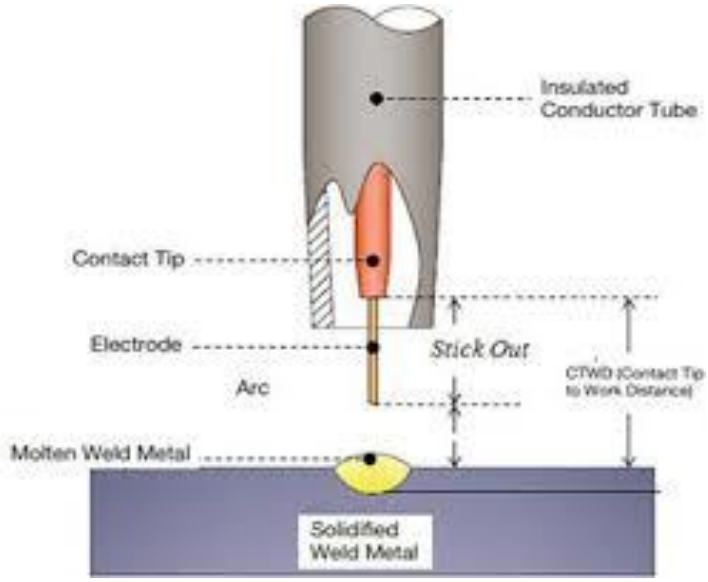

Figure 2-4: Electrode tip, Wire extension, and Arc Length (Punales & Alfaro, 2021)

(d) Welding gun

A standard GMAW welding gun includes several key components as illustrated in Figure 2-5:

1. Control switch (Trigger): Starts the wire feed, electric power, and shielding gas.
2. Contact tip: Delivers electrical energy to the electrode and directs it to the weld area.
3. Power cable: Connects the contact tip to the welding power source.
4. Gas nozzle: Releases shielding gas.
5. Electrode conduit and liner: Guides the electrode wire.
6. Gas hose: Provides shielding gas.

Before starting the welding process, the operator adjusts the voltage, wire speed, and gas flow to recommended levels. Once the gun is in place, activating the trigger begins gas flow and

creates an arc, allowing control over the distance from the nozzle to the workpiece, the angle, and the travel speed along the joint.

In Gas Metal Arc Welding (GMAW), it is crucial to maintain the appropriate contact tip to work distance (CTWD) to achieve high-quality weld cladding of 316LSi stainless steel on an A36 mild steel substrate, particularly for enhancing corrosion resistance in difficult environments. (CTWD is often mistaken for the electrode-to-work distance (ETWD)). The CTWD refers to the space between the end of the contact tip and the workpiece, while the ETWD is the distance from the electrode to the workpiece. Key points about its significance include:

Impact on Heat Input and Weld Quality:

A shorter ETWD can increase heat input, enhancing the melting of the filler wire and workpiece, which may improve fusion and reduce defects (Bhattacharya et al., 2016; Khrais, 2023).

Maintaining optimal ETWD is vital for a stable arc, affecting bead shape and overall cladding quality (Kah et al., 2022).

Correlation with Process Parameters:

Research shows that changes in ETWD significantly affect welding current and voltage, which are essential for achieving the desired cladding properties (Abioye et al., 2019).

Proper ETWD helps reduce corrosion rates, as indicated by fewer corrosion pits in clad samples when optimal parameters are used (Verma et al., 2017; Rakesh, 2021).

Conversely, excessive ETWD can lead to unstable arcs and increased spatter, which can compromise the protective qualities of the cladding. Thus, precise control of ETWD is essential for effective GMAW cladding applications (Young & Wang, 2024).

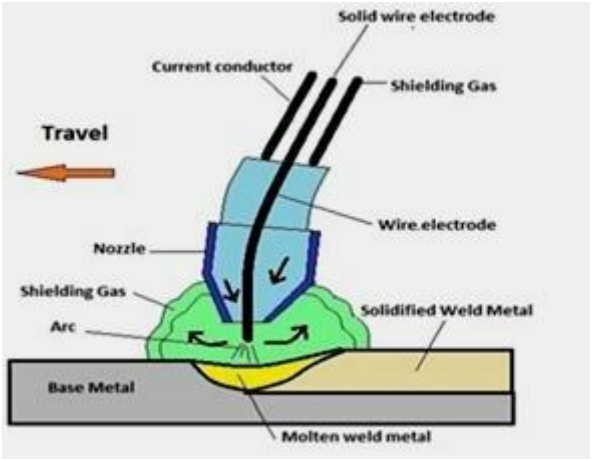

Figure 2-5: Welding gun (Pandya, 2018)

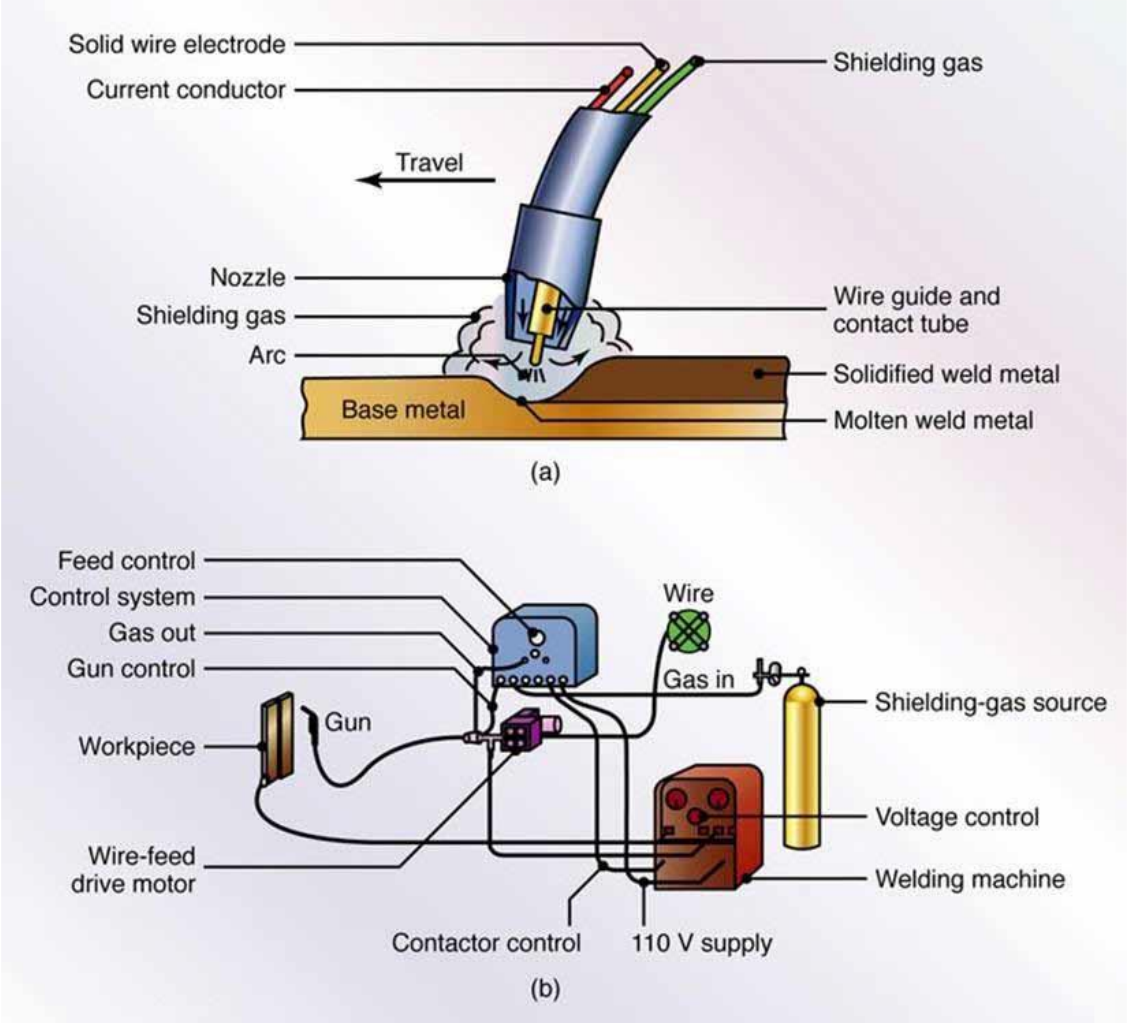

Figure 2-6: a) MIG Welding Process b) MIG welding hardware block diagram (Aytekin, 2021)

(e) Shielding gas supply and Gas Hoses

The shielding gas safeguards the molten weld pool from atmospheric gases like oxygen, nitrogen, and hydrogen, which helps to avoid defects such as porosity and excessive spatter. It also stabilizes the arc, increases productivity, and improves the mechanical properties of the weld metal. The gas is stored in a cylinder and delivered through a hose to the welding gun, along with electrical current and voltage cables, to ensure effective welding. Common shielding gases used include Argon (Ar), Carbon dioxide (CO_2), Helium (He), Hydrogen (H_2), and Nitrogen (N_2) (Ikpe et al., 2024).

GMAW Workstation

Gas Shielded Arc Welding workstations can be either manual or robotic, depending on the welder's preference.

GMAW Workstation

The Gas Shielded Arc Welding workstations can be either manual arc welding stations or robot workstations depending on the welder’s choice (Martinez et al., 2021).

(a) Manual System

A manual arc welding station shown in Figure 2-9 consists of only three major elements namely: the power source, the welding control, and the shielding gas supply.

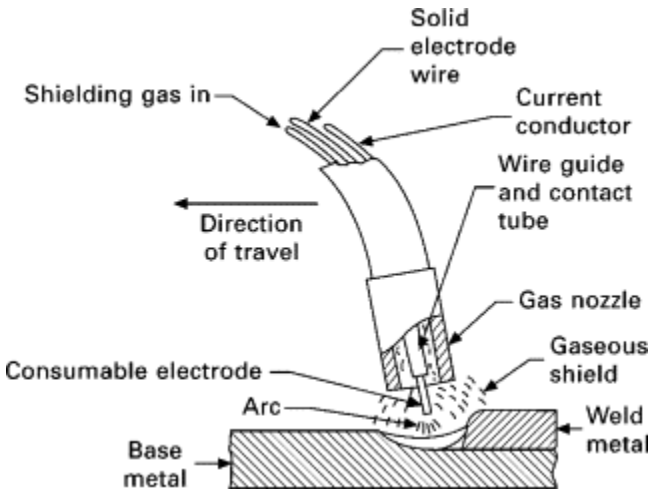

Figure 2-8: GMAW Gas Nozzle (Hickey, 2020)

(b) Automatic (Robotic) System

A robot is a versatile, programmable machine capable of performing diverse tasks through precise, pre-programmed movements, and manipulating materials, parts, tools, or custom devices. Effective robotic welding requires the operator to possess comprehensive training and extensive experience in both welding operations and robotic programming. A well-programmed robotic welder significantly enhances production, but achieving optimal results relies on precise operator inputs. The robot executes commands exactly, making operator input crucial for setting parameters like speed in the production of high-quality welds (Kajan et al., 2024).

2.1.3 GMAW Variables

There are numerous input variables in Gas Metal Arc Welding (GMAW) that are adjusted, each affecting the final weld differently. These variables include but are not limited to, polarity, voltage, current (wire feed rate), shielding gas flow rate, joint preparation, arc length, electrode extension, the size and type of filler wire, travel speed, travel angle, and the properties of the shielding gas, among others (Miller Electric Mfg. Co., 2018).

2.1.4 Versatility of GMAW

The GMAW process is very versatile, making it suitable for both manual and automated (robotic) welding tasks. As a result, GMAW workstations can be classified into manual arc welding stations or robotic workstations (Curiel et al., 2023).

(a) Manual Gas Metal Arc Welding Workstation

A manual arc welding station, as depicted in Figure 2-9, comprises three main components: the power source, welding control, and shielding gas supply. This type of station is easy to set up and does not require programming, as the human welder controls the torch movement. The welder manually adjusts the parameters before starting the welding process. In this scenario, personal protective equipment (PPE) is essential for the welder, unlike in robotic welding, where robots do not require PPE and do not experience fatigue. It is crucial to protect the welder from welding gases, electric radiation, and electric current, which is not a concern in automatic welding stations that typically have fewer accident risks (Driscoll Tim, 2020).

Figure 2-9: GMAW Process Welders in Action (Lincoln Electric, n.d.)

(b) Semi-Automatic Gas Metal Arc Welding System

Semiautomatic welding uses machinery to manage the arc and welding speed, enhancing both precision and accuracy. This method is commonly applied in processes like metal inert gas (MIG), metal active gas (MAG), tungsten inert gas (TIG), plasma arc welding (PAW), and submerged arc welding (SAW). Its popularity stems from its ability to provide better control compared to traditional manual welding techniques (Netto et al., 2023).

(c) Automatic (Robotic) Gas Metal Arc Welding System

Robots are adaptable, programmable machines capable of performing a variety of tasks with precision, including handling materials, parts, tools, or specialized devices. They provide numerous advantages, such as operating continuously (24/7), improving safety, and ensuring consistency (Saha and Santanu, 2020). Robots can undertake dangerous and repetitive tasks without fatigue, making them suitable for many applications.

Effective robotic welding requires skilled operators with significant experience in both welding and programming (Kajan et al., 2024). While robotic welders enhance production, the quality of welding relies heavily on accurate inputs from operators. The robot executes commands precisely, depending on operators to set parameters like speed.

The benefits of robotic welding include:

- Increased arc time and travel speed for higher productivity; one robot can replace more than two welders, reducing labor costs.
- Improved working conditions, as operators do not need to be near the intense heat of the arc.
- Enhanced efficiency through necessary reorganization and innovative thinking.
- Reduced challenges in hiring and retaining qualified welders (Kah et al., 2014).

However, establishing a robotic station requires extensive staff training for effective operation. Key considerations for transitioning to robotic welding include:

- Ensuring the robot can reach all necessary positions for welding.
- Monitoring welds so the robot controller can make adjustments for any deformations.
- Confirming that the robot fixtures are appropriate for the specific welding tasks.
- Achieving optimal weld sequences in robotic welding (Kah et al., 2014).

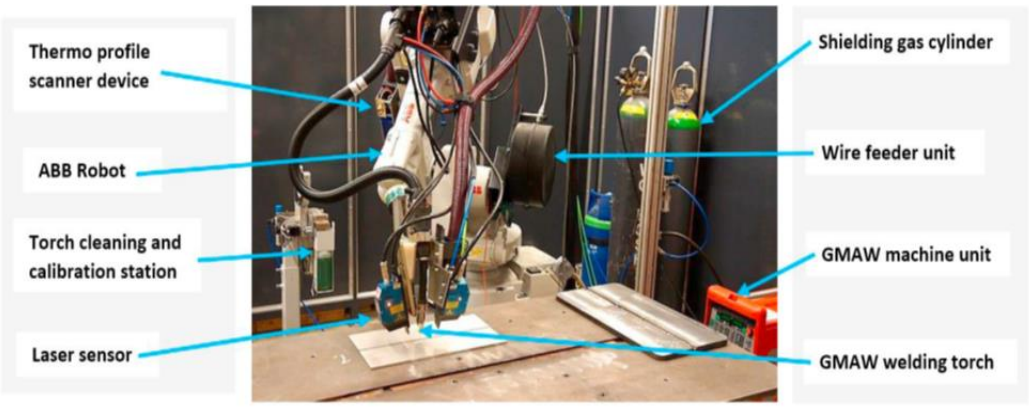

Figure 2-10: Automatic Welding GMAW equipment (Gyasi et al., 2019)

2.2 Modes of Metal Transfer

Metal transfer is the process in which the solid welding wire melts during welding and transfers across the arc to the weld pool depending on the amount of the applied energy (Boergert, 2021). The basic GMAW process has four distinctive metal transfers: Dip (Short-Circuiting) Transfer, Globular Transfer, Spray Arc Transfer, and Pulsed Spray metal transfer.

2.2.1 Dip (Short-Circuiting) Transfer

"Dip" or "Short-circuiting" describes the rapid contact of the wire electrode with the base metal, occurring up to 250 times per second, producing a sound similar to "crackling bacon." This contact cools and solidifies the wire quickly, allowing molten metal to flow onto the workpiece to create a weld. This cycle continues when the arc is reestablished. This method is particularly effective for thin materials like sheet metal. However, short-circuit transfer has some drawbacks:

1. Slow deposition rate
2. High risk of undercut, weld spatter, and lack of fusion (Boergert, 2021).

2.2.2 Globular Metal Transfer

In globular metal transfer, the filler metal is transferred across the arc in large droplets that exceed the diameter of the filler wire. These droplets fall randomly due to gravity, leading to a less stable process and a rough weld bead. This method is generally not preferred, except in flux-cored arc welding (FCAW) with specific shielding gases. Globular transfer often results in excessive spatter, which is inefficient and can cause cold lapping or incomplete fusion, requiring post-weld cleaning and additional costs. Its limitations include:

1. Uneven appearance due to spatter
2. Lower weld quality compared to other techniques

3. Limited to flat positions and horizontal fillet welds
4. Suitable only for metal thicknesses of 1/8” or 3.18 mm (Boergert, 2021).

2.2.3 Spray Metal Transfer

This metal transfer technique operates at high voltages, creating a spray of tiny molten droplets that move from the electrode wire to the substrate as the electrode is consumed. The droplets are smaller than the electrode diameter, and the intense heat from the arc melts both the electrode and the workpiece, aiding their transfer to the joint. The filler metal flows across the arc in a steady stream of fine droplets, which is different from globular transfer, resulting in a more stable arc. Spray transfer produces hundreds of droplets each second, with higher welding parameters like current and voltage compared to globular transfer. The benefits of spray arc transfer include:

a) High deposition rates

b) Effective fusion and penetration

c) Attractive bead appearance

d) Ability to use larger diameter wires

e) Minimal spatter

However, it has some limitations, such as:

1) Usable only on materials thicker than 3.175 mm for hand-held applications

2) Limited to flat and horizontal fillet weld positions

3) Requires precise fit-up due to the absence of open root capability (Boergert, 2021).

2.2.4 Pulsed Spray Transfer (GMAW-P)

This technique is an enhanced version of spray transfer that utilizes a high-frequency power source to alternate between high and low currents at a rate of 30 to 400 times per second. The high current effectively pinches off a droplet from the welding wire and propels it into the weld joint. This method is typically employed with a constant voltage power source, ensuring stable arcs and reducing the likelihood of weld defects. The current can exceed 100 amps, depending on the material's thickness and microstructure.

As noted by Boergert (2021), in pulse spray transfer (GMAW-P), the power source's pulse control generates high peak amperages that facilitate the spray transfer, while the background current is maintained at a level that sustains the arc without allowing metal transfer. This pause in metal transfer during the background phase allows the weld puddle to solidify slightly, unlike traditional spray transfer, where molten droplets are continuously moved. Consequently, this solidification enables pulsed spray transfer to be effective for thinner materials and enhances control during out-of-position welding. Pulsed spray transfer is suitable for all positions on both light and heavy-gauge metals.

2.3 Forces in the Arc

In Gas Metal Arc Welding (GMAW), various forces influence the molten metal droplets within the arc, impacting the transfer of metal from the wire electrode to the weld pool. When using Direct Current Electrode Positive (DCEP) polarity with Argon-based shielding, three primary forces assist in detaching droplets from the electrode:

- Lorentz force (electromagnetic pinch force)
- Gravitational force (assuming flat position welding)
- Aerodynamic drag force from the plasma flow

Additionally, research by Zhang et al. (2021) indicates that, "the relationship between a droplet's natural frequency and its size positions droplet resonance as a promising approach for accurately controlling droplet size."

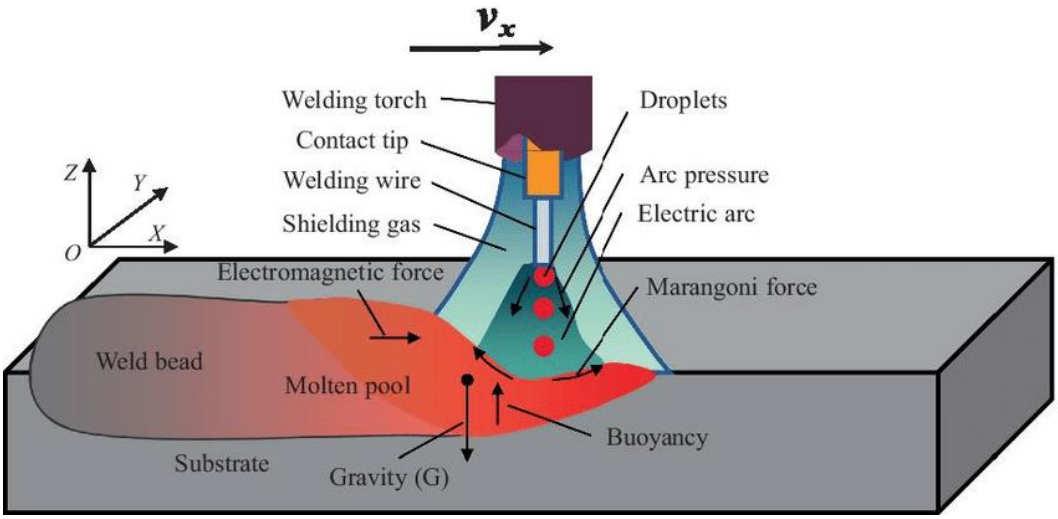

Figure 2-11: Forces acting on the droplet (Hu et al., 2021)

2.4 Weld Bead Characteristics

Welds are defined by their bead geometry, which includes:

- Weld bead penetration depth
- Bead reinforcement height
- Bead width, as shown in Figure 2-12

Furthermore, welded joints must possess specific mechanical properties, such as:

- Tensile strength
- Ductility
- Bending
- Toughness
- Resistance to aggressive environments (like acidic conditions for corrosion resistance)

According to AWS, "penetration refers to how far the fusion reaches into the base metal or previous weld pass from the melted surface during welding." This measurement is usually taken after each welding pass with a welding gauge, although other methods can also be used. The width of the weld bead reflects the amount of material deposited when joining base metals, while the height of bead reinforcement indicates the distance from the top of the deposited material to the surface of the welded joint (Khrais et al., 2023).

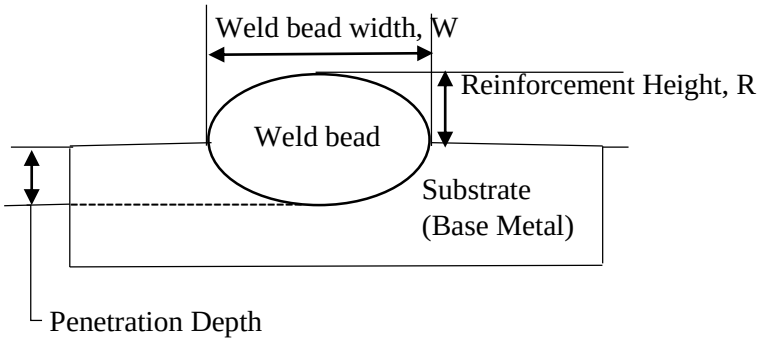

Figure 2-12: Bead Geometry (Zhang et al., 2021)

The goal of this study is to develop a composite material that exhibits enhanced properties such as tensile strength and corrosion resistance, along with applications in component repair. The process also addresses the dilution of the substrate into the weld, as depicted in Figure 2-14. Giarollo et al. (2022) state that "the bead geometries were measured using images of the cross sections of the beads." To achieve this, "the samples were cut (transversal to the weld bead) and metallographically prepared (sanded, polished, and chemically tested using dilute acid)." Their research measured "three dimensions in the weld bead geometry, including the bead width (l), reinforcement height (h), and weld penetration depth (p)," as illustrated in Figure 2-13.

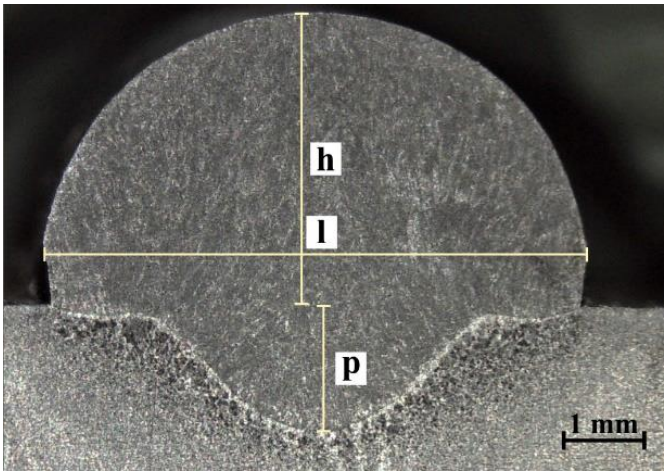

Figure 2-13: Clad bead geometry showing how dilution is calculated (Giarollo et al., 2022)

2.4.1 Weld Dilution

Weld dilution refers to the extent to which the substrate's composition blends with that of the filler wire during the welding process. In this study, it specifically pertains to how the melted

pool of A36 mild steel interacts with 316LSi stainless steel, with a minimal mix allowed to ensure the clad remains entirely stainless steel. Dilution in weld cladding can affect the mechanical properties and corrosion resistance of the overlay. Excessive dilution may result in a weld that fails to meet required specifications, impacting the overall performance of the welded joint. The clad consists of several sections: the substrate material layer, the weld interface zone (which determines dilution), the heat affected zone (HAZ), and the cladded layer (the filler wire layer in gas metal arc welding) (Souto et al., 2023).

The best dilution can be as low as less than 10%. For my study, it is the level at which the A36 mild steel melted pool mixes with the 316LSi stainless steel, and for this matter, a minimum mix is allowed such that the clad is purely stainless steel. According to Sayyid et al., 2017, "dilution is measured by D = 100 [$\frac{\text{Dilution Area A}}{\text{Dilution Area (A+B)}}$] = 100 [$\frac{A}{(A+B)}$] percent. A is the dilution area (Clad) between the filler metal and the clad area, and B is below the filler metal".

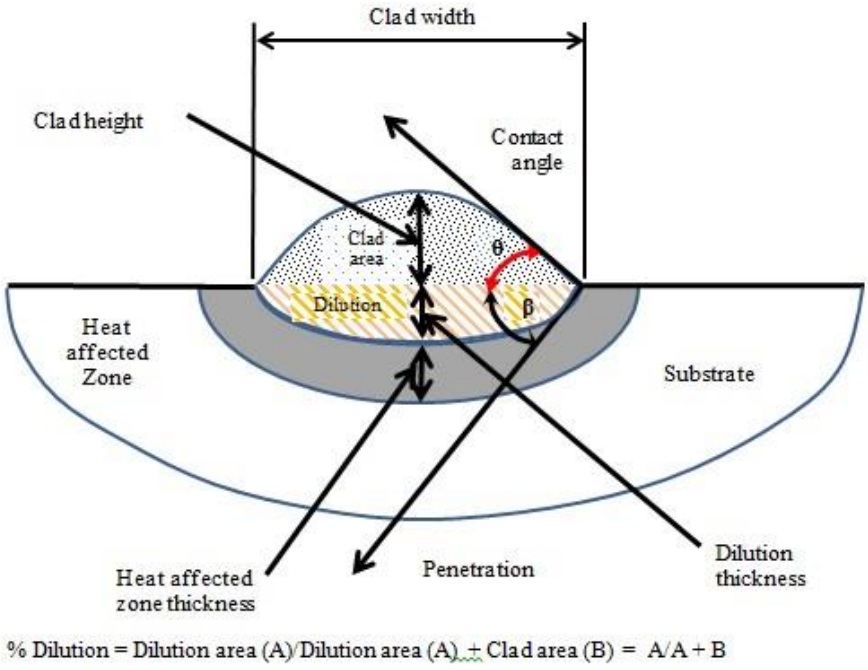

Figure 2-14: Weld Clad Geometry (Sayyid et al., 2017)

To simplify, Dr. Nuri et al. (2015) describe dilution using Equation 2-1: "Dilution, D % = (B/((B+A))) × 100% (approximately)... 2-1," where B represents penetration (depth of fusion) and A denotes reinforcement (thickness of the cladding). Dr. Nuri defines "dilution" as "the proportion of base metal present in the weld metal deposit," illustrated in Figure 2-15. He explains that a higher dilution percentage results in more base metal in the weld deposit, while

a lower percentage enhances surface properties due to less base metal in the weld. For cladding applications, a welding process that reduces dilution is preferred, as high heat input fuses the cladding and a significant part of the base material, forming a strong metallurgical bond. However, this fusion changes the cladding's composition, creating an alloy of the base metal and filler wire material.

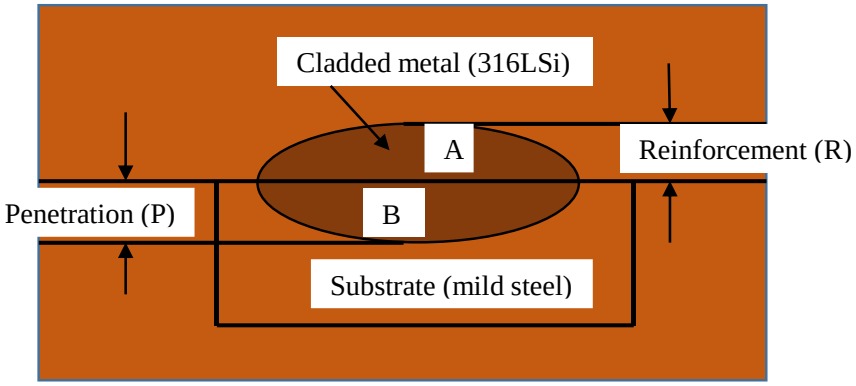

Figure 2-15: Schematic representation of the procedures adopted to calculate Dilution (Dr. Nuri et al., 2015)

The calculation of weld dilution involves dividing the penetration depth by the total of penetration depth and reinforcement height, a method commonly found in various research papers. This is the approach chosen by the researcher. To evaluate dilution in weld cladding based on penetration depth, several methodologies are utilized, mainly emphasizing mathematical modeling and machine learning techniques. These methods are essential for optimizing welding parameters to reduce dilution, which is vital for ensuring the quality of the weld (Zhang et al., 2021).

2.4.2 Response Surface Methodology (RSM)

RSM is a statistical and mathematical technique that models the connections between multiple explanatory variables and one or more response variables. It is used graphically to evaluate results and optimize input parameters, aiding in the reduction of dilution in processes like MIG welding (Vashisth et al., 2022).

2.5 Types of Weld Defects

A weld defect is a flaw that prevents the completed joint from bearing the applied forces or fails to meet the customer's aesthetic requirements. In Gas Metal Arc Welding (GMAW), defects can arise from inadequate joint design, excessively thin welds, high impurity levels in the base metal, or excessive amounts of specific alloys like boron in the filler metal. These issues can compromise the corrosion resistance of the weld, leading to premature pitting and crevice corrosion. Weld defects commonly include different types of cracks, such as crater cracks, hot cracks, and cold cracks. They also encompass cavities like blow holes, porosities, shrinkage, and pipes, in addition to issues like incomplete fusion and penetration (Hadzihafizovic, 2023).

2.5.1 Classification of Weld Defects

The American Society of Mechanical Engineers (ASME) identifies the causes of welding defects with the following distribution: 41% due to poor process conditions, 32% from operator error, 12% from incorrect techniques, 10% from unsuitable consumables, and 5% from faulty weld grooves. According to ASTM E-390 Vol-II, the allowed defects include shrinkage, cracks, lack of fusion, burn-through, and elongated porosity, while disallowed defects consist of incomplete penetration (up to level II), slag inclusion (up to level III), undercut (up to level IV), and porosity. Factors contributing to these defects may include poor welding design, incompatible materials, insufficient training, inadequate workmanship, incorrect welding patterns, and improper machine settings (like welding speed, current, voltage, shielding gas flow rate, and wire feed rate). Common welding defects are:

- Cracking, resulting from rapid cooling or improper techniques,
- Incomplete fusion, due to insufficient heat input or incorrect angles,
- Undercutting, caused by excessive welding speed or high current,
- Overlapping, from slow welding speed or excessive current,
- Slag inclusions, arising from inadequate slag removal or poor substrate cleaning.

The occurrence of welding defects can be minimized through effective prevention strategies and quality control measures. Reducing these defects enhances the reliability and safety of welded structures, improving their overall performance and lifespan. Welding defects are categorized into two types: external and internal.

External defects are visible to the naked eye or with a lens on the surface of the weld bead, base metal, or joint root. Examples include undercut, cracks, blow holes, surface porosity, excessive convexity, excessive concavity, incomplete root penetration, overlap, mismatch, uneven bead appearance, and spatters.

Internal defects are hidden within the weld bead or base metal and cannot be seen without special equipment. These include internal cracks, blowholes, porosity, slag inclusions, lack of fusion, lack of root penetration, and internal stresses.

Some defects, like cracks and blow holes, can be both external and internal (Hadzihafizovic, 2023; Ikpe et al., 2023) as seen from Figure 2-16 to Figure 2-20. Weld defects can appear as surface porosity, melted plate edges, excessive convexity (large welds or too much reinforcement), excessive concavity (insufficient throat thickness or fill), incomplete root penetration, excessive root penetration, overlap, mismatch, uneven bead appearance, and spatter. Internal defects consist of cracks, internal blowholes, porosity, slag inclusions, lack of fusion, insufficient root penetration, and internal stresses in restrained joints. Some defects, such as cracks and blowholes, can be classified as both external and internal. Common issues in welded joints include undercutting, porosity, and incomplete fusion. Undercutting is characterized by a groove along the weld toe, while wormholes are elongated cavities created by trapped gas during solidification, which can occur individually or in groups and may disrupt the weld surface. Figures 2-15 to 2-19 illustrate these defects.

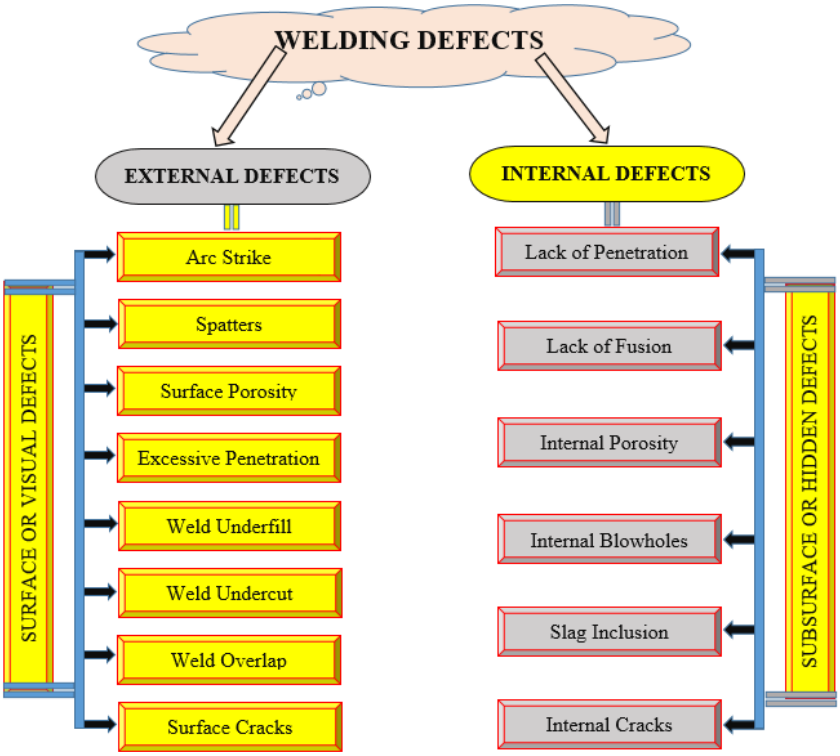

Figure 2-16: Types of weld defects (Ikpe et al., 2023)

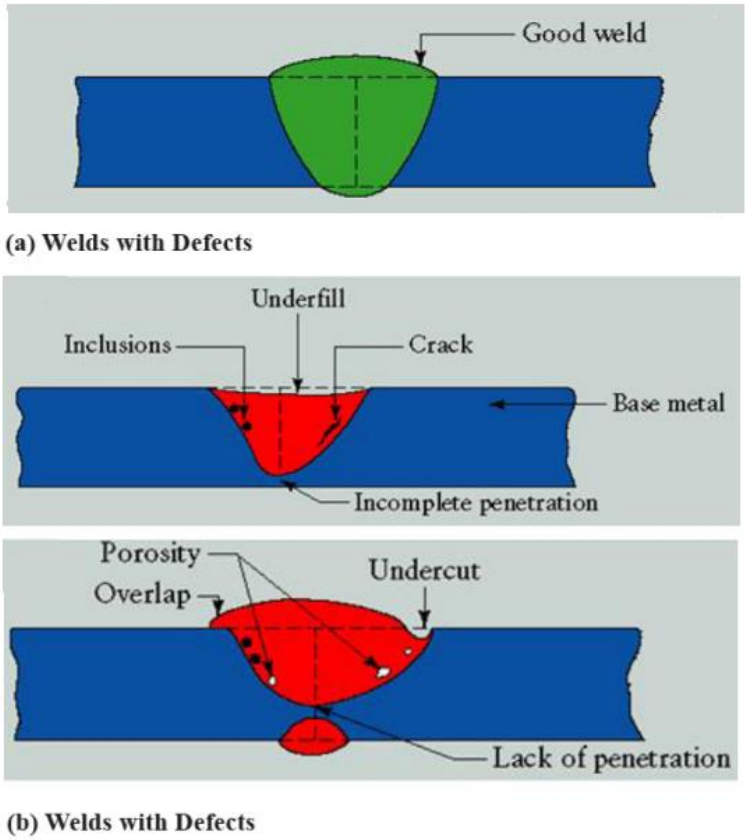

Figure 2-17: Nomenclature of the welding defects (Ikpe et al., 2023)

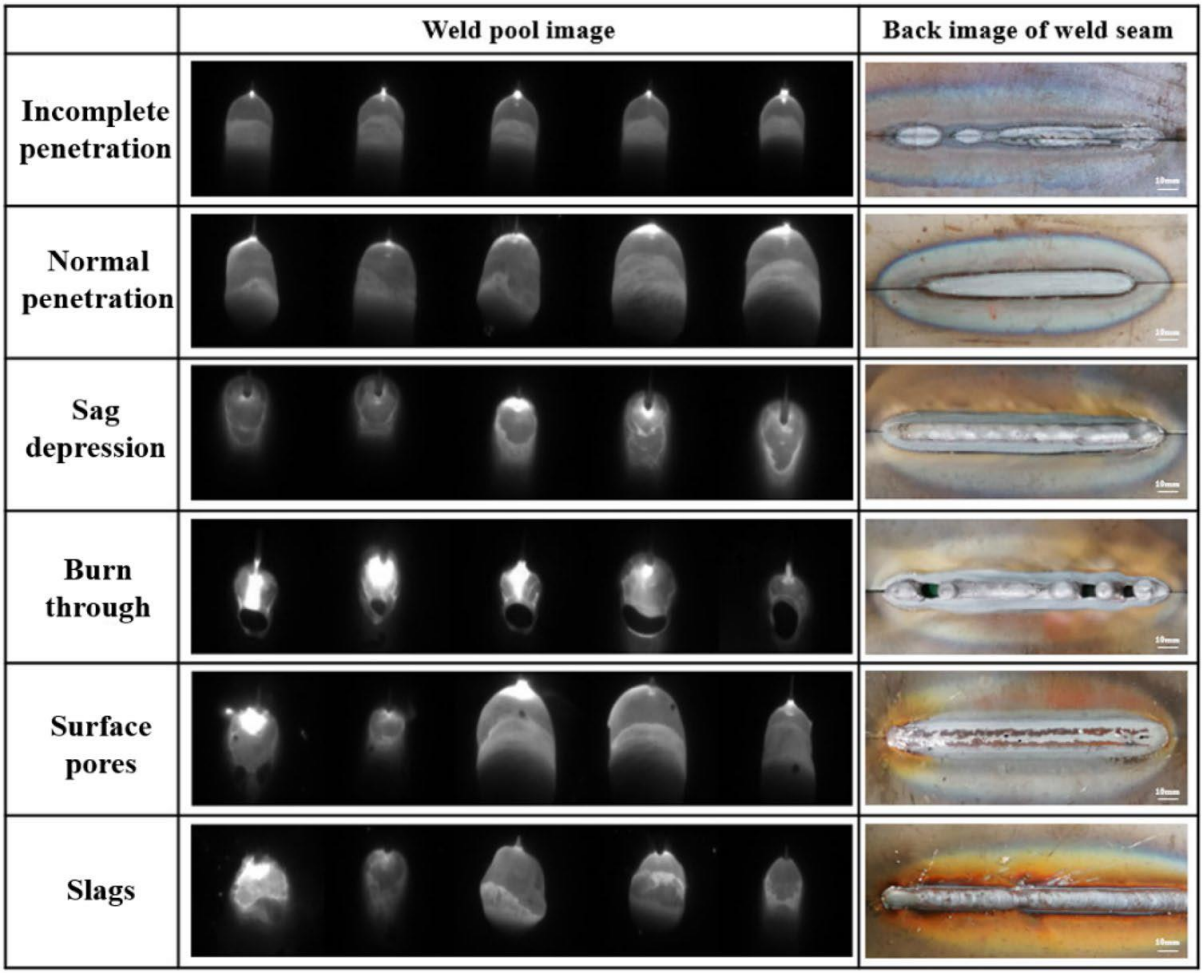

Figure 2-18: Chart of some of the welding defects (Li et al., 2023**)**

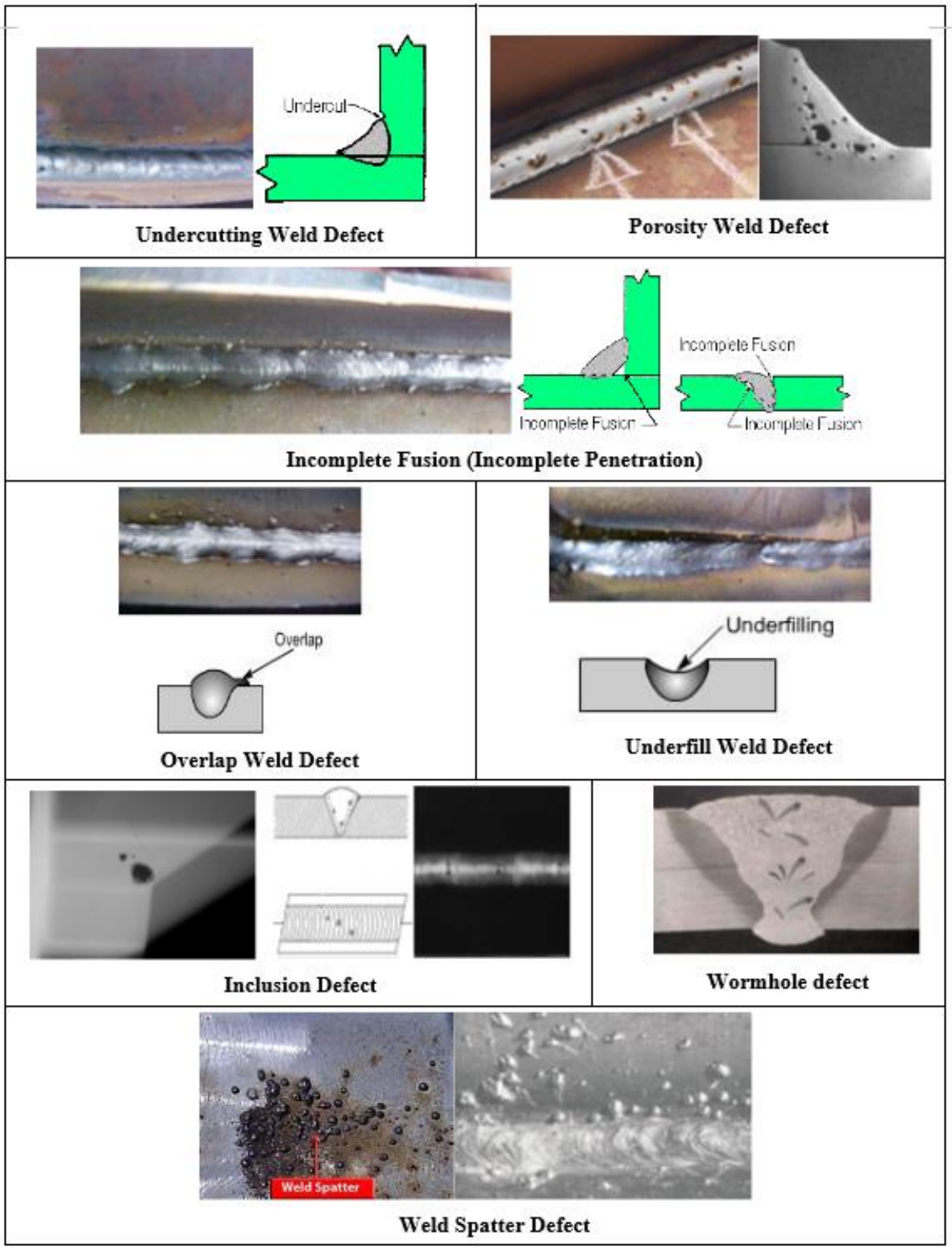

Figure 2-19: Pictorial Illustration of Weld Defects (Hadžihafizović, 2023)

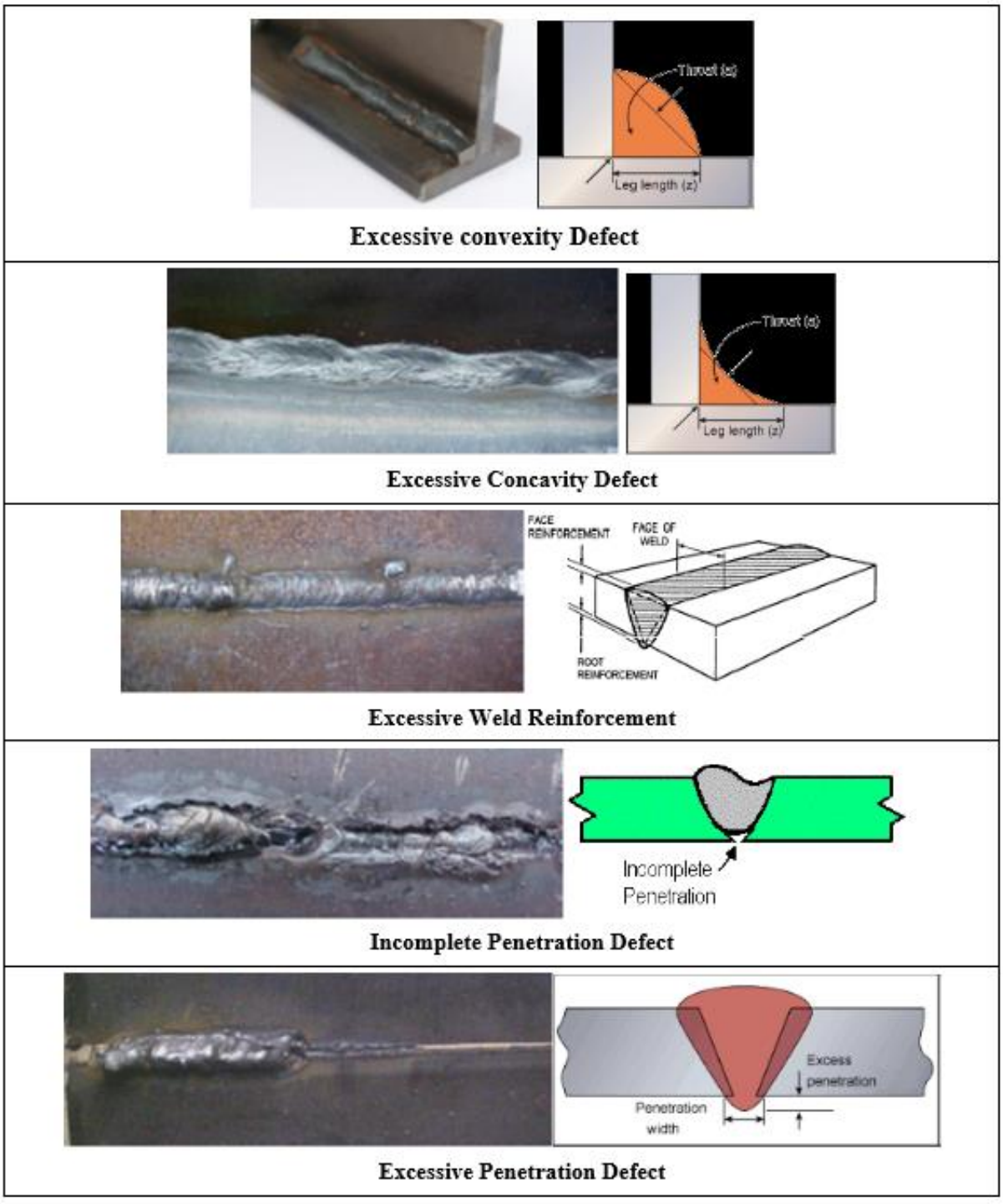

Figure 2-20: Pictorial Illustration of Weld Defects (Hadžihafizović, 2023)

2.6 Welding Parameters

Welding process parameters are crucial for achieving quality welds. The four key input parameters that can be adjusted significantly are welding current, wire electrode extension, welding voltage, and arc travel speed. For example:

(i) Welding Current: A higher current increases heat input, resulting in better fusion and deeper penetration. However, it also leads to a deeper clad layer with more dilution, while lower current results in a shallower clad layer with less dilution.

(ii) Welding Voltage: This affects arc stability and heat distribution. Higher voltages result in deeper penetration and wider beads, while lower voltages lead to shallower penetration and narrower beads. Insufficient voltage can cause excessive spatter, indicating instability. Insufficient voltage results in a great amount of spatter, i.e. process is unstable. The equipment-specific parameters are electrode type and size, arc current, polarity, preheat temperature, gas mixture, and flow/feed rate (Saha and Santanu, 2020, Roshan et al., 2023).

(iii) Wire Feed Rate: This controls the deposition rate of filler wire. A higher feed rate produces a thicker clad layer, whereas a lower feed rate results in a thinner layer. A higher feed rate leads to a thicker clad layer while a lower feed rate leads to a thinner clad layer (Gandhe et al., 2020).

(iv) Torch Angle: The angle between the torch and the workpiece should be optimal for uniform bead geometry; an incorrect angle can create uneven shapes.

(v) Shielding Gas: It protects the weld pool from contamination. Proper gas improves bead quality and corrosion resistance, while inadequate gas can lead to porosity and oxidation. Achieving the desired properties involves balancing these parameters (Saha and Santanu, 2020).

Balancing these parameters is essential for achieving desired welding properties

2.6.1 GMAW Wire Electrode

The most crucial aspect of the GMAW process is selecting the appropriate filler-wire electrode, as it influences other parameters like current, wire feed rate, and welding travel speed. The choice of electrode primarily depends on the metal composition being welded, taking into account factors such as process variation, joint design, material surface conditions, and the mechanical properties of the weld. These elements work together with the shielding gas, which affects the physical and mechanical characteristics of the final weld. There is a diverse range of electrodes that meet AWS (American Welding Society) standards. Key factors affecting the selection of filler wire for MIG welding include:

a) Chemical composition of the substrate
b) Mechanical properties of the substrate
c) Type of shielding gas used
d) Service type or specific requirements
e) Weld joint design (Ceweld Products, 2023).

2.6.2 Wire Electrode Extension

The wire extension, also known as stick-out, refers to the distance from the last point of electrical contact (typically the end of the contact tip) to the tip of the wire electrode, as illustrated in Figure 2-21. This region is where the heating effect (I^2R) takes place (Bose & Das, 2022).

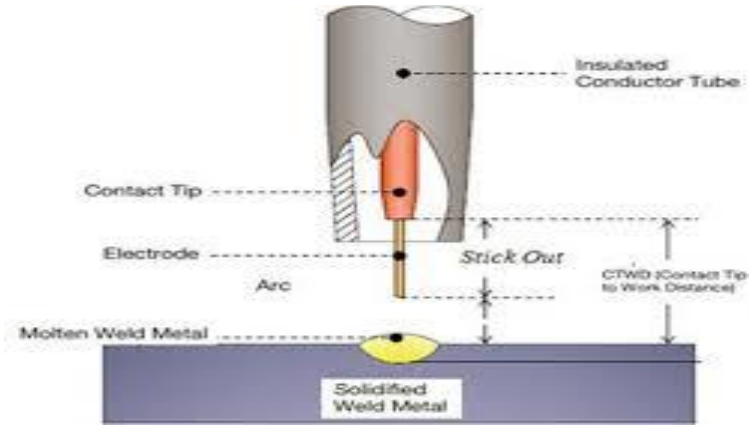

Figure 2-21: Electrode tip, Wire extension, and Arc Length (Punales & Alfaro, 2021)

Managing the electrode-to-work distance (ETWD) is crucial in GMAW. A shorter ETWD increases heat input, which can enhance the melting of both the filler material and the substrate, leading to better fusion and fewer defects. Maintaining the optimal ETWD is vital for a stable arc, which directly affects the bead shape and overall quality of the cladding. Consistent ETWD is necessary because a longer stick-out distance may cause the electrode to overheat and result in wasted shielding gas, as it escapes through the welding gun nozzle as shown in Figure 2-21.

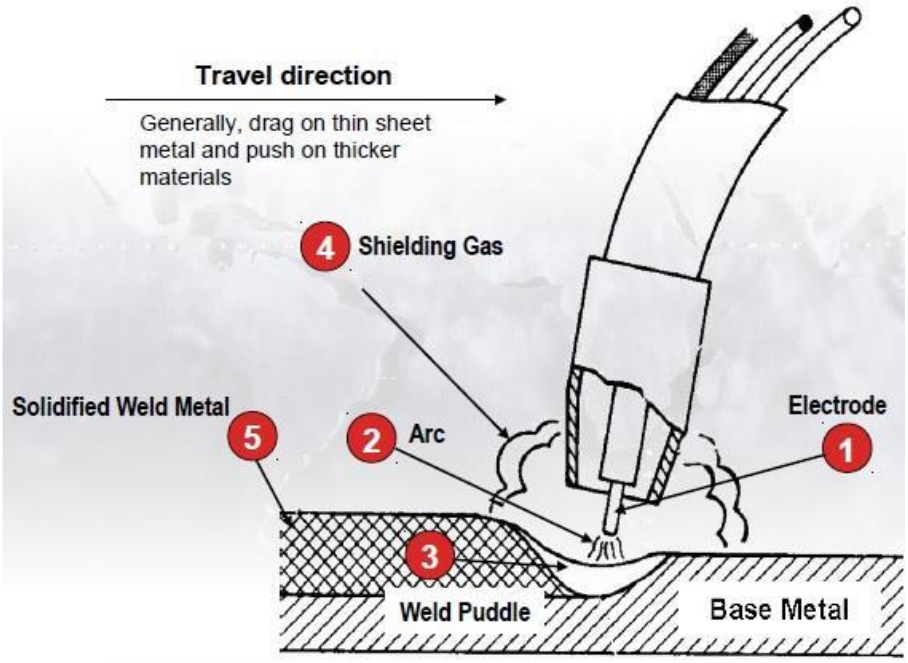

Figure 2-22: GMAW Shielding Gas Nozzle (Ahmed, 2022)

2.6.3 Arc Travel Speed

Arc travel speed refers to how quickly the arc moves across the workpiece. Key points to consider include:

(i) The travel speed should decrease as the thickness of the material increases.

(ii) For a specific material and joint design, increasing the welding current should lead to a higher arc travel speed.

(iii) The forehand welding technique allows for faster welding speeds. Maintaining a consistent contact tip-to-work distance (stick-out distance) is crucial, as a longer stick-out can cause the electrode to overheat and waste shielding gas (Sato et al., 2024).

2.6.4 Arc Voltage

Arc voltage plays a crucial role in determining the quality of a weld. It influences both heat input and penetration depth; while higher voltage can enhance penetration, it may also lead to increased spatter. The welding voltage primarily controls the arc length, which is the space between the molten pool and the wire filler metal melting in the arc. As the voltage increases, the weld bead tends to flatten and shows a larger width-to-depth ratio (Sato et al., 2024).

2.6.5 Welding current

The current affects both the melting rate and the shape of the weld bead. Maintaining proper control of the current is essential for stable arc performance. The welding current determines how deeply the weld penetrates into the base metal; higher current leads to greater penetration. Conversely, if the current is too low, it can result in inadequate fusion and a pointed bead profile (Pathak et al., 2020).

2.6.6 Wire feed rate (WFR)

The speed at which the filler wire is supplied impacts the shape of the weld bead, its penetration, and the rate of deposition. The wire feed rate (WFR) determines how much molten wire is deposited over a given length. When the feed rate is increased, it leads to smaller bead shapes due to a decrease in wire deposition. (Khrais et al., 2023).

2.6.7 Shielding gas

The type of shielding gas and its flow rate significantly affect arc stability, metal transfer, and the quality of the weld. Carbon dioxide typically creates a convex bead shape due to the arc and weld puddle's characteristics, offering adequate reinforcement but potentially causing overwelding. In contrast, argon blends produce a flatter bead face, which balances reinforcement and minimizes overwelding (Sato et al., 2024).

2.6.8 Stick-out (Arc length)

The arc length, or the distance from the electrode tip to the workpiece, also plays a crucial role in arc stability and bead shape. The distance between the electrode tip and the workpiece (arc length) influences both arc stability and bead geometry, as illustrated in Figure 2-13 (Surendra et al., 2019; Drosos & Kotsakis 2014). Changes in arc length are closely related to voltage, and adjusting it can significantly affect heat input and current. A shorter arc length increases heat input, causing the wire electrode to melt more quickly and maintain the original arc length.

2.6.9 Welding filler wire material

When cladding 316LSi stainless steel onto A36 mild steel using the gas metal arc welding (GMAW) process, several important factors must be taken into account:

- Shielding Gas Selection: It is crucial to choose the appropriate shielding gas for stainless steel welding. A mixture of argon with a small amount of oxygen or carbon dioxide is ideal as it enhances wetting and reduces excessive oxidation.
- Heat Input Control: To limit the dilution of the stainless-steel cladding into the mild steel base, the welder must manage the welding current, voltage, and wire feed speed to optimize heat input.
- Torch Angle: Proper torch angle is essential for controlling the geometry of the weld bead and the depth of penetration.
- Pre-heating: Pre-heating the A36 mild steel can help alleviate thermal stresses and enhance weld quality.

The main challenges include:

- Dilution: The melting point differences can cause dilution of the stainless-steel cladding into the mild steel, which may weaken the corrosion resistance of the cladding. Careful control of the welding process is necessary, and multi-pass overlays may be used to improve composition if needed. 316LSi stainless steel is advantageous for its corrosion resistance in harsh environments and its protection against rust and pitting.
- Differential Thermal Expansion: The differing thermal expansion rates of stainless steel and mild steel can create stresses and lead to cracking if not properly managed.
- Operator Skill: Skilled operators are vital for navigating the complexities of welding dissimilar metals and achieving the best results.

2.6.10 Process parameters for weld cladding

Weld cladding parameters are slightly similar to the above parameters like voltage, welding current, wire feed rate, welding speed, distance between nozzle and plate, electric angle, traverse speed, shielding gas type and composition, current pulsing, and others. According to Balasubramanian et al. (2023); Sild Siim, (2022), “the effects of parameters on cladding results are:

(i) Arc voltage

Impact: Arc voltage affects bead geometry and penetration. High voltage increases bead width and low voltage reduces bead width. The best is to optimize and find a balance for the desired bead shape as well as penetration.

(ii) Welding current

Higher currents lead to deeper penetration and wider bead width, and excessive heat can cause higher dilution, consequently affecting the microstructure of the weldment.

(iii) Welding wire feed rate (WFR)

WFR affects the deposition rate. Faster speeds increase dilution, while slower speeds allow better control over the bead shape.

(iv) Electrode diameter

Better selection of the size of the welding wire diameter is very vital".

There is a need to consult the welding standards (e.g., AWS D1.1, ISO 15614-1) for specific guidelines.

2.6.11 Practical applications

The practical applications of weld cladding are:

(i) Corrosion resistance: Proper parameter selection yields good corrosion resistance of the clad layer as long as the heat input can be controlled to an optimum level.

(ii) Microstructure characteristics: Optimal parameters lead to a fine-grained microstructure with minimal defects.

(iii) Weld bead geometry: Balancing parameters achieve the desired bead shape and width.

There is a need to consult the relevant welding standards (e.g., AWS D1.1, ISO 15614-1) for specific guidelines (de Lima et al., 2024).

2.7 Control Weld Quality Systems

Maintaining weld quality in GMAW cladding requires careful monitoring and control of various parameters, as illustrated in Figures 2-23 and 2-24. Weld bead geometry is managed through a passive vision system that uses sensors to track the width and height of the weld bead in real time, alongside an active vision system that emphasizes penetration control during the welding process. These systems are integrated into automation frameworks. If the welding process is intended to be fully automated, more sophisticated programming can simplify motion programming. Additionally, if the robot is equipped with auxiliary tools, their parameters must be programmed into the system with precision to optimize performance (Kah et al., 2014). The robotic programming modes include Online programming, Offline programming, and Adaptive control.

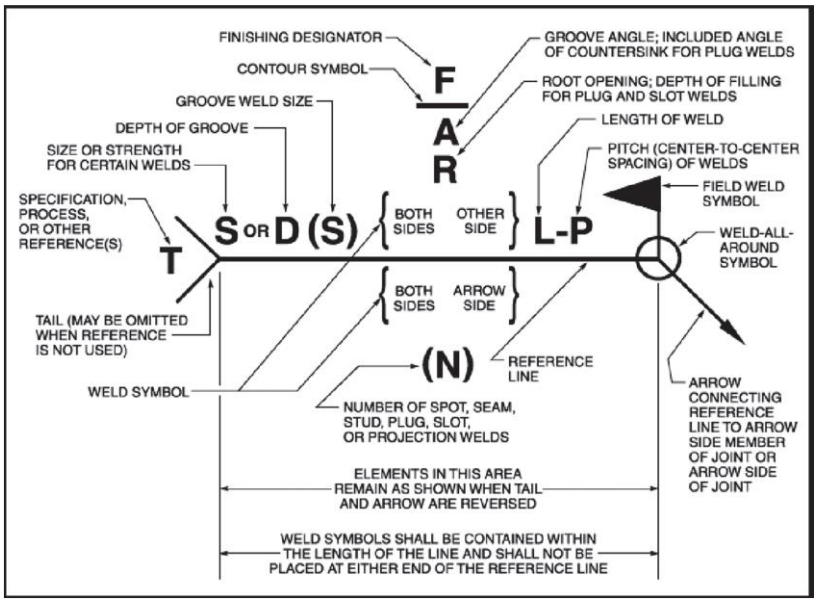

Figure 2-23: AWS Standard Locations of the Elements of a Welding Symbol (Hadzihafizovic, 2023)

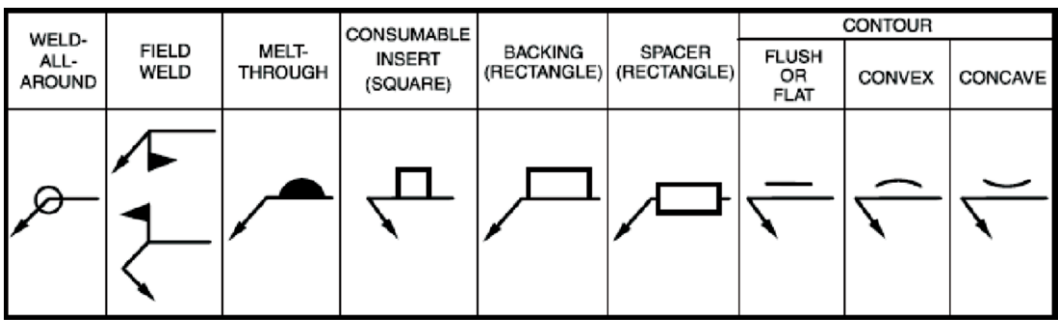

Figure 2-24: AWS Supplementary Symbols (Hadzihafizovic, 2023)

2.7.1 Online Weld Quality Systems

Maintaining weld quality in GMAW cladding requires careful monitoring and control of various parameters, as illustrated in Figures 2-23 and 2-24. Weld bead geometry is managed through a passive vision system that uses sensors to track the width and height of the weld bead in real time, alongside an active vision system that emphasizes penetration control during the welding process. These systems are integrated into automation frameworks. If the welding process is intended to be fully automated, more sophisticated programming can simplify motion programming. Additionally, if the robot is equipped with auxiliary tools, their parameters must be programmed into the system with precision to optimize performance (Kah et al., 2014). The robotic programming modes include Online programming, Offline programming, and Adaptive control (Hahn et al., 2023).

2.7.2 Offline Programming

Welding parameters such as wire feed, voltage, and current are modified via the power source and stored as a welding program for the robot to download, a process known as offline programming. This approach minimizes production downtime since adjustments to welding motions can be made without halting the robot station. It allows programming and welding to take place at separate times, thereby improving efficiency and productivity. Programmers can train and fine-tune robots for welding while keeping them in operation, a process referred to as automated offline programming (AOLP) (Liu et al., 2023).

2.7.3 Adaptive Control

This welding technology modifies the current in real time to enhance weld quality and maintain consistent processes. In automated welding, sensors monitor operational changes, activating actuators to manage the machines or devices. The controller settings are automatically adjusted to accommodate varying process conditions (Brush, 2018). An adaptive welding robot must effectively track and control the end effector's path and orientation to ensure precise joint alignment during welding. It should also manage welding process variables in real time, such as adjusting metal deposition according to the gap size between the components being welded (Biber et al., 2024).

2.8 Pipe Welding Positions, Codes and Standards

2.8.1 Pipe Welding Positions

The welding positions take the form of fillet F and G (F- fillet, G- butt) but in this study, we use G (welding positions for the pipework are those denoted by G). These positions include G1, G2, G5, G6, & G6R as shown in Figure 2-25 and Figure 2-26 (Kumar, 2024; Zheng, 2024).

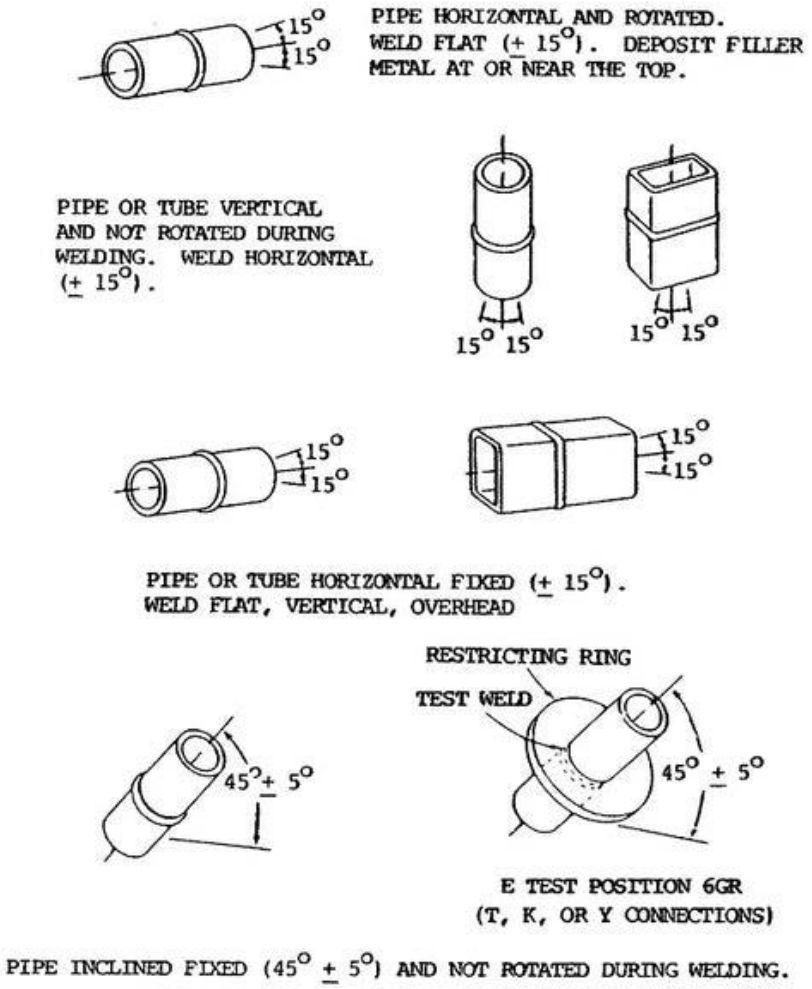

Figure 2-25: Welding position symbols for pipework (Zheng, 2024)

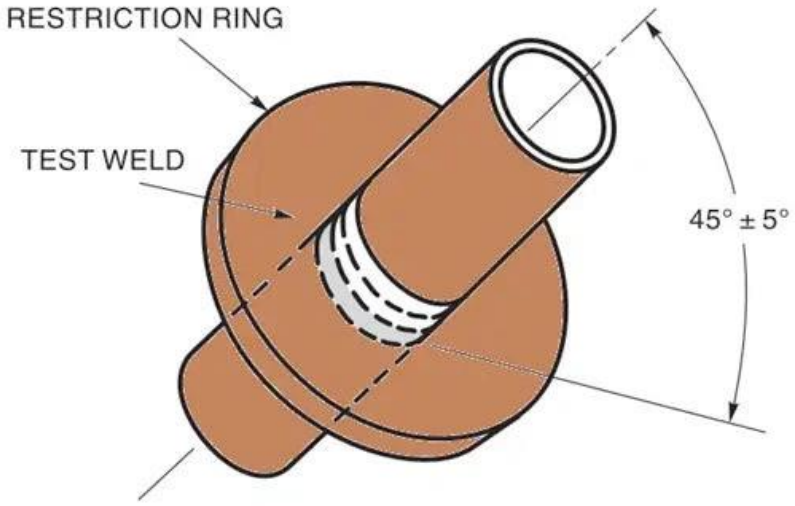

Figure 2-26: 6GR welding position for pipework (Zheng, 2024)

2.8.2 Welding Codes and Standards

Welding codes establish rules and regulations that define the minimum safety and quality levels for manufactured or fabricated materials. Standards are detailed documents that serve as long-term guidelines or definitions for various processes. Codes often reference these standards for specific details that go beyond the code's coverage. They are crucial in ensuring quality, safety, and consistency in weld cladding processes. Welding codes and standards provide essential guidelines, specifications, and procedures related to materials, fabrication, inspection, and testing. (Hadzihafizovic Dzevad, 2023).

2.8.2.1 American Welding Society (AWS).

The American Welding Society (AWS) is a prominent organization in the U.S. responsible for creating and publishing welding codes and standards. Their guidelines cover a range of welding techniques, including welding, brazing, soldering, and thermal spraying. Key standards include:

(i) AWS D1.1: Concentrates on structural welding.

(ii) AWS A2.4: Offers standard symbols for welding processes, brazing, and non-destructive testing.

(iii) AWS A3.0: Establishes standard terms and definitions related to welding.

(iv) AWS A5.1: Outlines requirements for carbon steel electrodes used in shielded metal arc welding (manual metal arc welding) (American Welding Society AWS (ANSI Z49.1), 2021).

2.8.2.2 American Society of Mechanical Engineers.

ASME codes mainly concentrate on welding procedures and the qualification of welders. These codes are extensively utilized in various industrial sectors, such as pressure vessels, boilers, and piping systems. Section IX specifically addresses the qualifications for welding and brazing. This standard outline the necessary requirements to ensure quality and precision in welding and brazing qualifications.

2.8.2.3 ISO Standards.

While not specific to the United States, ISO standards are internationally agreed upon by experts from specific nations where quality is a prerequisite to operations. ISO 18500 standards cover various aspects of welding, including terminology, procedures, and quality requirements. EN ISO 15614 addresses welding procedure qualifications and EN ISO 9606 covers the qualification of welders. ISO 6947:2019(E) is the standard that guides the pipe welding positions.

2.8.2.4 The American National Standards Institute (ANSI)

This focuses on the latest advancements in welding.

In summary, welding codes and standards ensure uniformity, quality, and safety across welding practices in whatever is done.

2.8.3 Welding Procedure Qualification (WPQ)

Standards such as ASME IX and EN ISO 15614 specify the requirements for qualifying welding procedures. They provide important welding parameters, including preheating, inter-pass temperature, and post-weld heat treatment (PWHT) for cladding processes. The Welding Procedure Qualification (WPQ) ensures that the cladding process remains both consistent and dependable.

2.8.4 Material selection and compatibility

Standards provide guidelines on selecting appropriate cladding materials based on the substrate and service conditions. They address issues related to dissimilar material welding, minimizing galvanic corrosion, and preventing intermetallic phases.

2.8.5 Quality Control and Inspection

Standards such as ASME IX and EN ISO 15614 specify the requirements for qualifying welding procedures. They provide important welding parameters, including preheating, inter-pass temperature, and post-weld heat treatment (PWHT) for cladding processes. The Welding Procedure Qualification (WPQ) ensures that the cladding process remains both consistent and dependable.

2.8.6 Documentation and Reporting.

Standards require detailed documentation of welding procedures including essential variables. The reporting formats for WPQ test results are standardized.

2.8.7 Environmental Considerations.

Some standards emphasize environmentally friendly practices, promoting energy-efficient welding processes and waste reduction. Adherence to these standards ensures safe and effective weld cladding practices in various industries (Hadzihafizovic Dzevad, 2023).

2.9 Common Deviations from Welding Standards that can Impact the Final Result

The common deviations from welding standards include:

(i) Chemical Compatibility: The cladding material's chemistry may not match the substrate, leading to reduced corrosion resistance or mechanical properties due to incorrect alloying or incompatible elements.

(ii) Heat input: The amount of heat applied during welding affects the microstructure of both the cladding and the heat-affected zone (HAZ). It is advisable to use low heat input methods, such as laser cladding, to reduce mixing in the HAZ and prevent the formation of undesirable phases that could compromise toughness and corrosion resistance.

(iii) Cracking: Welding can introduce cracking, such as solidification or hot cracks, which compromise integrity and corrosion resistance. Proper pre-heating, controlled cooling rates, and ensuring defect-free welds are essential for mitigation.

(iv) Surface Contaminants: Contaminants on the substrate surface can hinder bonding and affect corrosion resistance, so thorough cleaning and preparation are crucial.

(v) Quality Control: Inconsistent inspection practices can lead to undetected defects, compromising cladding quality. Adhering to rigorous inspection procedures and non-destructive testing (NDT) methods is vital for ensuring reliable and high-quality weld cladding (Sk Shrabon Nahidul Islam, 2024).

2.10 Strengths and Limitations of the GMAW Process

2.10.1 Strengths of the GMAW Process

Gas Shielded Metal Arc Welding (GMAW) offers numerous advantages over other welding methods, such as:

1) Versatility: GMAW can be applied to all types of metals and alloys, allowing for various deposition rates to efficiently create large and medium features on components.
2) Automation: The process can be fully automated, boosting productivity due to its straightforward equipment and easy management of tool paths with the consumable electrode.
3) Weld Position Flexibility: It can weld all commercial metals and alloys in any position.
4) Reduced Fumes: GMAW generates fewer fumes than FCAW or SMAW, resulting in a cleaner operation that requires less post-weld cleaning.
5) Operator Skill Requirement: It requires less skill from the operator compared to SMAW.
6) Continuous Electrode Feed: The continuous feeding of the electrode reduces defects since there is no need for restarts.
7) No Slag: GMAW does not create slag, which makes post-weld cleanup easier.
8) Good Weld Penetration: It offers excellent penetration, ensuring strong welds even in smaller sizes (Kumar et al., 2019).

2.10.2 Limitations of the GMAW Process

Gas Shielded Metal Arc Welding (GMAW) has several limitations:

- Control Challenges: Managing the welding current and wire feed speed (WFS) can be difficult.
- Titanium Welding Issues: GMAW is not suitable for titanium due to unstable arcs, which can result in poor weld quality from inconsistent droplet transfer.
- Spatter Production: Conventional short circuit transfer may produce spatter, regardless of the transfer method.
- Safety Risks: There are safety hazards if precautions are not followed; welders need to wear personal protective equipment (PPE) to guard against heat and flames.
- Equipment Complexity: The equipment is more complex and expensive than other welding methods and is heavier than SMAW equipment.
- Air Motion Sensitivity: It is ineffective in areas with strong air movement, as this can disrupt the shielding gas.
- Space Limitations: GMAW is less effective in confined spaces due to the design of the welding torch and the requirement for close gas shielding.
- Cleanliness Requirement: The base materials must be very clean and free of rust for effective welding.
- Lower Deposition Rates: GMAW has lower deposition rates compared to FCAW when welding in non-flat positions.
- Parameter Sensitivity: Precise adjustment of process parameters is crucial to avoid fusion defects, especially on thicker materials. (Kumar et al., 2019)

Summary of Factors Affecting Weld Bead Characteristics

Voltage: Higher voltage can lead to flatter, wider weld beads with reduced penetration. It also increases droplet size while decreasing their quantity, but may negatively impact bead height.

Wire Feed Rate: A higher feed rate results in more metal being deposited, which enhances both the width and height of the weld bead.

Wire Diameter: Increasing the diameter of the wire leads to a wider bead, as larger diameters produce bigger droplets during welding.

Overall, the experimental parameters like voltage, current, feed rate, and the type of stainless steel wire play a significant role in determining weld bead geometry, dilution, and corrosion resistance. Understanding these interactions is essential for optimizing welding processes.

Voltage and Current: Higher welding current enhances penetration and bead width, while also reducing dilution (J et al., 2023; Gowthaman et al., 2022).

Voltage adjustments can affect the heat input, affecting the overall bead geometry and dilution ratios (Yadav & Khanna, 2022; da Cruz Junior et al., 2024).

Feed Rate: An optimal wire feed rate is essential; lower travel speeds combined with higher feed rates yield better penetration and reduced dilution (Gowthaman et al., 2022).

The wire-feeding angle and distance from the substrate also play critical roles in droplet transfer and bead formation (Shin et al., 2023).

Stainless Steel Wire: The choice of stainless steel wire, such as ER 2209, affects the weld bead's characteristics, including its geometry and corrosion resistance (Abregeenst, 2023).

Studies indicate that specific wire types can enhance the mechanical properties of the weld, contributing to improved corrosion resistance (Yadav & Khanna, 2022).

CHAPTER THREE: METHODOLOGY

3.1 Experimental Design

This research approach involves creating a series of procedures to explore the connection between input variables and response parameters. The goal of the experimental design is to determine how individual or groups of independent variables influence the dependent variable(s). This was done in a controlled and objective environment to maximize precision; later conclusions were drawn. Based on the research data, 316LSi stainless steel is suitable for weld cladding A36 mild steel pipe substrates, offering improved mechanical and wear resistance properties. This project was executed with a specific objective (i) (to establish the GMAW process parameters that control the weld bead geometry in welding stainless steel onto a mild steel substrate). Pulsed spray gas metal arc welding is preferred in this study because it addresses issues like wider heat-affected zone (HAZ), coarse-grained weld-metal microstructure, and higher dilution encountered in other metal transfers to achieve objective number (ii) (to determine the GMAW process variables that influence the dilution in welding stainless steel onto a mild steel substrate). This is achieved by adjusting the welding current to achieve proper penetration and deposition; control of welding speed to ensure good weld bead geometry; and minimization of dilution. The wire feed rate is appropriately set for consistent deposition. Lastly, the filler wire recommended for use, 316LSi stainless steel, for weld cladding onto an A36 mild steel substrate to protect from corrosion in aggressive media and observe an achievement in objective number (iii) (to optimize the GMAW process variables for high-quality GMAW welding of stainless steel onto a mild steel substrate). There are three primary types of experimental design: pre-experimental research design, true-experimental design, and quasi-experimental design. The researcher opted for the true experimental design, which is regarded as one of the most precise research methods. This design employs statistical analysis to offer scientific evidence and determine cause-and-effect relationships. A true experimental design is essential for validating or refuting a researcher's hypothesis and is recognized for providing specific scientific evidence. Notably, only true experimental designs can establish cause-effect relationships within a group, making it a common choice in the physical sciences.

3.2. Experimentation

3.2.1 Description of Materials

The substrate is an A36 mild steel pipe (60.3 mm diameter, 5.0 mm thickness, and 1 m length). The cladding material is a 316LSi stainless steel wire electrode. The process parameters chosen by the researcher that were varied are arc voltage, welding current, and wire feed rate while maintaining other welding parameters. The focus was on achieving corrosion resistance (using 316LSi stainless steel over mild steel substrate), low dilution, good weld bead geometry, and favorable microstructural characteristics.

A cladding surface weld was made with an AISI 316LS stainless steel filler metal wire using the GMAW process over the A36 mild steel pipe substrate. The substrate measuring 60.3 mm in diameter, 5 mm thick, and 1 m long was used in the experiment. The 316LSi austenitic stainless steel wire offers excellent corrosion resistance, making it suitable for cladding applications. The workpiece was A36 mild steel; the substrate material provides a strong base for cladding.

Table 3-1: Composition of the substrate (base metal) as per ASTM A36 mild steel and the filler wire ER316LSi (wt. %)

Elements	C	Si	Mn	P	S	Ni	Cr	Al	Mo	Cu	V	Fe
Base metal (M.S)	0.26	0.4 max	1.02	0.04	0.05	0.4	0.043	0.027	0.15	0.2	0.08	98
Filler metal (S.S) ER316LSi	0.03	0.65-1.00	1.0-2.5	0.03 max	0.03 max	11-14	18 - 20	0	2.0-3.0	0.75 max	0	Bal.

UNS = Unified numbering system

Bal. = Balance

M.S = Mild Steel

S.S = Stainless Steel

Note that 1.0% maximum for the sum of Cu, Ni, Cr, Mo, and V. Increase of Mn allowed above maximum up to 1.35% at a rate of 0.06% per 0.01% C reduction.

Quality control and inspection

Quality control and inspection of weld cladding can be ensured by monitoring parameters like dilution, penetration depth, and reinforcement depth. Visual inspection and non-destructive testing (NDT) methods like ultrasonic testing and radiographic testing are commonly used for quality assurance in weld cladding processes. The test was done using an optical microscope.

Standards and Practical Implications

The researcher referred to international fabrication standards for guidance on welding procedures and quality control. There was consideration of the implications of heat input, energy efficiency, and waveform control. Additionally, the practical implications included cost-effectiveness, productivity, and overall performance. All tests followed AWS D1.1 (2020) Section 8.1.4.2.

3.2.2 Workpiece Preparation

The mild steel substrate was thoroughly cleaned to remove contaminants. The researcher ensured proper fit-up and alignment between the stainless-steel wire and the substrate. The welding table and the workpiece were cleaned to remove impurities and coatings from the surfaces; without tampering with the material. The cleaning of the table and the workpiece is key to the production of quality products, maintaining consistent productivity levels, and minimizing costs; especially post-weld cleaning, reworks, and downtime. Cleaning was done to avoid contaminants that might cause unstable arcs that could lead to welding defects like porosity, spatters, inclusions, and poisonous gasses during welding. The impurities include rust, paint, grease, oils and other types of dirt or mill scale create resistance and sometimes weld splash that cause danger to the welder and/or the environment. The welding table was well-cleaned before fixing the workpiece. The workpiece was then clamped in the vice on the welding table to prepare it for cleaning. Fixtures were used to clamp the workpiece in protection against mechanical damage. The cleaning tools that were prepared for the cleaning process include among others; files, reamers, sandpapers of different sizes, and very clean cotton wool. After the cleaning process, the experimentation was kicked off immediately to ascertain the material couldn’t get dirty again due to environmental changes. Lead, zinc, or lead or zinc compounds were avoided while welding due to the potential for hot cracking. Cutting tools such as grinding disks, saw blades, and files that were used on

carbon steels were not reused for stainless steels. Grinding was performed using an iron-free abrasive wheel. The surfaces intended for weld metal deposition, including adjacent areas, were thoroughly cleaned to eliminate organic contaminants and surface oxides. All surfaces were free from defects like fins, tears, laminations, and cracks that could compromise weld quality. Any unacceptable surface defects were removed through machining, ensuring that the remaining thickness met material specifications and that the surface was uniformly filled after defect removal. Relevant nondestructive testing (NDT) methods were specified in the literature and were fully implemented.

3.2.3 Experimental Setup

The experiment was done both manually and in semiautomatic welding. The human hand (manual welding) handled the welding torch. The filler wire and shielding gas were provided automatically from the filler wire feeder via the welding gun (Semi-automatic welding). The workpiece was clamped using fixtures onto the welding table and the weld was performed by moving (while waving) the welding torch while the specimen kept stationary. The nine experimental runs carried out were planned using the Taguchi design of experiment (DoE) on a W069 MAG inverter-based arc welding power source (MASTERMIG 400-TELWIN) shown in Figure 3-1. The equipment and materials used to conduct the experiments are:

(i) A direct current gas metal arc welding machine W069 MAG inverter-based gas metal arc welding power source (MASTERMIG 400 - TELWIN),
(ii) Wire feeder,
(iii) Filler material stainless steel welding wire; diameter of 1.2 mm (ER316LSi),
(iv) Gas cylinder with 100% Carbon dioxide,
(v) Mild steel pipe substrate (ASTM grade A36).

Figure 3-1: The equipment used for the nine experimental runs

The experimental setup (Figure 3-2) included a MIG/MAG (Metal Inert Gas/Metal Active Gas) welding machine that provided adjustable power settings for voltage and current. It also powered an automatic wire feeder that delivered the welding filler wire. The wire feeder had rollers that guided the wire to the gun connector, where the welding wire was energized. The wire then traveled through the welding conduit to the welding gun. When the gun was activated, the wire extended from the gun and contacted the workpiece. The substrate, a mild steel pipe, was connected to the neutral terminal, allowing the energized wire to complete the circuit, causing it to melt and fuse at the contact point (weld pool). The presence of air led to oxide formation, resulting in spatter and surface blemishes. To mitigate this, an inert gas or active carbon dioxide gas was introduced from a gas cylinder through a hose to the welding gun, protecting the weld from atmospheric air and preventing oxide and spatter formation.

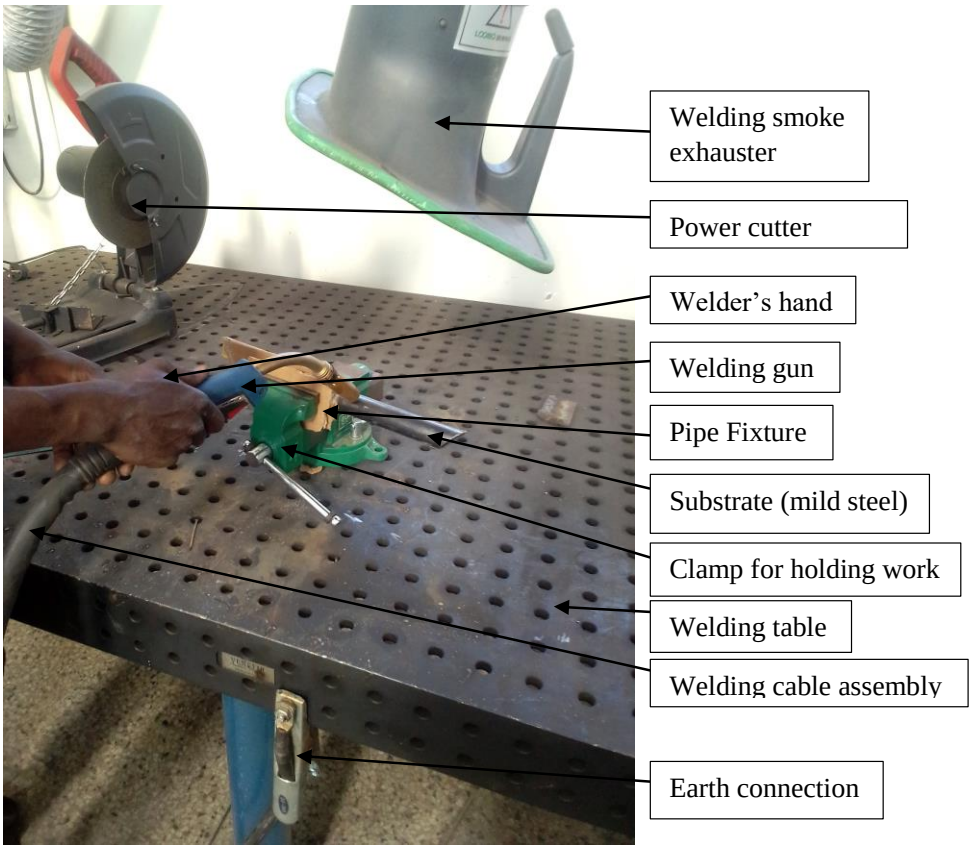

Figure 3-2: Experimental setup

3.2.4 Experimental Design

The researcher chose gas metal arc welding (GMAW) for the weld cladding process because of its benefits compared to other welding techniques. What are the advantages of GMAW?

(i) High-quality welds with good appearance and low spatter

(ii) Better control over the welding process with less clean up required

(iii) Higher welding speeds and efficiency

(iv) Good for welding thin materials

(v) Easiest type of welding to learn

(vi) Process is more forgiving for the robot

(vii) GMAW applications are more forgiving

The disadvantages of GMAW are:

(a) Requires a shielding gas, adding to the cost

(b) More complex equipment setup

The Taguchi method aims to reduce process variation through effective experimental design, with the primary objective of producing high-quality products at lower manufacturing costs. Gas metal arc welding (GMAW) is selected for cladding 316LSi stainless steel onto an A36 mild steel pipe due to its enhanced corrosion resistance and mechanical properties. Below are the advantages of using GMAW for this purpose.

Enhanced Corrosion Resistance

AISI 316L stainless steel exhibits superior corrosion resistance compared to mild steel, making it ideal for applications in corrosive environments. Additionally, the cladding process effectively protects the underlying mild steel from corrosion, extending the lifespan of the substrate.

Improved Mechanical Properties

The pulsed current GMAW (PC-GMAW) technique results in finer microstructures and reduced dilution, leading to increased hardness and wear resistance of the cladded layer. Besides, studies show that PC-GMAW cladding can achieve a 15.83% increase in hardness and a 20.18% reduction in wear rate compared to the mild steel substrate.

Microstructural Benefits

The GMAW process allows for better control over the heat-affected zone (HAZ), minimizing coarse grain formation and enhancing the overall microstructural integrity of the cladded layer. This is done by adjusting the travel speed, use of heat treatments (preheating and post-heating), and use of a low-carbon filler metal. While GMAW offers significant advantages, it is essential to

consider potential challenges, such as the initial cost of stainless steel and the need for skilled operators to ensure optimal cladding quality.

The Taguchi Design of Experiments (DOE) plays a vital role in optimizing the gas metal arc welding (GMAW) process for cladding 316L stainless steel onto A36 mild steel, aiming to improve corrosion resistance. This method systematically evaluates the influence of various parameters, ensuring optimal performance and quality of the cladding process.

Enhanced Corrosion Resistance

Material Properties: 316L stainless steel is known for its excellent corrosion resistance, which is further enhanced when cladded over mild steel, providing a protective layer against environmental degradation.

Microstructural Integrity: The laser cladding process results in a refined microstructure, promoting better bonding and reducing defects, which are critical for corrosion resistance.

Process Optimization

Parameter Influence: The Taguchi method allows for the systematic variation of laser power, speed, and powder flux, which significantly affects dilution and microstructural features, ultimately influencing corrosion resistance.

Layer Configuration: Studies indicate that single-layer cladding exhibits superior corrosion resistance compared to multi-layer configurations, which can introduce vulnerabilities due to increased hardness and reduced ductility.

In contrast, while Taguchi DOE optimizes cladding parameters, it is essential to consider that variations in environmental conditions and substrate preparation can also significantly impact the overall corrosion performance of the cladded materials.

To clearly state: “The methodology for welding stainless steel cladding onto mild steel pipe substrates using the GMAW process is based on philosophical principles that focus on material

enhancement and process optimization. This strategy highlights the use of advanced welding techniques to enhance the mechanical and corrosion-resistant properties of mild steel".

The methodology for welding cladding stainless steel onto mild steel pipes using the GMAW process is based on enhancing materials and optimizing processes. This method focuses on using advanced welding techniques to improve the mechanical and corrosion-resistant properties of mild steel. Key adjustments include:

(i) Arc Voltage: Modified to ensure proper penetration and bead width.
(ii) Welding Current: Optimized for stable metal transfer and reduced spatter.
(iii) Wire Feed Speed: Controlled to achieve the desired deposition rate.
(iv) Travel Speed: Managed for uniform cladding.
(v) Shielding Gas: Selected to protect the weld pool.

In this study, a 316LSi stainless steel layer was deposited on mild steel, with parameters like welding current and wire feed rate affecting bead width and penetration depth. Arc voltage was also optimized for bead reinforcement height. The experimental design, detailed in Table 3-2, utilized the Taguchi method to manipulate independent variables. The choice of GMAW and Taguchi methods was based on their effectiveness in optimizing complex welding processes while minimizing costs and time, providing systematic approaches to enhance welding quality and performance.

GMAW Advantages

GMAW is favored for its versatility and efficiency in various welding applications, allowing for high-speed operations and adaptability to different materials.

The process is less prone to defects, which is crucial in industries requiring high-quality welds, such as the aerospace and automotive sectors.

Taguchi Method Benefits

The Taguchi method employs orthogonal arrays to systematically analyze the impact of multiple parameters on welding performance, leading to robust designs that minimize variability.

Additionally, it was applied in various welding processes, demonstrating its effectiveness in optimizing settings for improved quality.

Design of Experiments (DOE)

DOE facilitates the exploration of interactions between variables, allowing for a comprehensive understanding of the welding process and enabling the identification of optimal conditions efficiently. This method reduces the number of experiments needed, saving time and resources while ensuring reliable results.

While GMAW, Taguchi, and DOE are powerful tools, some may argue that simpler methods could suffice for less complex welding tasks. However, the integration of these advanced techniques is essential for achieving high precision and quality in demanding applications.

Table 3-2: Experimental Design (L9 Orthogonal array of the 9 experimental runs)

Experiment No.	Current (A)	Voltage (V)	Filler Wire Feed Speed (m/min)
1	150	24	3.0
2	150	26	3.5
3	150	28	4.0
4	160	24	3.5
5	160	26	4.0
6	160	28	3.0
7	170	24	4.0
8	170	26	3.0
9	170	28	3.5

Table 3-3: Fixed parameters (Variables that remained unchanged)

Nozzle to work distance, D (mm)	Shielding gas, Ar/CO_2 (%)	Gas flow rate, $\dot{Q}$ (Liter/min)	Filler metal diameter, d (mm)	Welding travel speed, S (mm/min)	Electrode angle, θ (^{o})	Arc length, L_a (mm)
12	75/25	16	1.2	27	45±5	2.54

3.2.5 Experimental Procedure

The primary goal of weld cladding is to apply a protective or functional layer onto a substrate. The process begins with cleaning the surface and selecting the cladding material, which in this case is 316LSi stainless steel. Next, the substrate is positioned and secured, followed by the adjustment of welding parameters such as current, voltage, and wire feed rate. The experiment is executed using the GMAW process to melt the cladding material onto the substrate, ensuring control over heat input and fusion. After cooling, metallurgical bonding is achieved.

Post-processing involves inspecting for defects like cracks and porosity, assessing properties such as corrosion resistance and microstructural characteristics, and performing necessary finishing tasks like grinding or machining. Quality assurance is conducted to ensure proper bonding and minimal dilution while confirming the desired properties are met.

During the welding, a mild steel pipe with a diameter of 60.3 mm and a thickness of 5 mm was horizontally mounted using pipe fixtures. Cladding welds were performed with consistent parameters, including an open arc voltage of 28V and a torch angle of 15 degrees to the specimen's perpendicular line. A 1.2 mm diameter ER316LSi filler wire was utilized, with a gas flow rate of 16 liters/min and a contact tip-to-work distance of 12 mm. Maintaining low dilution is crucial for preserving the cladding material's properties, such as corrosion resistance and mechanical strength. Good weld bead geometry is vital for structural integrity and aesthetics, and proper control of welding parameters ensures uniform and strong weld beads. The experimental runs were carried out as planned, with measurements taken as scheduled, followed by result analysis.

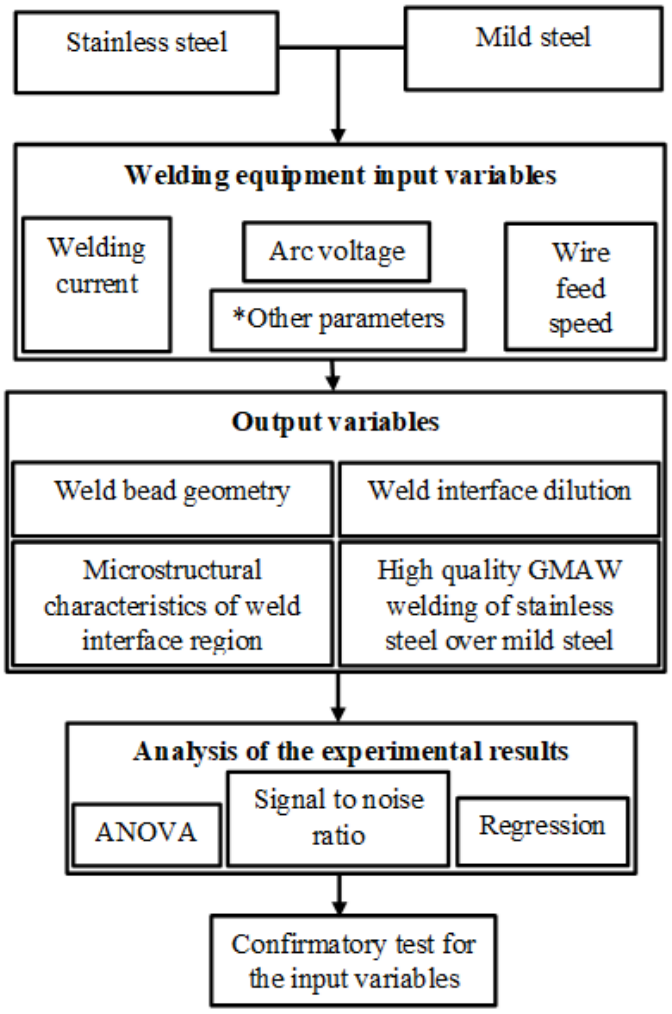

Figure 3-3: Architectural layout of the experiments

3.3 Weld Quality Analysis

The weld claddings are inspected to establish defects (e.g., lack of fusion, porosity, undercut). The cladding thickness was measured to verify adherence to specifications; additionally, destructive testing was done to establish the clad profile. After the welding process was completed, a visual examination using unaided eyes was done to check the weld integrity. The defects identified beyond control limits included low-clad and nonlinear bead profiles. The defects indicated that the weld cladding process was not essential. This resulted in repeating the experimental runs to correct the anomalies. The factors for the defects were eliminated towards the end of the experiments. Then the specific weld quality analyses were done. They included weld bead measurement, dilution of the weld at the interface zone weld interface microstructure analysis, and pitting

corrosion test. Subsequently, the obtained weld quality results were optimized using the Taguchi signal-to-noise (S/N) ratio, regression, and ANOVA by using the design expert software. The independent parameters will be optimized individually as well as in combinations using the Taguchi method and ANOVA (Analysis of Variance). The microstructural analysis was done using an optical microscope to check for any defects in the weld and the weld bead thickness was measured using a digital vernier caliper. The confirmatory tests using the optimal parameters were performed to verify the best GMAW process parameters in the current study.

3.3.1 Measurement of Weld Bead Characteristics

Weld bead measurements were conducted using the TWI Welding Gauge (Cambridge UK). This gauge measures bead width (W), reinforcement height (R), and penetration depth (P). The dilution of the weld bead (D) was calculated using equation 3-1. The standard height for both single and overlap weld bead samples should not exceed 3.2mm. The gauge also assesses preparation angles (0 to 60º), excess weld metal, undercut depth, pitting depth, fillet weld throat size, leg length, misalignment, and linear measurements up to 60mm. Weld bead geometry is defined by width (W), reinforcement height (R), and penetration depth (P). To measure bead height, the gauge was placed on the substrate surface, with a pointer indicating the top of the weld bead. For penetration depth, destructive testing was employed, cutting the weldment to access the cross-section for measurement. All samples adhered to the American Welding Society (AWS D1.1 – 2020) inspection criteria, ensuring no incomplete penetration, cracks, or fusion issues, and that undercut did not exceed 10% of the substrate thickness.

$$D = \left(\frac{P}{P+R}\right) \quad \text{3-1}$$

Where: D = Dilution,
P = Penetration, and,
R = Reinforcement.

The use of the TWI welding gauge is to measure the experimental results for the weld bead geometry (Bead Width, W, Penetration depth, P, and Reinforcement height, R) as the experiment is under progress.

3.3.2 Microstructure Analysis

The substrate, ASTM A36 Grade B - mild steel pipe and clad weld-stainless steel (ER316LSi), were checked at two levels. The examination of material graphic sections of welded joints is commonly carried out at two levels of inspection, i.e. macro-level examination using the naked eye and micro-level examination using an optical microscope, Figure 3-7. For micro examination techniques and hardness traverse, the provision of a polished, optically flat surface is required.

Using an optical microscope for the microstructural characteristics of the interface zone. A polished, optically flat surface is prepared for optical microscopy through the following process:

(i) Cutting the specimen of the desired size from a suitable location on the welded product,

(ii) Grinding the sample to a flat surface,

(iii) Polishing the sample to a mirror-like finish,

(iv) Etching to reveal the microstructure, and,

(v) After polishing and etching, the specimen is examined under the metallurgical optical microscope (Figure 3-7).

The microstructural features of the weld examined include the voids, special phases, segregation, HAZ, and base structure

3.3.3 Pitting Corrosion Loss Test

The pitting corrosion test is a localized form of corrosion that can have serious implications for metal structures. It first appears as tiny holes or cavities that are invisible to the human eye. However, it can rapidly progress both horizontally and vertically below the substrate's surface. Pitting corrosion can be severe, leading to structural failures and even catastrophic collapses. The testing and evaluating pitting corrosion include the ASTM G48 Test, density of pits, and pitting factor. The pitting factor was used and is given by Equation 3-2. To prevent pitting corrosion, consider proper surface cleaning and removal of contaminants from the substrate surface, optimizing welding parameters, filler wire, and shielding gas. Pitting corrosion is influenced by chloride ions that can break the passive oxide film on metal surfaces, leading to localized attack,

temperature and PH, and material properties (for example austenitic stainless steels e.g., 316LSi exhibit better resistance due to their chromium content; surface condition like roughness, inclusions and defects; mechanical stress; welding parameters; fluid velocity; and galvanic effects. The pitting corrosion rate was calculated using the equation 3-2.

$$COR = \frac{W}{D.A.T} \quad \text{..... 3-2}$$

Where:

COR = corrosion rate in millimeters per year

W = metal weight loss in milligrams

D = metal density in grams per cubic millimeter

A = area of the sample in square millimeters

T = total time in years.

CHAPTER FOUR: RESULTS AND DISCUSSION

4.1 Results

4.1.1 Output Process Parameters Weld Bead Geometry

The weld bead geometry was assessed using a TWI Welding Gauge and documented in Table 4-1. The width of the bead increased due to the weaving of the welding torch, which helps control the weld pool, regulate heat input, and ensure proper fusion and penetration. Torch weaving is crucial for maintaining the necessary heat input; it slows down the travel speed, thus enhancing heat input at specific points on the substrate. This technique also improves the penetration depth of the weld bead and the overall quality of the weld joint. Compliance with various welding standards, such as AWS D10.11, AWS D10.12, and AWS D10.18, is essential. Additionally, standards like API RP 577 and AS/NZS 1554.6 provide guidelines for welding practices. According to ASME sect. 1, PW-40.3.4(d) and AWS-D1.1, the maximum weld bead width for any electrode should not exceed four times the electrode core diameter.

Table 4-1: Measured Weld Bead Geometry (Weave Width, W1, Bead Width, W, Penetration depth, P, and Reinforcement, R)

Exp. No.	Independent Parameters			Dependent Parameters (Bead Geometry)			
	Arc Voltage, V (V)	Welding Current, I (A)	Wire Feed Speed, S (m/min)	Weave Width (W1) [2d.p] (mm)	Bead Width (W = 1/3W1) [2d.p]	Penetration Depth (P) [2d.p] (mm)	Reinforcement (R) [2d.p] (mm)
1	24	150	3.0	10.90	3.63	0.25	1.75
2	24	160	3.5	11.42	3.81	0.20	1.91
3	24	170	4.0	10.21	3.40	0.66	2.09
4	26	150	3.5	14.33	4.78	0.18	2.57
5	26	160	4.0	13.16	4.39	0.22	2.28
6	26	170	3.0	15.66	5.22	0.23	2.48
7	28	150	4.0	14.21	4.74	0.21	1.84
8	28	160	3.0	16.33	5.44	0.19	2.66
9	28	170	3.5	17.77	5.92	0.22	2.24

4.1.2 Cladding Thickness

The weldment workpieces were tested for weld quality by measuring the thickness of the weld bead using a digital vernier calliper to check for the evenness of the weld surface, Table 4-1. Cladding thickness affects the dilution in overlay welding processes. Increasing cladding thickness can lead to changes in the dilution levels of the barrier layer. The relationship between cladding thickness and dilution ratio is crucial for ensuring the quality of the overlays. Dilution was tested and from Table 4-1, the optimized parameters are

Arc Voltage	**Welding Current**	**Wire Feed Rate**
28V	160A	3.0mm/min

The following specifications, codes, and standards are utilized:

1. AWS D10.11: Guidelines for root pass welding in pipes.
2. AWS D10.12: Standards for welding mild steel pipes.
3. AWS D10.13: Specifications for brazing copper tubes.
4. AWS D10.18: Standards for welding stainless steel pipes.
5. BS 4515-2: Specification for welding steel pipelines both on land and offshore, including duplex stainless steel pipelines.
6. ISO 13847: Standards for welding pipelines in the petroleum and natural gas industries.

Testing for the Cladded Layer Thickness

The nine specimens were tested for the cladded layer thickness to check if the cladding was done well. Therefore, five different positions were selected and the results are shown in table 4-2 and measurement was done using a digital Vernier Calliper.

Table 4-2: Effects of Parameters on Cladding Thickness, T = (P + R)

Test Runs (Parameter Variation)	Position 1 Thickness (mm)	Position 2 Thickness (mm)	Position 3 Thickness (mm)	Position 4 Thickness (mm)	Position 5 Thickness (mm)
Test Run 1	2.00	1.85	1.93	2.10	2.15
Test Run 2	2.11	2.13	2.30	2.33	2.10
Test Run 3	2.45	2.41	2.50	2.37	2.18
Test Run 4	2.75	2.80	2.59	2.61	2.54
Test Run 5	2.51	2.53	2.62	2.43	2.55
Test Run 6	2.71	2.80	2.55	2.62	2.65
Test Run 7	2.02	2.32	2.41	2.22	2.08
Test Run 8	2.85	2.60	2.51	2.56	2.79
Test Run 9	2.53	2.65	2.54	2.62	2.51

4.1.3 Pitting Corrosion Loss

The Taguchi Design of Experiments (DOE) plays a vital role in optimizing the gas metal arc welding (GMAW) process for cladding 316L stainless steel onto A36 mild steel, aiming to improve corrosion resistance.

$$\text{Pitting Corrosion Loss} = \text{Weight loss} / (\text{Area exposed} \times \text{Time of exposure}) \quad \ldots 4\text{-}2$$

Table 4-3: Values for Calculation of Pitting Corrosion Loss

Weight Loss (lbs)	Area Exposed (m^2)	Time of Exposure (hrs)	Pitting Corrosion Loss (kg)
0.000108	0.00189342	48	5.39×10^{-4}

4.1.4 Inferential Analysis of Bead Width Variation with Process Parameters

Values of reinforcement and penetration for each specimen were noted, and the percentage dilution was calculated. The values of reinforcement height, R, and penetration depth, P, were picked from Table 4-1. They are meant to be used in the calculation of dilution, D, as per Equation 3-1. Where the dilution was found to be minimum at 6.67%, that is the optimal value and, therefore, the independent parameters were taken as shown in Table 4-3.

In this report, key values were established based on factors such as bead width, reinforcement height, penetration depth, corrosion resistance, and dilution. The analysis was conducted using "Design Expert 13" software, and the results were presented accordingly. The Analysis of Variance (ANOVA) assessed bead width in relation to welding parameters like arc voltage, welding current, and wire feed rate. The Model F-value of 13.23 indicates significant experimental results, with A being an important model term. Values exceeding 0.1000 imply that model terms are not significant. If many terms are insignificant (excluding necessary ones for hierarchy), simplifying the model may improve its effectiveness. The Lack of Fit F-value of 0.72 suggests that the Lack of Fit is not significant compared to pure error, with a 69.63% likelihood that such a Lack of Fit F-value could result from noise. The Predicted R^2 of 0.5080 is reasonably close to the Adjusted R^2 of 0.6588, as the difference is less than 0.2. Adequate Precision, which indicates the signal-to-noise ratio, should be above 4; a ratio of 9.593 shows a sufficient signal. The coefficient estimate indicates the expected change in response per unit change in factor value, while keeping other factors constant.

Table 4-4: Dilution of weld after cladding

Expt. No.	**Voltage (V)**	**Current (A)**	**WFS (m/min)**	**P (mm)**	**R (mm)**	**P + R (mm)**	**% Dilution** $\{[\frac{P}{P+R}] \times 100\%\}$
1	24	150	3.0	0.25	1.75	2.00	12.50
2	24	160	3.5	0.20	1.91	2.11	9.48
3	24	170	4.0	0.36	2.09	2.45	14.69
4	26	150	3.5	0.18	2.57	2.75	8.72
5	26	160	4.0	0.22	2.28	2.50	8.80
6	26	170	3.0	0.23	2.48	2.71	8.49
7	28	150	4.0	0.18	1.84	2.02	8.91
8	28	160	3.0	0.19	2.66	2.85	6.67
9	28	170	3.5	0.22	2.24	2.46	8.94

Table 4-5: ANOVA of Bead Width

Source	Sum of Squares	df	Mean Square	F-value	p-value	Remark
Model	65.54	3	21.85	13.23	0.0001	Significant
A-Arc voltage	60.07	1	60.07	36.36	< 0.0001	
B-Welding current	0.3329	1	0.3329	0.2015	0.6595	
C-Wire feed speed	0.4624	1	0.4624	0.2799	0.6040	
Residual	26.43	16	1.65			
Lack of Fit	16.24	11	1.48	0.7242	0.6963	Not significant
Pure Error	10.19	5	2.04			
Cor. Total	91.98	19				
Fit Statistics 1						
Std. Dev.	1.29		**R^2**	0.7126		
Mean	14.00		**Adjusted R^2**	0.6588		
C.V. %	9.18		**Predicted R^2**	0.5080		
			Adeq. Precision	9.5932		

Intercept	13.90	1	0.2903	13.29	14.52			
A-Arc voltage	2.39	1	0.3958	1.55	3.23		1.04	
B-Welding current	0.1482	1	0.3302	-0.5518	0.8482		1.03	
C-Wire feed speed	-0.2220	1	0.4196	-1.11	0.6675		1.07	
Run Order	**Actual Value**	**Predicted Value**	**Residual**	**Leverage**	**Internal Residuals**	**External Residuals**	**Cook's Distance**	**Fitted Value DFFITS**
1	10.90	11.59	-0.6879	0.382	-0.681	-0.669	0.071	-0.525
2	11.42	11.51	-0.0941	0.155	-0.080	-0.077	0.000	-0.033
3	10.21	11.44	-1.23	0.328	-1.168	-1.182	0.166	-0.825
4	14.33	13.75	0.5773	0.103	0.474	0.462	0.006	0.156
5	13.16	13.68	-0.5190	0.159	-0.440	-0.429	0.009	-0.186
6	15.66	14.27	1.39	0.210	1.216	1.235	0.098	0.636
7	14.21	15.92	-1.71	0.304	-1.592	-1.681	0.277	-1.111
8	16.33	16.51	-0.1798	0.204	-0.157	-0.152	0.002	-0.077
9	17.77	16.44	1.33	0.221	1.176	1.191	0.098	0.634

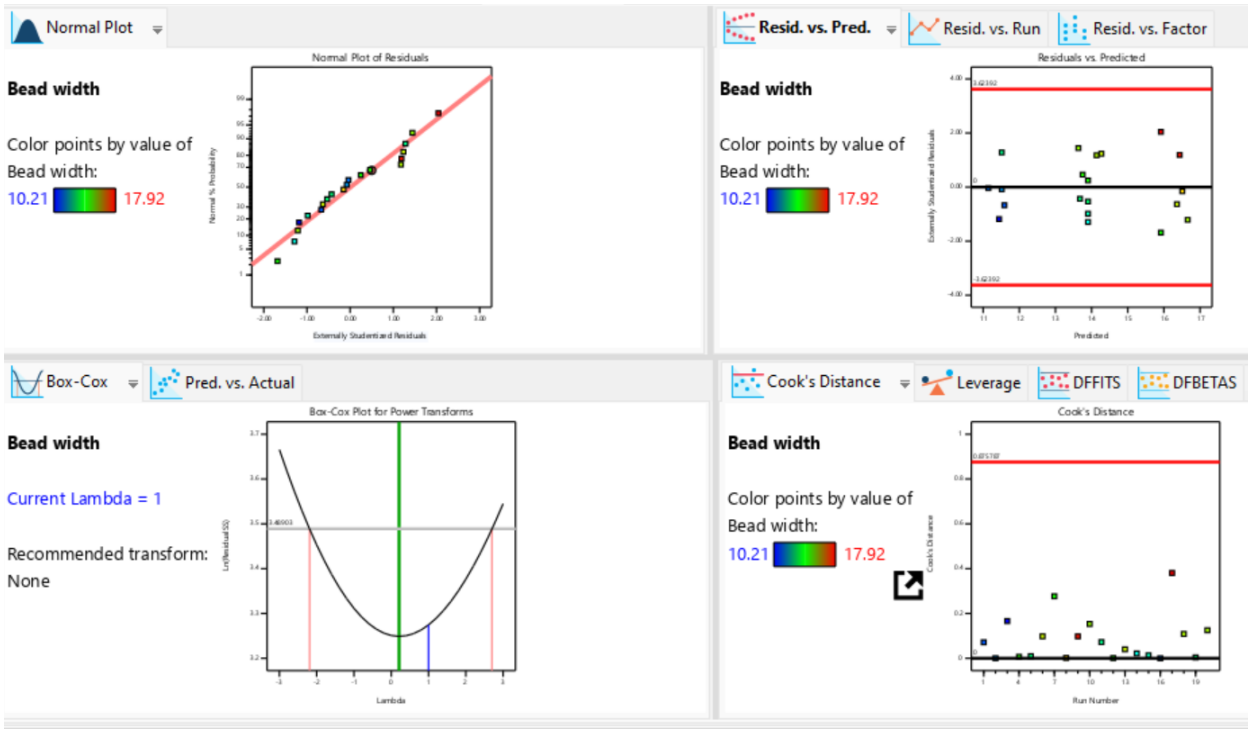

Figure 4-1: The inferential plots for bead width (from Design Expert 13)

To explain the graphs in Design Expert 13, it is essential to understand the types of analyses and visualizations the software provides. The software employs various statistical methods, including response surface methodology (RSM) to optimize experimental conditions and visualize results.

Types of Graphs in Design Expert 13

Response Surface Plots: These illustrate the relationship between independent variables and the response variable.

Contour Plots: These provide a two-dimensional view of the response surface, helping to identify regions of optimal responses.

Causal Graphs: These graphs help in understanding the causal relationships between variables, enhancing the interpretation of experimental data.

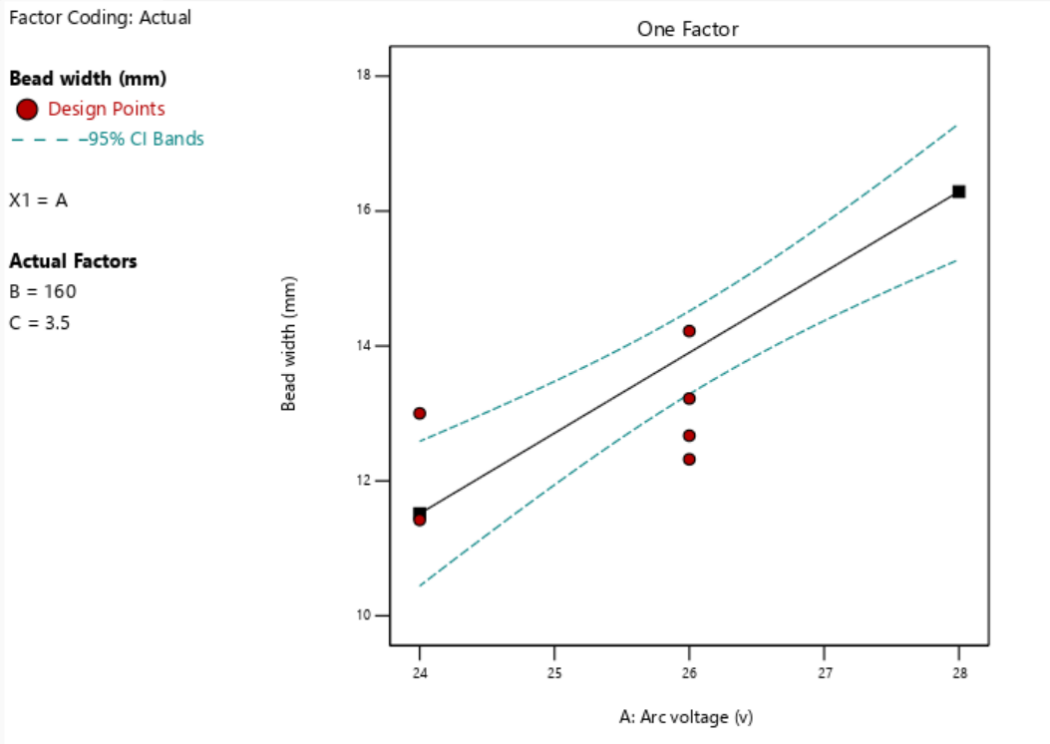

Figure 4-2: Bead width against arc voltage for one factor (DESIGN EXPERT 13)

4.1.5 Inferential Analysis of Penetration Variation with Process Parameters

The Model F-value of 3.42 indicates that the model is significant, with only a 4.28% likelihood that such an F-value could result from noise. P-values below 0.0500 demonstrate that model terms are significant, making C an important term in this analysis. The Lack of Fit F-value of 0.78 implies that the Lack of Fit is not significant compared to pure error, with a 66.07% chance that this Lack of Fit F-value could arise from noise. A non-significant lack of fit is beneficial, as it suggests a good model fit. A negative Predicted R^2 indicates that the overall mean might predict the response better than the current model, and sometimes a higher-order model may provide better predictions. The ratio of 6.353 indicates an adequate signal.

Here are some other ways to interpret results from Design Expert:

(i) Residual plots

Design Expert provides residual plots to check assumptions like constant variance and normality. You can check for non-constant variance by using the "residuals versus predicted value" graph. If the variation in the residuals increases as the response increases, then the variance constant. This means that it is harder to predict larger response values as precisely as smaller ones.

(ii) Normal probability plot

You can check for a well-behaved (nearly normal) distribution by using a normal probability plot. The residuals should be approximately normally distributed.

(iii) R-squared

A rule of thumb is that the adjusted and predicted R-squared values should have a maximum difference 0.2 of each other. A low R-squared indicates that there is individual variation that the current model does not explain.

(iv) Graphs

Design Expert offers a variety of graphs to help you visualize your results and identify standout effects.

Table 4-6: ANOVA for Penetration

Source	Sum of Squares	df	Mean Square	F-value	p-value	Significance
Model	0.1756	3	0.0585	3.42	0.0428	Significant
A-Arc voltage	0.0091	1	0.0091	0.5295	0.4773	
B-Welding current	0.0172	1	0.0172	1.00	0.3316	
C-Wire feed speed	0.1416	1	0.1416	8.28	0.0109	
Residual	0.2738	16	0.0171			
Lack of Fit	0.1731	11	0.0157	0.7812	0.6607	Not significant
Pure Error	0.1007	5	0.0201			
Cor Total	0.4494	19				
Fit statistics						
Std. Dev.	0.1308		**R^2**	0.3908		
Mean	0.3430		**Adjusted R^2**	0.2766		
C.V. %	38.14		**Predicted R^2**	-0.0401		
			Adeq Precision	6.3533		

Factor	Coefficient Estimate	df	Standard Error	95% CI Low	95% CI High	VIF
Intercept	0.3482	1	0.0295	0.2855	0.4108	
A-Arc voltage	-0.0293	1	0.0403	-0.1147	0.0561	1.04
B-Welding current	0.0337	1	0.0336	-0.0376	0.1049	1.03
C-Wire feed speed	0.1229	1	0.0427	0.0323	0.2134	1.07

Run Order	Actual Value	Predicted Value	Residual	Leverage	Internal Residuals	External Residuals	Cook's Distance	Influence on Fitted Value DFFITS
1	0.2500	0.2210	0.0290	0.382	0.282	0.274	0.012	0.215
2	0.2000	0.3775	-0.1775	0.155	-1.476	-1.538	0.100	-0.658
3	0.6600	0.5340	0.1260	0.328	1.175	1.190	0.168	0.831
4	0.1800	0.3145	-0.1345	0.103	-1.086	-1.092	0.034	-0.369
5	0.2200	0.4710	-0.2510	0.159	-2.092	-2.377	0.206	-1.032
6	0.2300	0.2590	-0.0290	0.210	-0.249	-0.242	0.004	-0.124
7	0.2100	0.4081	-0.1981	0.304	-1.815	-1.972	0.360	-1.303
8	0.1900	0.1960	-0.0060	0.204	-0.051	-0.050	0.000	-0.025
9	0.3500	0.3525	-0.0025	0.221	-0.022	-0.021	0.000	-0.011

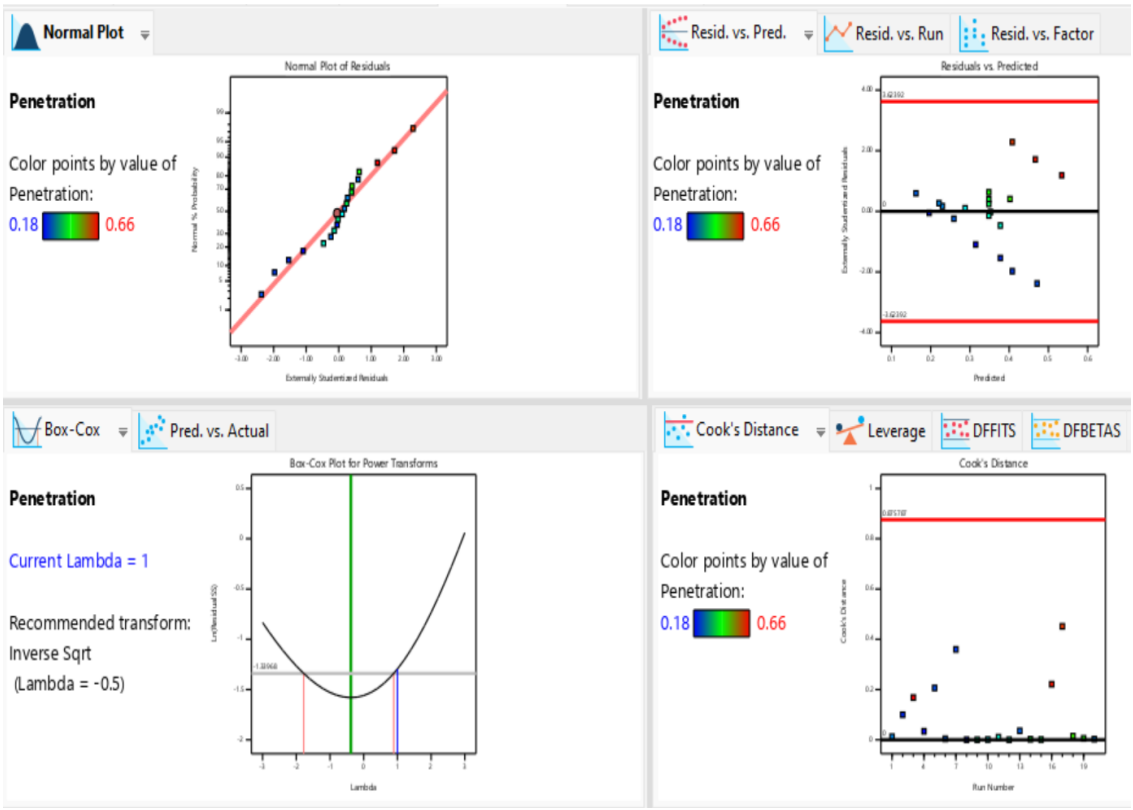

Figure 4-3: Inferential plots for penetration (DESIGN EXPERT 13)

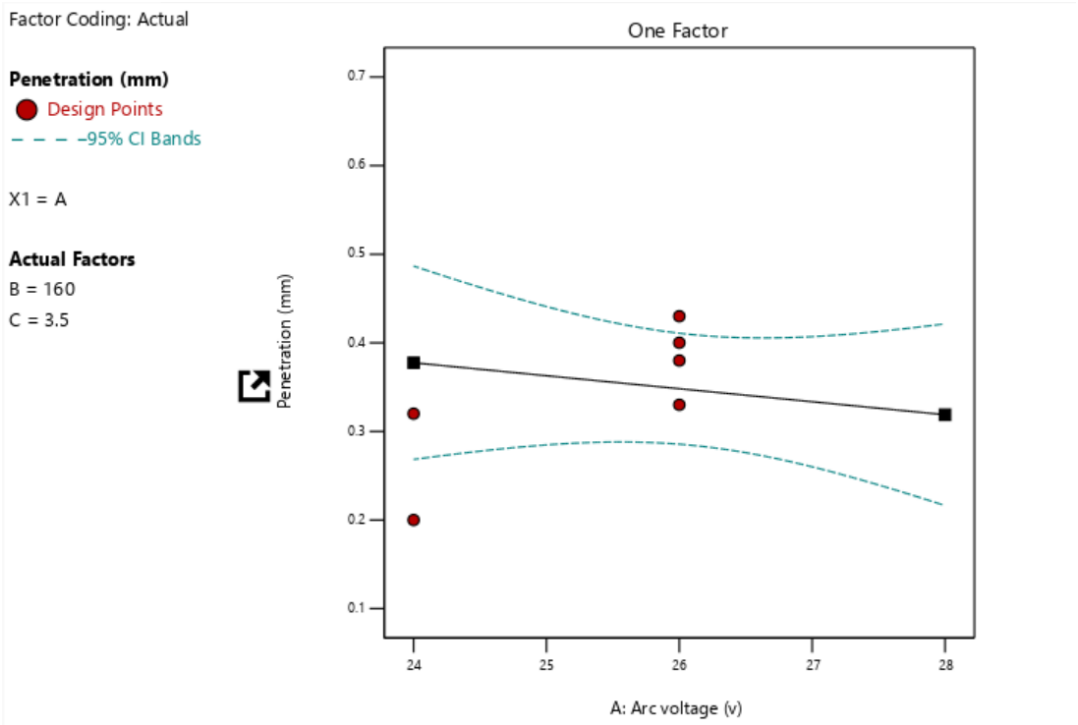

Figure 4-3: Penetration against arc voltage for one factor (DESIGN EXPERT 13)

4.1.6 Inferential Analysis of Reinforcement Variation with Process Parameters

The Model F-value of 3.37 indicates that the model is statistically significant, with only a 3.60% probability that this F-value is due to random chance. P-values lower than 0.0500 show that the model terms are significant, highlighting AC as an important factor in this analysis. The Lack of Fit F-value of 1.08 implies that the Lack of Fit is not significant when compared to pure error, with a 46.84% chance that this Lack of Fit F-value could result from noise. The F-value is the ratio of the mean square of the term to the mean square of the residuals.

Degrees of freedom (df) are crucial in statistics, representing the number of independent parameters that can change within a system. R-squared assesses the goodness-of-fit but may be misleading if too many variables are included. Adjusted R-squared and predicted R-squared provide more reliable results by addressing this issue. In Design-Expert software, a p-value below 0.05 is generally regarded as statistically significant.

In Design-Expert software, a lack of fit (LOF) test is a model-validation statistic that measures how much model predictions differ from observations. A statistically significant LOF test indicates that the model is not fitting the data well.

An analysis of variance (ANOVA) is typically paired with a model-validation statistic known as the lack of fit (LOF) test. A significant LOF test can concern researchers as it suggests the model may not adequately fit the data. LOF is an algorithm that detects outliers by assessing how much a data point deviates from its neighbors. The "Cor. Total" row indicates the total variation around the mean of the observations, with the model accounting for part of it and the residuals explaining the remainder. The sample standard deviation (s) is calculated as the square root of the sample variance, which shows how much the data points vary from the expected values. The Coefficient of Variation (C.V. %) expresses the standard deviation as a percentage of the mean. Adequate Precision refers to a signal-to-noise ratio that assesses the relationship between variability in predicted outcomes and the standard error of those predictions. Lastly, "residuals" are the differences between observed response values and the expected values based on the model's predictions.

The leverage is a numerical value between 0 and 1 that indicates the potential for a design point to influence the model fit.

Cook's Distance is a measure of an observation or instance's influence on a linear regression.

Factor coding involves converting categorical variables into integer values, allowing for easier manipulation and analysis within datasets.

DFFITS stands for "difference in fits". It is calculated by measuring the change in predicted values that occurs when that response value is deleted. The larger the value of DFFITS, the more it influences the fitted model. Another way to explain DFFITS is that the externally studentized residuals are magnified at high leverage points and shrunk by low leverage points. In statistics, studentized means dividing a statistic by a sample standard deviation. This is similar to standardizing and normalizing.

A run is considered influential when the value of the DFFITS is outside the limits. The limits are calculated as $\pm \max\left(1, 3\sqrt{\frac{p}{n}}\right)$.

Where n is the number of runs in the design, and p is the number of terms in the model. We use the DFFITS to judge the influence of suspected outliers.

Table 4-7: ANOVA for Reinforcement

Source	Sum of Squares	df	Mean Square	F-value	p-value	Remarks		
Model	1.01	9	0.1121	3.37	0.0360	Significant		
A-Arc voltage	0.0397	1	0.0397	1.19	0.3006			
B-Welding current	0.0096	1	0.0096	0.2877	0.6034			
C-Wire feed speed	0.0477	1	0.0477	1.43	0.2588			
AB	0.0108	1	0.0108	0.3245	0.5815			
AC	0.3986	1	0.3986	11.98	0.0061			
BC	0.0429	1	0.0429	1.29	0.2827			
A^2	0.1505	1	0.1505	4.52	0.0594			
B^2	0.0011	1	0.0011	0.0318	0.8621			
C^2	0.0022	1	0.0022	0.0657	0.8029			
Residual	0.3328	10	0.0333					
Lack of Fit	0.1726	5	0.0345	1.08	0.4684	Not significant		
Pure Error	0.1602	5	0.0320					
Cor Total	1.34	19						
Run Order	**Actual Value**	**Predicted Value**	**Residual**	**Leverage**	**Internally Studentized Residuals**	**Externally Studentized Residuals**	**Cook's Distance**	**Influence on Fitted Value DFFITS**
1	1.75	1.77	-0.0158	0.958	-0.422	-0.404	0.403	-1.921
2	1.91	2.04	-0.1285	0.396	-0.906	-0.897	0.054	-0.726
3	2.09	2.06	0.0320	0.769	0.365	0.348	0.044	0.636
4	2.57	2.28	0.2864	0.202	1.758	2.006	0.078	1.009
5	2.28	2.21	0.0730	0.583	0.620	0.600	0.054	0.709
6	2.48	2.49	-0.0098	0.707	-0.099	-0.094	0.002	-0.146
7	1.84	1.83	0.0071	0.489	0.054	0.052	0.000	0.051
8	2.66	2.50	0.1627	0.357	1.113	1.128	0.069	0.841
9	2.24	2.25	-0.0098	0.707	-0.099	-0.094	0.002	-0.146

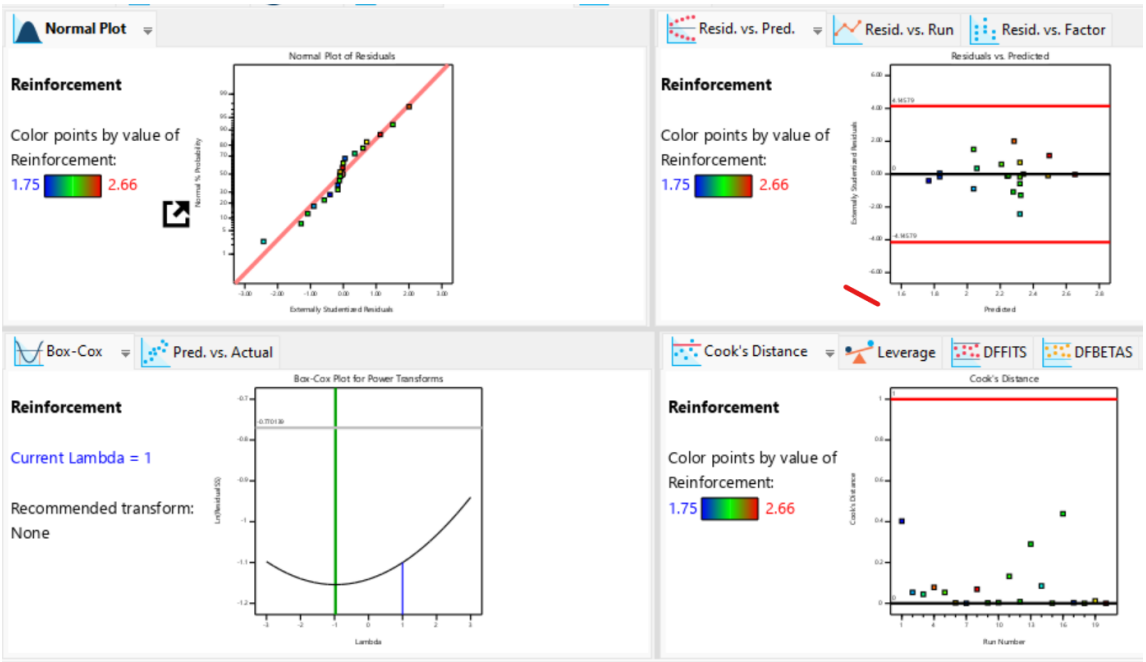

Figure 4-4: Graphs of inferential plots for reinforcement (DESIGN EXPERT 13)

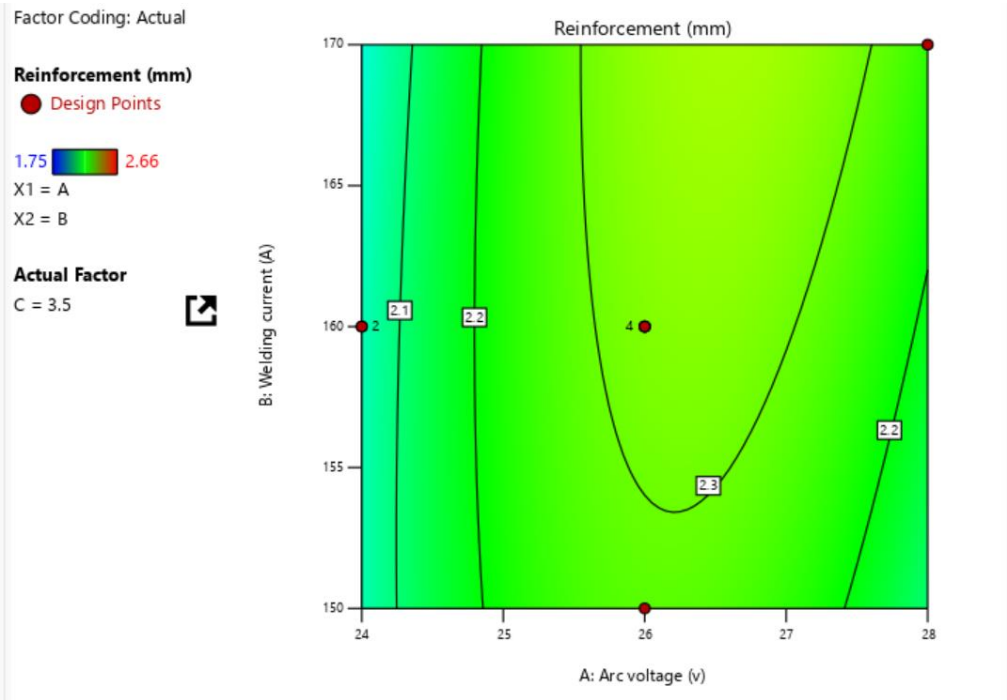

Figure 4-5: Graph of welding current against arc voltage on reinforcement (DESIGN EXPERT 13)

4.1.7 Microstructure of Cladding Region

From Table 4-2, the best dilution parameters are Voltage = 28V, Current = 160A, and Wire Feed Speed = 3.0mm/min, where there was a minimum dilution (6.67%). The test results for the microstructural analysis results for test run 1-9 shown in Appendix B. The resulting cladding exhibited the desired characteristics, corrosion resistance, and favorable optical microstructure, as shown in Figure 4-7. The observed microstructural characteristics were the fusion zone (FZ) exhibited a fine-grained structure due to the rapid solidification during welding, the heat-affected zone (HAZ) showed some grain growth but remained relatively refined, and the substrate retained its original microstructure, consisting of pearlite and ferrite phases. Minimal dilution from the cladding process ensured that the base metal properties were largely unaffected. Other microstructural characteristics images shown in Appendix F.

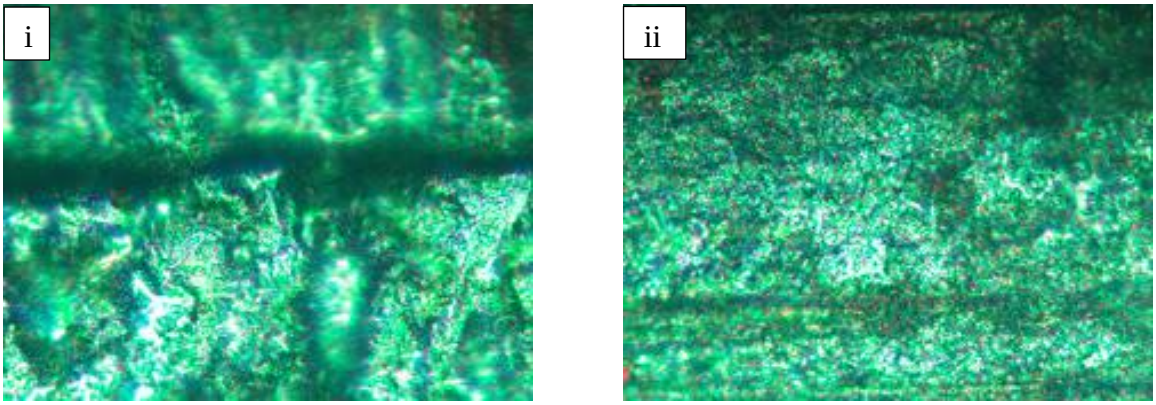

Figure 4-7: (i) Fusion interface microstructure (ii) Surface microstructure for specimen test run 1

4.2 Discussion of Results

The results were analyzed separately according to the defined specific objectives. Specific **Objective (i): To Identify the GMAW Process Parameters that Influence Weld Bead Geometry**. This experimental method effectively highlighted the significance of each parameter in managing the geometry of the weld bead.

Welding Current: Higher current increases heat input, leading to wider and deeper weld beads. However, excessive current can cause burn-through or excessive dilution.

Arc Voltage: Increased voltage can enhance arc stability and penetration, affecting bead shape. Higher voltage typically results in a flatter bead profile.

Wire Feed Rate: A higher feed rate can lead to increased bead width and height, while a lower feed rate may produce a narrower bead. Balancing feed rate with current and voltage is crucial for optimal bead geometry.

The variations in the welding current, arc voltage, and wire feed rate affected the weld bead geometry, and the optimized values were 28V, 160A, and 3.0mm/min, respectively.

Specific Objective (ii): To determine the GMAW process variables that influence the weld dilution of the interface region

Corrosion Resistance: Stainless steel cladding protects underlying materials from corrosion, making it ideal for chemical processing and marine environments.

Aesthetic Appeal: Stainless steel enhances the visual appearance of buildings and structures, often used in architectural designs.

Thermal Insulation: Cladding can provide thermal insulation, improving energy efficiency in buildings.

Structural Support: Stainless steel adds strength and durability to structures, commonly used in construction and infrastructure projects.

Hygienic Surfaces: Stainless steel is easy to clean, making it suitable for food processing and healthcare facilities.

These applications highlight the versatility and benefits of stainless steel cladding in various industries.

From Table 4-4, the minimum dilution was 6.67%. This was the best dilution in all the experiments.

Specific Objective (iii): To optimize the GMAW process variables for high-quality GMAW Welding Cladding

To optimize the Gas Metal Arc Welding (GMAW) process variables for high-quality welding cladding, several key factors must be considered:

(i) Welding wire feed rate: Increasing the wire feed rate enhances the amount of deposited material, leading to a larger fusion zone and improved joint integrity.

(ii) Voltage and Amperage: Fine-tuning the voltage and amperage settings is crucial for achieving the desired bead profile and minimizing defects.

(iii) Shielding Gas Composition: The type and flow rate of shielding gas influence the arc stability and the quality of the weld, requiring careful selection based on the materials being welded.

(iv) Electrode Diameter: Choosing the appropriate electrode diameter can enhance the deposition rate and improve the weld's mechanical properties.

By systematically analyzing these variables, it is possible to achieve optimal conditions that enhance the quality and performance of GMAW welding cladding.

In general, the best dilution can be as low as less than 10%. Dilution is the level at which the composition(s) in the substrate mixes with that in the filler wire when welding is taking place. For my study, it is the level at which the A36 mild steel melted pool mixes with the 316LSi stainless steel, and for this matter, a minimum mix should be allowed such that the clad is purely the stainless steel.

CHAPTER FIVE: CONCLUSIONS AND RECOMMENDATIONS

5.1 Conclusions

The primary goal of this study was to develop the cladding process for depositing austenitic stainless steel (AISI 316LSi) onto mild steel (A36) pipe substrate using the GMAW process. The specific objectives were achieved as follows:

Specific objective (i): To establish the GMAW process parameters that control the weld bead geometry in welding stainless steel onto a mild steel substrate.

The process parameters that were optimized: Welding voltage (28 V), Welding Current (160 A), and Welding wire feed rate (3.0 m/min). From research:

Welding Current: Optimal current settings significantly influence bead geometry. Studies indicate that a current of around 160 A yields favorable bead height and width, while lower currents (e.g., 120 A) can minimize distortion and shrinkage.

Arc Voltage: It is generally accepted that maintaining a stable arc voltage is crucial for consistent weld quality and penetration depth and some researcher was quoted as having 28V as the optimum value.

Wire Feed Rate: The feed rate must be balanced with current and voltage to achieve optimal fusion and bead characteristics. A feed rate of approximately 3.5 m/min has been shown in research to enhance bead formation.

Specific objective (ii) To determine the GMAW process variables that influence the dilution in welding stainless steel onto a mild steel substrate.

The 316LSi stainless steel cladding achieved a lower dilution rate of 6.67% compared to many researches where in literature a researcher got 12% dilution.

Specific objective (iii) To optimize the GMAW process variables for high-quality GMAW welding of stainless steel onto a mild steel substrate.

The pitting corrosion loss in 48 hours is 0.539 grams. This implies the 316LSi stainless steel cladding over the A36 mild steel pipe substrate was very significant. Research indicates that in a 0.5 M sulfuric acid solution, mild steel experiences a weight loss of approximately 2.99 grams after 48 hours.

The absence of a mathematical model shows that the optimization was based on empirical experimentation results. The significant parameter for this study is arc voltage and bead width that gave the p-value of < 0.0001 followed by the reinforcement height whose p-value is 0.0061, and welding current whose p-value is 0.6040. The focus was achieving corrosion resistance, low dilution, good weld bead geometry, as well as favorable microstructural characteristics. The obtained results show that the bead width was at 99.99% (with a p-value of 0.0001), penetration at 95.72% (p-value of 0.0428), and reinforcement at 96.4% (p-value of 0.0360) were significant (since they are less than 0.0500), all outputs optimized at 95% confidence interval.

5.2 Recommendations and Practical Implications of Weld Cladding

5.2.1 Recommendations for Future Work

(i) Automated Cladding Systems: Implementing automated systems can help reduce human error and improve quality assurance and inspection.

(ii) Eco-Friendly Processes: Utilizing eco-friendly welding methods, such as laser cladding, can lower energy consumption and emissions.

5.2.2 Practical Implications of Weld Cladding

(a) Corrosion Resistance: The stainless-steel overlay significantly enhances corrosion resistance, making it ideal for harsh environments like chemical processing and marine applications.

(b) Improved Mechanical Properties: The cladding improves the substrate's mechanical properties, enabling it to endure higher stresses and temperatures.

(c) Cost-Effectiveness: Using mild steel as a substrate lowers costs while still providing the advantages of stainless steel, making it practical for various applications.

(d) Weld Quality Control: Maintaining proper welding parameters is essential to minimize dilution and ensure the cladding's integrity, which is crucial for performance.

These aspects highlight the value of this cladding technique in industries that require durable and resistant materials.

REFERENCES

Abioye, T.E., Kanu, C.O., Ogedengbe, T.I. and Adebiyi, D.I. (2019) 'Parametric optimization of gas metal arc dissimilar welding on AISI 304 stainless steel and low carbon steel'. *Int. J. Microstructure and Materials Properties*, *14*(2), 155–169. http://dx.doi.org/10.1504/IJMMP.2019.10020468

Ahmed M. Aly. (2022, May 07). *Gas Metal Arc Welding (GMAW) | MIG Welding Guide*. Welding Technology. Workshop insider.

Akpanyung, K.V., & Loto, R.T. (2019). Pitting corrosion evaluation: a review. *Journal of Physics: Conference Series 1378*(2019) 022088. IOP Publishing. hpps:www.doi.org:10.1088/1742-6596/1378/2/022088

Borba A. Jeff. (2020). American Welding Society (AWS) - Guide-for-AWS-D1.1-2020-Visual-Weld-Inspection-1. www.technicalinspector.com

American Welding Society ANSI Z49.1 (2021). Safety in Welding, Cutting, and Allied Processes.

American Welding Society (AWS) D l Committee on Structural Welding. (2019, December 9). Structural Welding Code - Steel. *AWS D1 .1/D1 .1 M: 2020 - An American National Standard, 24th Edition*. Supersedes AWS Dl.1/D1.lM:2015. ISBN Print: 978-1-64322-087-1. ISBN PDF: 978-1-64322-088-8

American Welding Society (AWS) D1 Committee on Structural Welding. (2020). Structural Welding Code — Steel. *AWS D1.1/D1.1M:2020 - An American National Standard, 24th Edition.* ISBN Print: 978-1-64322-087-1ISBN PDF: 978-1-64322-088-8, © 2020 by American Welding Society

American Welding Society (AWS) D1 Committee on Structural Welding. (2017, January 9). Structural Welding Code — Stainless Steel. *AWS D1.6/D1.6M:2017 - An American National Standard, 3rd Edition.* ISBN (PDF): 978-0-87171-906-5 © 2017 by American Welding Society

American Welding Society. (2017). Standards, reference books, online education, and more: With access to more info than ever - 11 Modules with Pre & Post Quizzes - *ANSI 49.1 National Standard - Safety & Health Fact Sheets.*

Anand, S. (2022). ASME material specification and grades for pipes, tubes, forgings, castings, fittings, valves, nuts, and bolts. *ASME codes and standards, steel.*

Anirban Bhattacharya & Tarun Kumar Bera (2014), Development of Automatic GMAW Setup for Process Improvements: Experimental and Modeling Approach. *Materials and Manufacturing Processes*, *29*(8), 988-995, http://dx.doi.org/10.1080/10426914.2014.892611

Arabaci, H., & Laving, S. (2019). Weld Defect Categorization from Welding Current Using Principle Component Analysis. *(IJACSA) International Journal of Advanced Computer Science and Applications*, *10*(6), 204-211. www.ijacsa.thesai.org

Arc Machines, Inc. (2022, September 01). *Understanding the basics of the stainless steel cladding process*, Engineering Department; orbital welding-pipe welding. https://www.resources.arcmachines.com/?

Arthur Casarini, João P. Coelho, Émillyn T. Olívio, Manuel Braz-César, and João Ribeiro, (2020), "Optimization and Influence of GMAW Parameters for Weld Geometrical and Mechanical Properties Using the Taguchi Method and Variance Analysis". *International Congress on Engineering — Engineering for Evolution*, *KnE Engineering*, 781–794. http://dx.doi.org/10.18502/keg. v5i6.7097

Asal, V.D., Prof. Patel, R.I., Choudhary, A.B. (2013, March-April). Optimization of Process Parameters of EDM Using ANOVA Method. *International Journal of Engineering Research and Applications (IJERA)*, *3*(2), 1119-1125. ISSN: 2248-9622 www.ijera.com

Aslam, Mohd & Kumar Sahoo, Chinmaya. (2022, May 01). Numerical and experimental investigation for the cladding of AISI 304 stainless steel on mild steel substrate using Gas Metal Arc Welding. *CIRP Journal of Manufacturing Science and Technology*, *Volume 37*, 2022, 378-387, ISSN 1755-5817, https://doi.org/10.1016/j.cirpj.2022.02.017.

(https://www.sciencedirect.com/science/article/pii/S1755581722000414)

ASTM G48-11 (2020)e1. (2021, January 01). *Standard Test Methods for Pitting and Crevice Corrosion Resistance of Stainless Steels and Related Alloys by Use of Ferric Chloride*. ASTM International. Version: G0048-11R20E01.

Aytekin Ulutaş (2021, December 16). Joining Techniques like Welding in Lightweight Material Structures https://orcid.org/0000-0002-5230-7122 Edremit School of Civil Aviation, Balıkesir University, Turkey.

Bahador, A., Hamzah, E., & Mamat, M.F. (2015, June 17). Effect of Filler Metals On the Mechanical Properties of Dissimilar Welding of Stainless Steel 316l and Carbon Steel A516 GR 70. *Jurnal Teknologi, 75*(7), 61–65. www.jurnalteknologi.utm.my, eISSN 2180–3722

Balasubramanian, K., Vikram, R., Sambath, S. et al. (2023 August 24). Optimization of flux-cored arc welding parameters to minimize dilution percentage of AISI 316LSi stainless steel cladding on mild steel. *Int J Interact Des Manuf.* https://doi.org/10.1007/s12008-023-01487-2

Bao, Y., Xue, R., Zhou, J., Liu, H., & Xu, Y. (2023). The Influence of Oscillation Parameters on the Formation of Overhead Welding Seams in the Narrow-Gap GMAW Process. *Appl. Sci., 13*(5519), 1-11. https://doi.org/10.3390/app13095519

Biber. A., Sharma, R., & Reisgen, U. (2024, March 27). Robotic welding system for adaptive process control in gas metal arc welding. *Researchgate*. https://doi.org/10.1007/s40194-024-01756-y https://www.researchgate.net/publication/379361445

Biserova-Tahchieva, A., Biezma-Moraleda, M.V., Llorca-Isern, N., Gonzalez-Lavin, J., Linhardt, P. (2023, February 24). Additive Manufacturing Processes in Selected Corrosion Resistant Materials: A State of Knowledge Review. *Materials, 16*, 1893. https://doi.org/10.3390/ma16051893 *Carbon Steel Handbook.* EPRI, Palo Alto, CA: 2007. 1014670.

Boergert, R.L., Stephen. (2021, January 12). Mode of Metal Transfer-Gas Metal Arc Welding

(GMAW). *Researchgate*, https://www.researchgate.net/publication/348419138 *WeldPower, Corp 2008* www.weldpowercorp.com

Bunaziv I, Olden, V., & Akselsen, O.M. (2019, August 1). Metallurgical Aspects in the Welding of Clad Pipelines—A Global Outlook. *Appl. Sci.*, *9*(3118), 1-24. https://doi.org/10.3390/app9153118. *www.mdpi.com/journal/applsci*

Cárcel-Carrasco, F-J., Pascual-Guillamón, M., García, L.S., Vicente, F.S., & Pérez-Puig, M-A. (2019, August 9). Pitting Corrosion in AISI 304 Rolled Stainless Steel Welding at Different Deformation Levels. *Appl. Sci. 9*(3265), 1-12; https://doi.org/10.3390/app9163265 www.mdpi.com/journal/applsci

Cayo, E.H., Alfaro, S.C.A. (2009). GMAW process stability evaluation through acoustic emission by time and frequency domain analysis. *Journal of Achievements in Materials and Manufacturing Engineering 34*(2), 157-164.

Chaubey, V., Dr. Rao, P.S., & Gupta, S.K. (2018, November). Cladding of Mild Steel Plates Using GMAW Process. *International Journal of Emerging Technologies in Engineering Research (IJETER)*, *6*(11), 1-9. ISSN: 2454-6410 www.ijeter.everscience.org

Coors, T., Faqiri, M.Y., Saure, F., Kahra, C., Büdenbender, C., Peddinghaus, J., Prasanthan, V., Pape, F., Hassel, T., Herbst, S., et al. (2022). Investigations on Additively Manufactured Stainless Bearings. *Coatings*, *12*(1699), 1-20. https://doi.org/10.3390/coatings12111699

Curiel, D., Veiga, F., Suarez, A., & Villanueva, P. (2023). Advances in Robotic Welding for Metallic Materials: Application of Inspection, Modeling, Monitoring, and Automation Techniques. *Metals*, *13*(711). https://doi.org/10.3390/met13040711

Curiel, D., Veiga, F., Suarez, A., & Villanueva, P. (2023, January 18). Methodology for the Path Definition in Multi-Layer Gas Metal Arc Welding (GMAW). *Symmetry*, *15*(268). https://doi.org/10.3390/sym15020268

da Cruz Junior, E.J., Varasquim, F.M.F.A., De Mendonca, V.R., Ventrella, V.A., Goncalves, A.C., Fagundes Junior, J.G., Zambon, A., Calliari, I. (2024, October 24). Impact of Heat Input on

the Cladding of Super Austenitic Stainless Steel Through the Gas Tungsten Arc Welding Process on ASTM A516 Grade 70 Steel. *Coatings*, *14*(1356). https://doi.org/10.3390/coatings14111356

de Lima, J.S., da Silva Neto, J.F., Maciel, T.M. et al. (2024, March 05). Effect of wire arc additive manufacturing parameters on geometric, hardness, and microstructure of 316LSi stainless steel preforms. *Int J Adv Manuf Technol* 131, 5981-5996 (2024). https://doi.org/10.1007/s00170-024-13240-4

Dr. Nuri M. Bhieh1, Dr. Thoria G. Sharef, Eng. Abdullah A. Abdullah (2015, November 2-5). Optimization of Welding Parameters of Gas Metal Arc Welding on Cladding of Stainless Steel on Low Carbon Steel. *3rd International Conference in Africa and Asia on Welding and Failure Analysis of Engineering Materials*, Luxor, Egypt

Driscoll, Tim (2020, July). CONTROLLING FUMES AND ULTRAVIOLET RADIATION EXPOSURE FROM WELDING AND MINIMISING THE ASSOCIATED RISK OF CANCER – REVIEW OF PUBLISHED EVIDENCE. ELMATOM Pty Ltd. Controlling fumes and ultraviolet radiation exposure from welding – July 2020 – Final report. https://research.isbrr.com.au/_data/assets/pdf_file/0007/2357071/254_REP_RES_R01_Welding-exposures-and-controls-VWA-Final-report.pdf.

Eswaran, S., & Kumar, R. D. (2023). Review Paper on Optimization of Metal Inert Gas Welding on Stainless Steel AISI 410 by Taguchi Method. *International Journal for Research in Applied Science and Engineering Technology*, *11*(3), 1149–1154. https://doi.org/10.22214/ijraset.2023.49610

Farkade, V. & Ravanan, F.P.M. (2015, August). Modification in Weld Overlay for Productivity and Corrosion Resistance. *IJSTE - International Journal of Science Technology & Engineering*, *2*(2), 37-41. ISSN (online): 2349-784X. www.ijste.org

Fırat Alemdar, Z., & Alemdar, F. (2023, March 22). Investigation of Corrosion Effects on Collapse of Truss Structures. Buildings, 13, 826. https://doi.org/10.3390/buildings13030826

Gandhe, S., Aher, V.S., Wakchaure, V.D. (2020, January 04). Influence of GMAW Process Parameters and Selection Techniques on the Quality of a Welded Joint. *International Journal for Research in Applied Science & Engineering Technology (IJRASET)* , *7*(XII), 741-758. ISSN: 2321-9653; IC Value: 45.98; SJ Impact Factor: 7.177. www.ijraset.com

Giarollo, D.F., Hackenhaar, W., Mazzaferro, C.C.P., & Mazzaferro, J.A.E. (2022). Bead geometry prediction in pulsed GMAW welding - a comparative study on the performance of the artificial neural network and regression models. *Soldagem & Inspeção, 27: e2722*. https://doi.org/10.1590/0104-9224/SI27.22

Giron-Cruz, J.A., Pinto-Lopera, J.E., & Alfaro, S.C.A. (2022). Weld bead geometry real-time control in gas metal arc welding processes using intelligent systems. *Int J Adv Manuf Technol 123*, 3871-3884. https://doi.org/10.1007/s00170-022-10384-z.

Gulhane, U.D., Dixit, A.B., Bane, P.V., & Salvi, G.S. (2012). Optimization of Process Parameters for 316l Stainless Steel Using Taguchi Method and ANOVA. *International Journal of Mechanical Engineering and Technology (IJMET), 3*(2), 67- 72. ISSN 0976 – 6340(Print), ISSN 0976 – 6359(Online), www.iaeme.com/ijmet.html

Gyasi, E. A. et al. (2019). Digitalized automated welding systems for weld quality predictions and reliability. *(FAIM2019), June 24-28, 2019*, Limerick, Ireland.

Hadžihafizović, Dževad. (2023, August 16). Guide to weld inspection for structure steel. *Researchgate*, https://www.researchgate.net/publication/373160685.

Hadžihafizović, Dževad. (2023, January 5). Welding Defects, Causes & Remedy. *Researchgate*, https://www.researchgate.net/publication/366897608. University of Sarajevo. https://doi.org/10.13140/RG.2.2.24115.91689

Hadzihafizovic Dzevad. (2023, April 04). Standard Symbols for Welding. *Researchgate*. https://www.researchgate.net/publication/369764334

Hickey, K. (2020). *Gas metal arc welding: Introduction*. High energy density welding arc welding main-blog AHSS blog tool & Die Professionals homepage.

Hu, Z., Lin Hua, Qin, X., Ni, M, Ji, F., & Wu, M. (2021). Molten pool behaviors and forming the appearance of robotic GMAW on the complex surface with various welding positions. *Journal of Manufacturing Processes, 64* (2021) 1359–1376. www.elsevier.com/locate/manpro

Ikpe, A.E., Ikpe, E.O., & Etuk, E.M. (2024, March). Shielding gases in conventional welding applications: A glimpse of weld integrity in the manufacturing sector. *Researchgate*, p.324-341. https://www.researchgate.net/publication/379037279. ISARC (International Science and Art Research Center.

Ikpe, A.E., Idiong, K.E., & Bassey, M.O. (2023, December 4). A Comprehensive Overview of Welding Defects and Associated Failure Mechanisms in Metal Joining Process. *5th International Black Sea Modern Scientific Research, I*, ISBN: 9 7 8 - 1 - 9 5 5 0 9 4 - 6 2 – 7. https://www.researchgate.net/publication/376189204.

Jayavelu Jeyaganesh, D., Ziout, A., & Abu Qudeiri, J.E. (2018). *Multi-objective optimization of welding parameters in a gas metal arc welding process using Taguchi and Grey relation analysis*. United Arab Emirates University, Al Ain 15551, UAE; 201870228@uaeu.ac.ae. *Metals*, *11*(11), 1858

Kaewsakul, N., Putrontaraj, R. & Kimapong, K. (2015). The Effects of GMAW Parameters on Penetration, Hardness, and Microstructure of AS3678-A350 High Strength Steel. *International Journal of Advanced Culture Technology*, *3*(1), 169-178. http://dx.doi.org/10.17703/IJACT.2015.3.1.169

Kajan, S., Trebul'a, M., Duchoň, F., Kovaríková, Z., Švolík, M. & Švec, D. (2024, May 22). Robotic Vision Inspection of Weld Quality Using Convolutional Neural Networks. *25th International Carpathian Control Conference (ICCC)*, Krynica Zdrój, Poland, 2024, pp. 01-05. https://doi.org/10.1109/ICCC62069.2024.10569157.

https://ieeexplore.ieee.org/stamp/stamp.jsp?tp=&arnumber=10569157&isnumber=10569149

Kah, P., Ogheneluona Edigbe, G., Ndiwe, B., & Kubicek, R. (2022, September 11). *SN Applied*

Sciences, (2022) 4:268, 1-22. https://doi.org/10.1007/s42452-022-05150-5. Springer Nature. onlineservice@springernature.com.

Kah, P. (2021, July). Advancements in Intelligent Gas Metal Arc Welding Systems. *Researchgate – Elsevier*: ISBN9780128239056

Kah, P. (2021, September 3). Exploring the potential of Gas Metal Arc Welding in ensuring the productivity and competitiveness of welding production. *Researchgate, Elsevier.com*

Kah, P., & Martikainen, J. (2012, April 12). Influence of shielding gases in the welding of metals. *Int J Adv Manuf Technol 64*(2013), 1411–1421. https://doi.org/10.1007/s00170-012-4111-6. *Researchgat*e. https://www.researchgate.net/publication/257336726

Kah, P., Shrestha, M., Hiltunen, E. & Martikainen, J. (2015). Robotic arc welding sensors and programming in industrial applications. *International Journal of Mechanical and Materials Engineering*, *10*(13), 1-17. http://dx.doi.org/10.1186/s40712-015-0042-y

Kah, P., Suoranta, R., & Martikainen, J. (2012). Advanced gas metal arc welding processes. *Int. J. Adv. Manuf. Technol. (2013)* 67. 655–674. https://doi.org/10.1007/s00170-012-4513-5. https://www.researchgate.net/publication/257337180

Kannan, T., & Murugan, N., (2006, May). Prediction of ferrite number of duplex stainless steel clad metals using RSM. *Welding Journal*, 124, 91-99. *Supplement to the Welding Journal*. Sponsored by the American Welding Society and the Welding Research Council.

Karimi, M.R., Wang, S.H., & Jelovica, J. (2022, September 03). Taguchi-based experimental investigation into weld cladding of Ni-WC MMC overlays by CMT process. *Int J Adv Manuf Technol.; 122*(5-6), 2433-2461. Epub 2022 Sep 3. PMID: 36147551; PMCID: PMC9482915 https://doi.org/10.1007/s00170-022-09816-7

Keane, M., Stone, S. & Chen, B. (2010, February 23). Welding fumes from stainless steel gas metal arc processes contain multiple manganese chemical species. *Journal of Environmental Monitoring*, *12*, 1133–1140. http://dx.doi.org/10.1039/b922840c

Khalid, N., Nadila P.Z., Zamanhuri and Baharin, F.A.S. (2017, March). A Study of Weld Defects of Gas Metal Arc Welding with Different Shielding Gasses. *ARPN Journal of Engineering and Applied Sciences, 12*(6), 2006-2011. ISSN 1819-6608

Khan, A., Agrawal, B.P., Siddique, A.N., & Satapathy, S.N. (2018, March-April). An Investigation on Cladding of Stainless Steel on Mild Steel using Pulse Current GMAW. *International Journal of Engineering Trends and Applications (IJETA), 5*(2), 1-6. ISSN: 2393-9516 www.ijetajournal.org

Khrais, S., Al Hmoud, H., Abdel Al, A., & Darabseh, T. (2023, June 29). Impact of Gas Metal Arc Welding Parameters on Bead Geometry and Material Distortion of AISI 316L. *J. Manuf. Mater. Process, 7*(123). https://doi.org/10.3390/jmmp7040123

Kumar Das, R., Sahana, S., Dutta, S., & Chandra Moi, S. (2023, April). Analysis of dissimilar joining of stainless steel and mild steel using MIG welding. *International Journal of Creative Research Thoughts (IJCRT), 11*(4), h367-h373. ISSN: 2320-2882. www.ijcrt.org © 2023 IJCRT.

Kumar, Anup Dey (2024, June 02). Construction, Mechanical, Piping Design, Basics, Piping Interface. What is piping (A blog for Engineers)? anup.piping@gmail.com.

Kumar, H., Kumar, N., & Manmohan. (2021, May 20). A survey on Gas Metal Arc Welding (GMAW)-Review. IJSRD – International Journal for Scientific Research & Development, 7(01). ISSN (online):2321-0613. https:///www.researchgate.net/publication/351711395.

Kumar, S., & Kumar, D. (2019, October). Effect of Welding Parameters and Electrodes on Bead width using Gas Metal ARC Welding. *International Journal of Engineering and Advanced Technology (IJEAT) 9*(1), 1338-1343. ISSN: 2249-8958. https://doi.org/10.35940/ijeat.A1162.109119 Journal Website: www.ijeat.org. Published By: Blue Eyes Intelligence Engineering & Sciences Publication

Kumar, V., Singh, G., & Khan Yusufzai, M.Z. (2012, August). Effects of process parameters of Gas Metal Arc Welding on dilution in cladding of stainless steel on mild steel. *MIT*

International Journal of Mechanical Engineering, *2*(2), 127-131. ISSN: 2230-7680

Lee, V.T. A preliminary study on gas metal arc welding-based additive manufacturing of metal parts. *Sci. Tech. Dev. J.*, *23*(1), 422-429.

Li, H., Ma, Y., Duan, M., Wang, X., & Che, T. (2023). Defects detection of GMAW process based on convolutional neural network algorithm. *Scientific Reports*, *0123456789*(13), 21219. www.nature.com/scientificreports. https://doi.org/10.1038/s41598-023-48698-x.

Liu, Y., Tang, Q., Tian, X., & Yang, S. (2023). A novel offline programming approach of robot welding for multi-pipe intersection structures based on NSGA-II and measured 3D point-clouds. *Robotics and Computer-Integrated Manufacturing*, *83*(102549). ISSN 0736-5845. https://doi.org/10.1016/j.rcim.2023.102549. (https://www.sciencedirect.com/science/article/pii/S073658452300025X)

Madesh, R. (2020, December). Performance characteristics of GMAW process parameters of multi-bead overlap weld claddings. *IOP Conf. Ser.: Mater. Sci. Eng*. 988 012013 https://www.researchgate.net/publication/347805729 https://doi.org/:10.1088/1757-899X/988/1/012013

Mallick, P.K. (2021). *Materials, Design and Manufacturing for Lightweight Vehicles (Second Edition).* Woodhead Publishing in Materials, 321-371. ISBN: 9780128187128. https://doi.org/10.1016/B978-0-12-818712-8.00008-2. https://www.sciencedirect.com/science/article/pii/B9780128187128000082.

Manney, Dave. (2024, June 04). *Hard-facing and Cladding: What do you know about these 2 processes?* FAB TIMES: SCHUETTE Metals Blog. https://www.schuettemetals.com

Martinez, R.T., Alvarez Besterd, G., Almeida Silva, A.M., & Alfaro, S.C.A. (2021, January 15). Analysisof GMAW process with deep learning and machine learning techniques. Journal of manufacturing processes, p.1-10. https://doi.org/10.1016/j.jmapro.2020.12.052. 1526-6125/© 2020 The Society of Manufacturing Engineers. Published by Elsevier Ltd.

Miller Electric Mfg. Co. (2018). *Guidelines for Gas Metal Arc Welding (GMAW).* MIG (GMAW)

Welding. *Processes*, 154 557 D. www.MillerWelds.com

Mirzaei, N.E., Pal, N. E., and Per Hilletofth (2021). Challenges to competitive manufacturing in high-cost environments: checklist and insights from Swedish manufacturing firms. *Operations Management Research*, 14, 272–292.

Mohammad, H.M., Naeem, U.J., & Jasim Al Hasan, N.H. (2023). Study of welding parameters' effects on residual stress and hardness in 316 stainless steel pipes: Experimental and analytical investigations. *Cogent Engineering*, *10*(2), 2283343, https://doi.org/10.1080/23311916.2023.2283343

Moinuddin, S.D., Hameed, S.S., Dewangan, A.K., Kumar, K.R. & Kumari S. (2021). A study on weld defects classification in gas metal arc welding process using machine learning techniques. *Materials Today: Proceedings*, *43*(1), 623-628. ISSN: 2214-7853. https://www.doi.org/110.1016/j.matpr.2020.12.159. https://www.sciencedirect.com/science/article/pii/S2214785320398448

Mondal, S., & Bose, G.K. (2023, September 11). Parametric optimization for hardness of TIG welded duplex stainless steel. *Materials science - Journal of Industrial Optimization, 4*(2). https://doi.org/10.12928/ijio.v4i2.7756

Moon, J., Ha, H-Y., Kim, K-W., Park, S-J., Lee, T-H., Kim, S-D., Jang, J.H., Jo, H-H., Hong, H-U., Lee, B.H., Lee, Y-J., Lee, C., Suh, D-W., Han, H.N., Raabe, D. & Lee, C-H. (2020, July 22). A new class of lightweight, stainless steel with ultra-high strength and large ductility. *Scientific Reports, (2020), 1-10*. https://1010.1038/s41598-020-69177-7

Mvola, B., Kah, P., & Martikainen, J. (2014). Welding of dissimilar non-ferrous metals by GMAW processes. In *International Journal of Mechanical and Materials Engineering, 9*(1). University of Malaya. https://doi.org/10.1186/s40712-014-0021-8

Nadzam. J., Armao, F., Byall, L., Kotecki, D. & Miller, D. (2014, August). Gas Metal Arc Welding Guidelines - Product and Procedure Selection. www.lincolnelectric.com. © *Lincoln Global Inc. All Rights Reserved*

Nele, L., Mattera, G., & Vozza, M. (2022). Deep Neural Networks for Defects Detection in Gas Metal Arc Welding. *Appl. Sci.*, *12*(3615). https://doi.org/10.3390/app12073615

Netto, A.; Njock Bayock,F.M.; Kah, P. (2023). Optimization of GMAW Process Parameters in Ultra-High-Strength Steel Based on Prediction. *Metals*, *13*(1447), 1-20. https://doi.org/10.3390/met13081447

Odinikuku, W.E., Udumebraye, J.E., & Atadious, D. (2020). Prediction of Weld Bead Geometry of Mild Steel Using Taguchi Technique and Multiple Regression Analysis. *Journal of Engineering Research and Reports 13*(4): 31-46, 2020; Article no. JERR.57894. ISSN: 2582-2926

Ogbonna, O.S., Akinlabi, S.A., Madushele, N, O.S. Fatoba, O.S., & Akinlabi, E.T. (2023, February 11). Grey-based Taguchi method for multi-weld quality optimization of gas metal arc dissimilar joining of mild steel and 316 stainless steel. *Results in Engineering 17*(100963), 1-8. www.sciencedirect.com/journal/results-in-engineering

Oliveira, A.S., Santos, R.O.d., Silva, B.C.d.S., Guarieiro, L.L.N., Angerhausen, M., Reisgen, U., Sampaio, R.R., Machado, B.A.S., Droguett, E.L., da Silva, P.H. & Coelho, R.S. (2021). A Detailed Forecast of the Technologies Based on Lifecycle Analysis of GMAW and CMT Welding Processes. *Sustainability*, *13*(3766), 1-23. https://doi.org/10.3390/su13073766

Pandya, D. (2018). Optimization of MIG welding process parameter using Taguchi Method.

Pathak, R.D., Pratap Singh, S. Gaur, et al. (2020, May 31). To study the influence of process parameters on weld bead geometry in shielded metal arc welding, *Materials Today: Proceedings, xx* (xx), xxx. https://doi.org/10.1016/j.matpr.2020.06.164

Pavaret Preedawiphat, P., Mahayotsanun,N., Sa-ngoen, K., Noipitak, M., Tuengsook, P., Sucharitpwatskul, S., and Dohda, K. (2020, August 30). Mechanical Investigations of ASTM A36 Welded Steels with Stainless Steel Cladding. *Coatings 10*(844), 2-17. https://doi.org/10.3390/coatings10090844 www.mdpi.com/journal/coatings

Punales, E.M. & Alfaro, C.A., (2021). Stability of the process. *IntechOpen Journals*.

http://dx.doi.org/10.5772/intechopen.90386

Rakesh, K., Harsimran, S., & Santosh, K. (2021). OVERVIEW OF CORROSION AND ITS CONTROL: A CRITICAL REVIEW. *Proceedings on Engineering Sciences, 03*(1), 13-24, https://doi.org/10.24874/PES03.01.002**.** *Researchgate* https://www.researchgate.net/publication/384227150. www.pesjournal.net

Ramos-Jaime, D. López-Juárez, I. & Perez, P. (2013). Effect of process parameters on robotic GMAW bead area estimation. *The 2013 Iberoamerican Conference on Electronics Engineering and Computer Science- Procedia Technology*, *7*, 398 – 405

Ranjan, R., & Anil Kumar Das, A.K. (2023). A brief review of enhancing mechanical and corrosion qualities using metal inert gas weld hard-facing. *Journal of Physics: Conference Series, 2484* (012018), 1-8. IOP Publishing. https:doi.org/10.1088/1742-6596/2484/1/012018.

Riswanda, R. Akhyar A., Kadir H., Sugianto S., & Saragih, A.D. (2024, March 1). The effect of heat input on tensile strength, Vickers hardness, and microstructure on DMW of AISI 1015 and 304L SS through the GMAW process. *Journal of Achievements in Materials and Manufacturing Engineering.* ISSN: 1734-8412 https://doi.org/10.5604/01.3001.0054.4920. www.azojete.com.ng. https://www.researchgate.net/publication/349802208

Roshan, R., Kumar Naik, A., Kumar Saxena, K., Singh Arora, K., Shajan, N., Msomi, V., & Mehdi, H. (2023). Effect of welding speed and wire feed rate on arc characteristics, weld bead and microstructure in standard and pulsed gas metal arc welding. *Journal of Adhesion Science and Technology*. https://doi.org/10.1080/01694243.2023.2192314

Sada, S. O., & Enyi, L. C. (2020, December). Parametric Optimization and Determination of a Suitable Welding Process for Stainless Steel-Mild Steel Dissimilar Metals Weld. *Arid Zone Journal of Engineering, Technology & Environment, 16*(4):803-812 Print ISSN: 1596-2490, Electronic ISSN: 2545-5818

Saha, M.K. & Das, S. (2018, June). Gas Metal Arc Weld Cladding and its Anti-Corrosive

Performance- A Brief Review. *Athens Journal of Technology and Engineering, 5*(2), 155-174. *Researchgate*, *5*(2). https://doi.org/10.30958/ajte.5-2-4

Sato, Y., Ogino, Y., & Sano, T. (2024, January 15). Process parameters and their effect on metal transfer in gas metal arc welding: a driving force perspective. *Welding in the World (2024)*68. 905–913

Sayyid, F.F., Ali Bash, M.A., Mohammed, A.I., Mustafa, A.M., & Resen, A.M. (2017, January). Effect of feed rate on laser surface cladding of cold rolled carbon steel. *Engineering and Technology Journal*, 35, Part A (9), pp.922 - 929. https://www.researchgate.net/publication/363353231

Sk Shrabon, Nahidul Islam. (2024, March 30). Welding defects & its prevention. Researchgate. https://www.researchgate.net/publication/379412460.

Sild Siim (2022, October 10). Welding Defects – Types, Causes, Prevention. https://www.fractory.com>welding-def...

Singh Singhal, T., & Kumar Jain, J. (2020). GMAW cladding on metals to impart anti-corrosiveness: Machine, processes and materials. *Materials Today: Proceedings*, *26*(2), 2432-2441, ISSN 2214-7853, https://doi.org/10.1016/j.matpr.2020.02.518. (https://www.sciencedirect.com/science/article/pii/S2214785320312736)

Souto, J.I.V., Ferreira, S.D., Lima, J.S., Castro, W.B., Grassi, E.N.D., & Santos, T.F.A. (2023). Effect of GMAW process parameters and heat input on weld overlay of austenitic stainless steel 316L-Si. *Soldagem & Inspeção. 28*:e2809. https://doi.org/10.1590/0104-9224/SI28.09

Sreeharan, B.N., Yoganandh, J., Sudhakar, R., & Kannan, T. (2022). Investigation of gas metal arc welding process parameters of aluminium alloy weldment using Taguchi-grey-fuzzy integrated approach. *Scientia Iranica B.*, *29*(6), 3084-3097. https://doi.org/10.24200/sci.2022.60003.6545 . http://scientiairanica.sharif.edu.

Sreeraj, Pathiyasseril. (2013). Prediction and optimization of weld bead geometry in gas metal arc welding process using RSM and fmincon. *Journal of Mechanical Engineering Research.*

5(8), 154-165. https://doi.org/10.5897/JMER2013.0271; https://www.researchgate.net/publication/272909740

Sreeraj, P., Kannan, T., and Maji, S. (2013, November). Prediction and optimization of weld bead geometry in gas metal arc welding process using RSM and fmincon. *Journal of Mechanical Engineering Research, 5*(8), 154-165. https://doi.org/10.5897/JMER2013.0292. ISSN 2141-2383 © 2013 Academic Journals. http://www.academicjournals.org/JMER. https://www.researchgate.net/publication/272909740

Tandon, D., Li, H., Pan, Z., Yu, D., & Pang, W. (2023). A Review on Hardfacing, Process Variables, Challenges, and Future Works. *Metals, 13*, 1512. https://doi.org/10.3390/met13091512

Tang, W., Chatzidakis, S., Schrad, C.M., Miller, R.G., & Howard, R. (2024). Study of Mechanical Properties, Microstructure, and Residual Stresses of AISI 304/304L Stainless Steel Submerged Arc Weld for Spent Fuel Dry Storage Systems. *Metals, 14*(262). https://doi.org/10.3390/met14030262

Telwin SPA (2020, July 1) MASTERMIG 400 230-400V. www.telwin.com. Via della Tecnica 3 - 36030 VILLAVERLA (VI) ITALY.

Terner, M., Bayarsaikhan, T.A., Hong, H.U. and Je-Hyun Lee, J.H. (2017, January 03). Influence of Gas Metal Arc Welding Parameters on the Bead Properties in Automatic Cladding. *Journal of Welding and Joining, 35*(1), pp16-25. https://doi.org/10.5781/JWJ.2017.35.1.16

Tesfaye, F.K. (2023, April). Parameter optimizations of GMAW process for dissimilar steel welding. *International Journal of Advanced Manufacturing Technology*, http://dx.doi.org/10.1007/s00170-023-11356-7

Tran, N.-H., Bui, V.-H., & Hoang, V.-T. (2023). Development of an Artificial Intelligence-Based System for Predicting Weld Bead Geometry. *Appl. Sci., 13*(4232). https://doi.org/10.3390/app13074232

Valiente Bermejo, M.A., Eyzop, D., Hurtig, K., & Karlsson, L. (2021, July 25). Welding of Large

Thickness Super Duplex Stainless Steel: Microstructure and Properties. *Metals, 11*(1184). https://doi.org/10.3390/met11081184.

Vashisth, D., Sharma, A., Verma, A., & Khanna, P. (February 2022). Mathematical Modelling to predict dilution in MIG welded aluminium 8011 plates. *Materials Today: Proceedings xxx* (xxxx) 1-7. Journal homepage: www.elsevier.com/locate/matpr. https://doi.org/10.1016/j.matpr.2022.02.065. *Researchgate*. https://www.researchgate.net/publication/358611102

Vasiliev, M., MacLeod, C.N., Loukas, C., Javadi, Y., Vithanage, R.K.W., Lines, D., Mohseni, E., Pierce, S.G., & Gachagan, A. (2021). Sensor-Enabled Multi-Robot System for Automated Welding and In-Process Ultrasonic NDE. *Sensors, 21,* 5077. https://doi.org/10.3390/s21155077

Volavanis, I. & Kosmopoulos, D. (2010, December). Multiclass defect and classification in weld radiographic images using geometric and texture features. *Expert systems with applications, 37*(12), 7606-7614. https://doi.org/10.1016/j.eswa.2010.04.082 . www.sciencedirect.com/s

Vora, J., Parmar, H. Chaudhari, R., Khanna, S., Doshi, M. Patel, V. (2022). Experimental investigations on mechanical properties of a multi-layered structure fabricated by GMAW-based WAAM of SS316L. *Journal of Materials Research and Technology 20*, 2748-2757. https://doi.org/10.1016/j.jmrt.2022.08.

Vu, M.D., et al. (2023). Prediction of the Welding Process Parameters and the Weld Bead Geometry for Robotic Welding Applications with Adaptive Neuro-Fuzzy Models. In: Nguyen, T.D.L., Verdo, E., Le, A.N. Ganzha, M. (eds) Intelligent Systems and Networks. ICISN 2023. Lecture Notes in Networks and Systems, vol 752. Springer, Singapore. https://doi.org/10.1007/978-981-99-4725-6_20

Wahidi, S.I., Oterkus, S., Oterkus, E. (2024). Robotic welding techniques in marine structures and production processes: A systematic literature review. *Marine Structures, 95*(103608). ISSN 0951-8339. https://doi.org/10.1016/j.marstruc.2024.103608. (https://www.sciencedirect.com/science/article/pii/S0951833924000364)

Wang, H., Klarif, S., & Havrlišan, S. (2024). Preliminary Study of Bead-On-Plate Welding Bead Geometry for 316L Stainless Steel Using GMAW. *FME Transactions (2024)*52, 563-572. https://doi.org/10.5937/fme2404563W

W ę g l o w s k i, S.M., H u a n g, Y., & Z h a n g, Y.M. (2008). AN INVESTIGATION OF THE METAL TRANSFER PROCESS IN GMAW. *ENGINEERING TRANSACTIONS • Engng. Trans. • 56*(4), 345–362.

Weck, R. (1965, April 6). "Failure of steel structures: Causes and Remedies." Proceedings of the Royal Society of London. *Series A, Mathematical and Physical Sciences, 285*(1400), 3-9. *JSOR*, http://www.jstor.org/stable/2415084.

Wu, K., Zhan, J., Xuanwei, C., Hong, X., & Xie, P. (2020, September). Dynamic metal transfer in double-wire DP-GMAW of Aluminium alloy under different pulse phases. *Journal of Manufacturing Science and Engineering, 143*(4), 1-28. https://doi.org/10.1115/1.4048439.

Yang, J. & Wang, A. (2024, November 07). Microstructure Evolution and Performance of AA2024 Alloy through Wire-Arc Additive Manufacturing under Different Heat Inputs. *Metals, 14*(1265), 1-13. https://doi.org/10.3390/met14111265

Yao, P., Lin, H., Wu, W., & Tang, H. (2021). Influence of Duty Ratio and Current Mode on Robot 316L Stainless Steel Arc Additive Manufacturing. *Metals, 11*(508). https://doi.org/10.3390/met11030508

Zhai, P., Xue, S., Wang, J., Chen, W., Chen, T., & Ji, S. (2020, May 20). Effects of Arc Length Adjustment on Weld Bead Formation and Droplet Transfer in Pulsed GMAW Based on Datum Current Time. *Metals, 10*(665). http://dx.doi.org/10.3390/met10050665 www.mdpi.com/journal/metals

Zhang, Z., Huang, X., Yao, P., & Xue, J. (2021, January 11). A New Method for Weld Dilution Calculation through Chemical Composition Analysis. *Metals, 11*(131). https://doi.org/10.3390/met11010131

Zhang, S., Xie, F., Wu, X., Luo, J., Li, W., & Yan, X. (2022). The Microstructure Evolution and

Mechanical Properties of Rotary Friction Welded Duplex Stainless Steel Pipe. *Materials*, *16*(9), 3569. https://doi.org/10.3390/ma16093569

Zhao, L., Sun, Y., Shi, Z., & Yang, B. (2023). Analysis of Crack Propagation Behaviors in RPV Dissimilar Metal Welded Joints Affected by Residual Stress. *Materials*, *16*(6578), 1-16. https://doi.org/10.3390/ma16196578 https://doi.org/10.1007/s40194-023-01670-9

Zheng, Lety (2024, January 18). Welding positions explained. Pipe welding positions. Blog for yeswelder.com/blog https://www.wcwelding.com/. https://www.weldfabworld.com/. https://www.weldfabworld.com/.

APPENDICES

APPENDIX A: EQUIPMENT

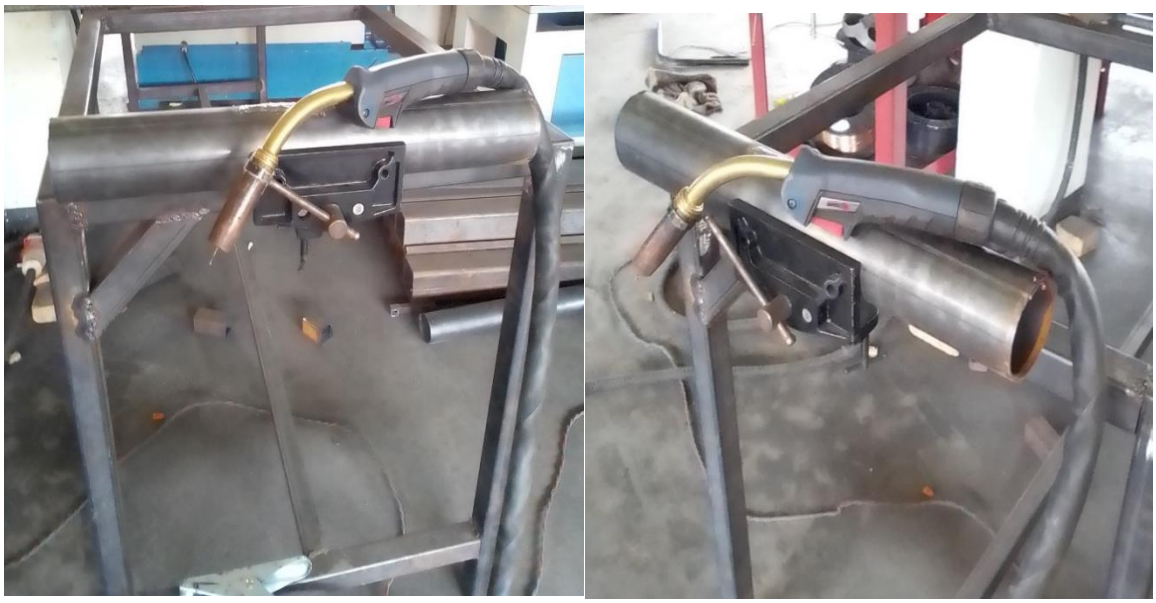

Figure A1-1: experimental setup for the 11-run experiments

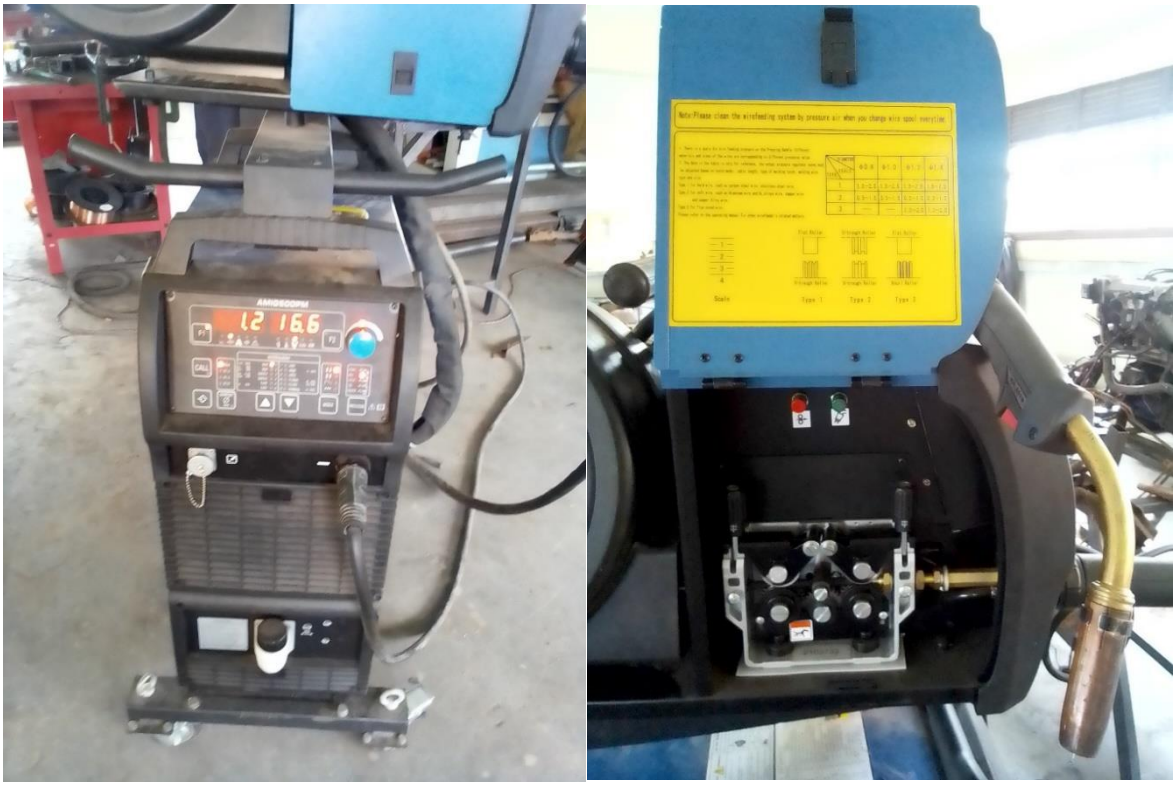

Figure A1-2: Electrode wire feeder equipment

Figure A1-3: Shielding gas cylinder with gas control unit (left) and vermack GMAW welding set (right)

Figure A1-4: TWI Welding Gauge (Cambridge UK) (GAU/0002)

APPENDIX B: EXAMINATION TEST OF THE SAMPLE RUN 1

Objective Lens Used: **50X**/0.70

Eyepiece: WF**10X**/22

C-Mount Adapter: 3.1 MP

Camera Sensor: ½'' (8.00 mm)

Screen size: 18'' (18*25.4 = 457.2 mm)

Total magnification = Optical Magnification * Digital Magnification

Optical magnification = Objective Magnification * C-Mount Adaptor Magnification

Optical magnification = 50*3.1 = **155.0**

Digital magnification = screen size/sensor size

Digital magnification = 457.2 mm / 8.00 mm = **57.1375**

Therefore; Total magnification = 155.0 * 57.1375 = **8,856.3125** (for all images)

APPENDIX C: PIPE SCHEDULES (according to ASME/ANSI B36.10M

Projects Oil & Gas

ArcelorMittal

Pipe Schedules (according to ASME/ANSI B36.10M)

Nominal pipe size mm/inch	OD mm	20	30	STD	40	60	XS	80	100	120	140	160	XXS	Shipping vol/CBM
15 1/2	21.3			2.77 1.27	2.77 1.27		3.73 1.62	3.73 1.62				4.78 1.95	7.47 2.55	0.0004
20 3/4	26.7			2.87 1.69	2.87 1.69		3.91 2.20	3.91 2.20				5.56 2.90	7.82 3.64	0.0007
25 1	33.4			3.38 2.50	3.38 2.50		4.55 3.24	4.55 3.24				6.35 4.24	9.09 5.45	0.0011
32 1 1/4	42.2			3.56 3.39	3.56 3.39		4.85 4.47	4.85 4.47				6.35 5.61	9.70 7.77	0.0017
40 1 1/2	48.3			3.68 4.05	3.68 4.05		5.08 5.41	5.08 5.41				7.14 7.25	10.15 9.56	0.023
50 2	60.3			3.91 5.44	3.91 5.44		5.54 7.48	5.54 7.48				8.74 11.11	11.07 13.44	0.036
65 2 1/2	73.0			5.16 8.63	5.16 8.63		7.01 11.41	7.01 11.41				9.53 14.92	14.02 20.39	0.0053
80 3	88.9			5.49 11.29	5.49 11.29		7.62 15.27	7.62 15.27				11.13 21.35	15.24 27.68	0.0079
90 3 1/2	101.6			5.74 13.57	5.74 13.57		8.08 18.63	8.08 18.63				- -	- -	0.0103
100 4	114.3			6.02 16.07	6.02 16.07		8.56 22.32	8.56 22.32		11.13 28.32		13.49 33.54	17.12 41.03	0.0130
125 5	141.3			6.55 21.77	6.55 21.77		9.53 30.97	9.53 30.97		12.70 40.28		15.88 49.11	19.05 57.43	0.0199
150 6	168.3			7.11 28.26	7.11 28.26		10.97 42.56	10.97 42.56		14.27 54.20		18.26 67.56	21.95 79.22	0.028
200 8	219.1	6.35 33.31	7.04 36.81	8.18 42.55	8.18 42.55	10.31 53.08	12.70 64.64	12.70 64.64	15.09 75.92	18.26 90.44	20.62 100.92	23.01 111.27	22.23 107.92	0.048
250 10	273.1	6.35 41.77	7.80 51.03	9.27 60.31	9.27 60.31	12.70 81.55	12.70 81.55	15.09 96.01	18.26 114.75	21.44 133.06	25.40 155.15	28.58 172.33	25.40 155.15	0.074
300 12	323.9	6.35 49.73	8.38 65.20	9.53 73.88	10.31 79.73	14.27 108.96	12.70 97.46	17.48 132.08	21.44 159.91	25.40 186.97	28.58 208.14	33.32 238.76	25.40 186.97	0.104
350 14	355.6	7.92 67.90	9.53 81.33	9.53 81.33	11.13 94.55	15.09 126.71	12.70 107.39	19.05 158.10	23.83 194.96	27.79 224.65	31.75 253.56	35.71 281.70		0.126
400 16	406.4	7.92 77.83	9.53 93.27	9.53 93.27	12.70 123.30	16.66 160.12	12.70 123.30	21.44 203.53	26.19 245.56	30.96 286.64	36.53 333.19	40.49 365.35		0.165
450 18	457.2	7.92 87.71	11.13 122.38	9.53 105.16	14.27 155.80	19.05 205.74	12.70 139.15	23.88 254.55	29.36 309.62	34.93 363.56	39.67 408.26	45.24 459.37		0.209
500 20	508.0	9.53 117.15	12.70 155.12	9.53 117.15	15.09 183.42	20.62 247.83	12.70 155.12	26.19 311.17	32.54 381.53	38.10 441.49	44.45 508.11	50.01 564.81		0.258
550 22	558.8	9.53 129.13	12.70 171.09	9.53 129.13	- -	22.23 294.25	12.70 171.09	28.58 373.83	34.93 451.42	41.28 527.02	47.63 600.63	53.98 672.26		0.312
600 24	609.6	9.53 141.12	14.27 209.64	9.53 141.12	17.48 255.41	24.61 355.26	12.70 187.06	30.96 442.08	38.89 547.71	46.02 640.03	52.37 720.15	59.54 808.22		0.372
650 26	660.4	12.70 202.72	- -	9.53 152.87	- -		12.70 202.72							0.436
700 28	711.2	12.70 218.69	15.88 271.21	9.53 164.85	- -		12.70 218.69							0.505
750 30	762.0	12.70 234.67	15.88 292.18	9.53 176.84	- -		12.70 234.67							0.580
800 32	812.8	12.70 250.64	15.88 312.15	9.53 188.82	17.48 342.91		12.70 250.64							0.660
850 34	863.6	12.70 266.61	15.88 332.12	9.53 200.31	17.48 364.90		12.70 266.61							0.745
900 36	914.4	12.70 282.27	15.88 351.70	9.53 212.56	19.05 420.42		12.70 282.27							0.836
950 38	965.2			9.53 224.54			12.70 298.24							0.931
1000 40	1016.0			9.53 236.53			12.70 314.22							1.032
1050 42	1066.8			9.53 248.52			12.70 330.19							1.138
1100 44	1117.8			9.53 260.50			12.70 346.16							1.249
1150 46	1168.4			9.53 272.25			12.70 351.82							1.365
1200 48	1219.2			9.53 284.24			12.70 377.79							1.486

SI Units (Metric)
OD = mm
Wall thickness = mm
Weight = kg/m (plain end mass)

*For our complete range of structural tubulars, please refer to our stock program: www.arcelormittal.com/oilandgas/stockprogram

Africa
projects.africa@arcelormittal.com

China
projects.china@arcelormittal.com

India
projects.india@arcelormittal.com

South East Asia
projects.asia@arcelormittal.com

Caspian
projects.caspian@arcelormittal.com

Europe
projects.europe@arcelormittal.com

North America
projects.northamerica@arcelormittal.com

UAE
dvtc.sales@arcelormittal.com

ArcelorMittal

APPENDIX D: MATERIALS USED FOR TESTING FOR PITTING CORROSION

APPENDIX F: MICROSTRUCTURAL CHARACTERISTICS

Figure F-1: Image testing for microstructural characteristics of the fusion zone

Figure F-2: Metallurgical Optical Microscope used for testing microstructural characteristics

S/N	Microstructural Characteristics	Comments
S-1-A	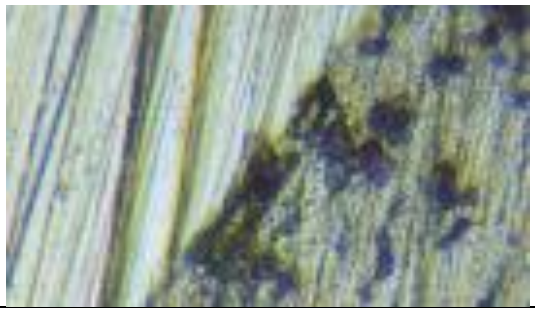	The microstructural characteristics of this specimen show that the material was well-cladded because there is little difference in the microstructure of both the substrate and the cladding material. The image is magnified further by two (×2). The parameters were arc voltage, welding current, and wire feed rate of 180A, 25V, 3.0 mm/min respectively.
S-1-B	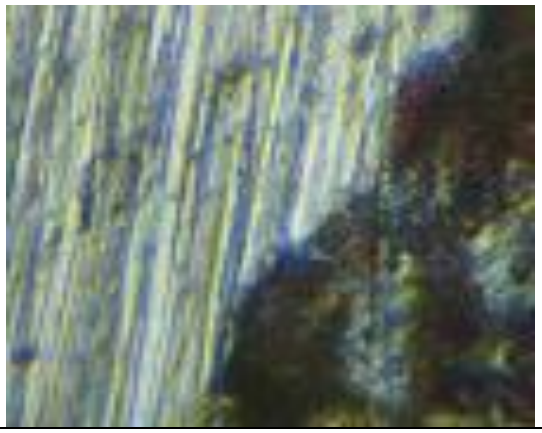	The microstructural characteristics of this specimen show that the material was well-cladded but had dirt on it at this joint because there is a difference in the microstructure of both the substrate and the cladding material. The image is magnified further by two (×2).
S-2-A	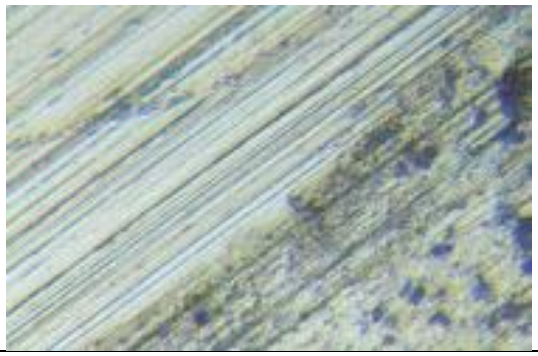	The microstructural characteristics of this specimen show that the material was well-cladded because there is little difference in the microstructure of both the substrate and the cladding material. The image is magnified further by two (×2). The parameters were arc voltage, welding current, and wire feed rate of 150A, 26V, and 3.5m/min respectively.
S-2-B	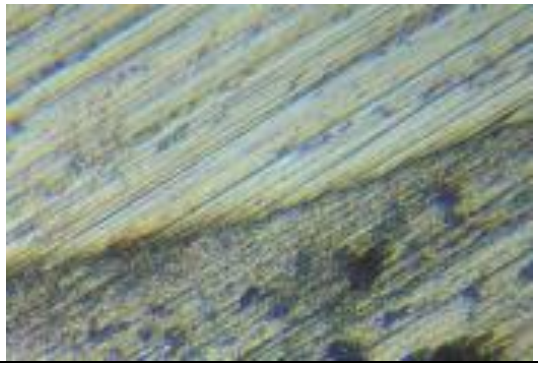	The microstructural characteristics of this specimen show that the material was well-cladded because there is little difference in the microstructure of both the substrate and the cladding material. The image is magnified further by two (×2).
S-3-A		The microstructural characteristics of this specimen show that the material was well-cladded because there is little difference in the

	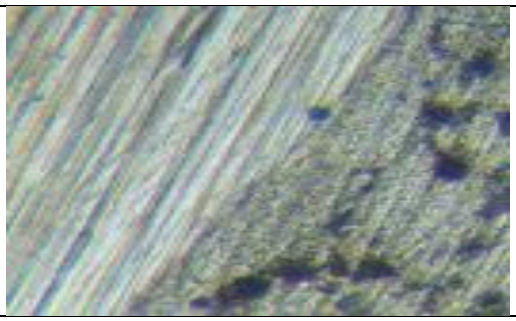	microstructure of both the substrate and the cladding material. The image is magnified further by two (×2). The parameters were arc voltage, welding current, and wire feed rate of 150A, 28V, and 4.0m/min respectively.
S-3-B	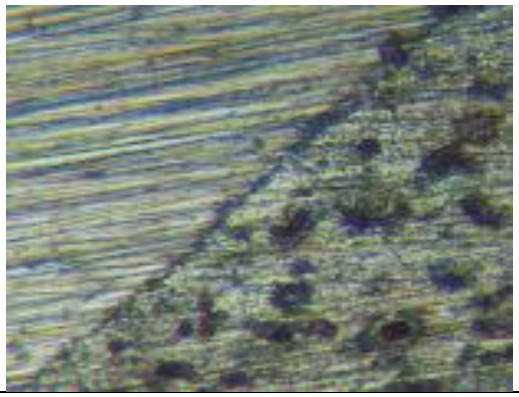	The microstructural characteristics of this specimen show that the material was well cladded because there is little difference in the microstructure of both the substrate and the cladding material. The image is magnified further by two (×2).
S-4-A	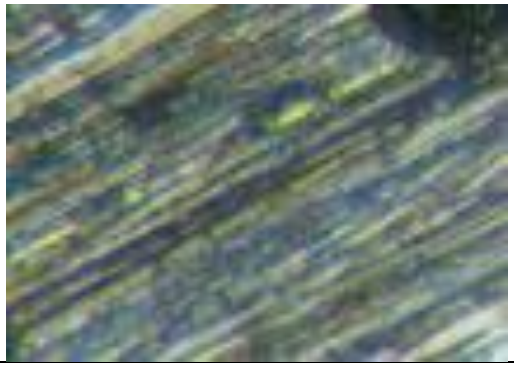	The material shows that the clad had a good mixing. The image is magnified further by two (×2). The parameters were arc voltage, welding current, and wire feed rate of 160A, 24V, and 3.5m/min respectively.
S-4-B	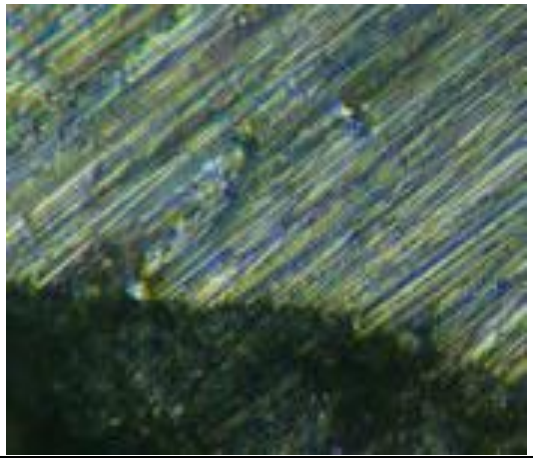	The material shows that the clad had a good mixing. The image is magnified further by two (×2).
S-5-A		

	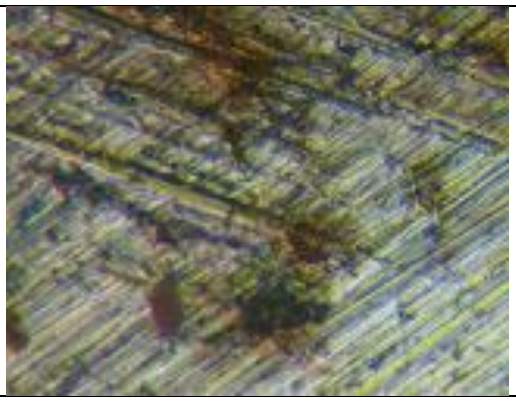	The microstructure of the cladding surface. It has scratches due to the use of the grinder. The image is magnified further by two (×2). The parameters were arc voltage, welding current, and wire feed rate of 160A, 26V, and 4.0 m/min respectively.
S-5-B	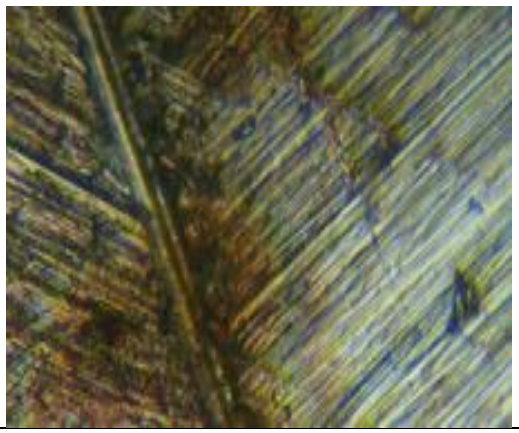	The microstructural characteristics of this specimen show that the material was well-cladded because there is little difference in the microstructure of both the substrate and the cladding material. The image is magnified further by two (×2).
S-6-A	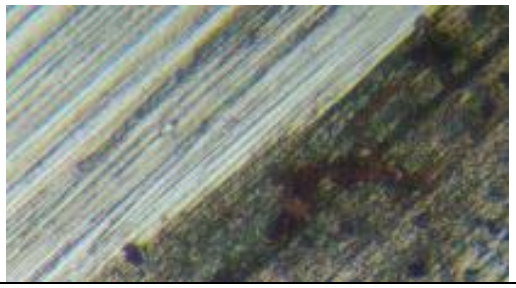	The microstructural characteristics of this specimen show that the material was well-cladded because there is little difference in the microstructure of both the substrate and the cladding material. The image is magnified further by two (×2). The parameters were arc voltage, welding current, and wire feed rate of 160A, 28V, and 3.0 m/min respectively.
S-6-B	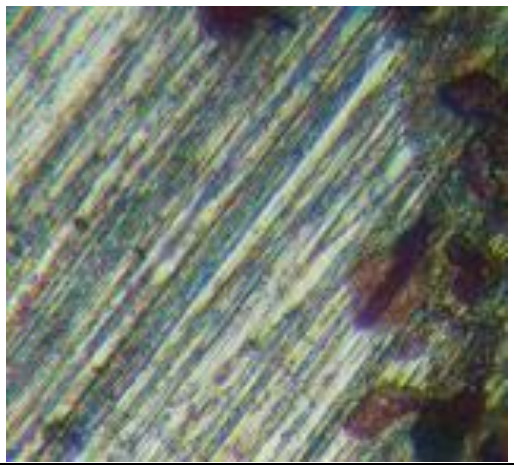	The microstructural characteristics of this specimen show that the material was well-cladded because there is little difference in the microstructure of both the substrate and the cladding material. The image is magnified further by two (×2).

S-7-A	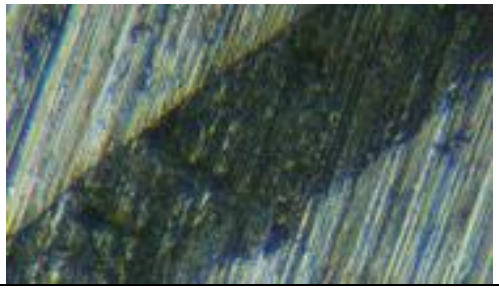	The microstructure of the fusion zone showing a unique microstructure due to the applied heat. The image is magnified further 170A, 24V, and 4.0 m/min. Image magnified by two (×2). The parameters were arc voltage, welding current, and wire feed rate of 170A, 24V, and 4.0 m/min respectively.
S-7-B	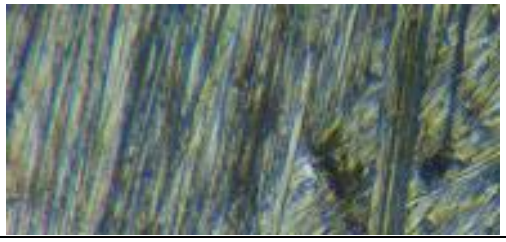	Uniform microstructure at the surface of the cladding. The image is magnified further by two (×2).
S-8-A	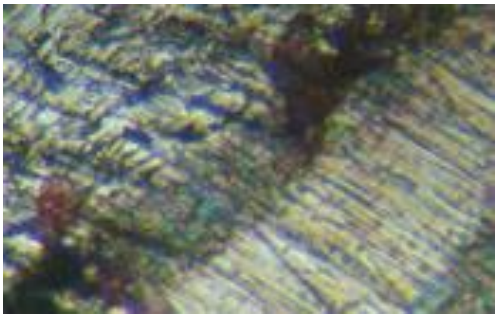	The microstructural characteristics of this specimen show that the material was well-cladded because there is little difference in the microstructure of both the substrate and the cladding material. There are little microstructural characteristics seen due to the change of the bulb of the optical microscope. The image is magnified further by two (×2). The parameters were arc voltage, welding current, and wire feed rate of 170A, 26V, and 3.0 m/min respectively.
S-8-B	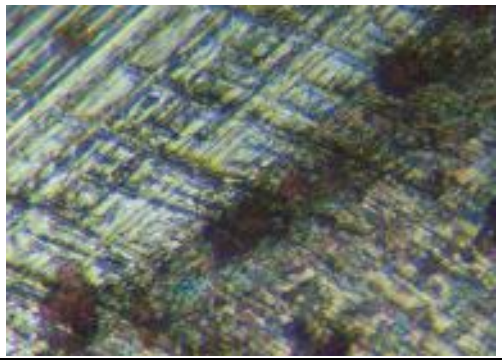	The microstructural characteristics of this specimen show that the material was well-cladded because there is little difference in the microstructure of both the substrate and the cladding material. There are little microstructural characteristics seen due to the change of the bulb of the optical microscope. The image is magnified further by two (×2).
S-9-A		The microstructure shows no difference, it was well-cladded. The image is magnified further by two (×2). The parameters were arc voltage, welding current, and wire feed rate of 170A, 28V, and 3.5 m/min respectively.

S-9-B	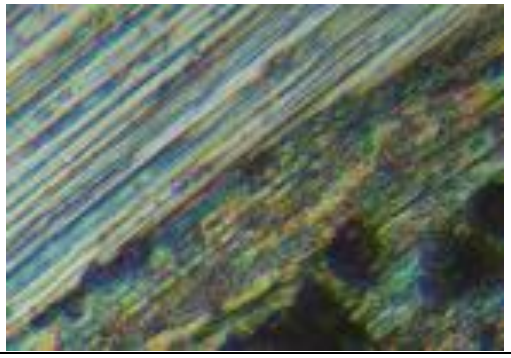	The microstructure is normal with little difference in the cladding region. The image is magnified further by two (×2).

At-Least Six People Killed in the Building Collapse (Sunday Vision, October 9, 2021)